ATG14L and ZBTB16: Critical Roles In Aggrephagy In STHdhQ7/Q7 Striatal Neurons

Vanessa Kissner

Thesis submitted to the University of Ottawa in partial fulfillment of the requirements for the MSc in Cellular and Molecular Medicine

Department of Cellular and Molecular Medicine
Faculty of Medicine
University of Ottawa

Abstract

Huntington's disease (HD) is a devastating neurodegenerative disease caused by a polyglutamine expansion repeat in exon one of the gene encoding the huntingtin protein. A hallmark of HD pathology is the accumulation of aggregates of the mutant huntingtin protein (mHtt). Macroautophagy (MA) is an intracellular catabolic process responsible for the degradation of cytoplasmic constituents, including misfolded protein aggregates, as are found in HD. Selective MA which degrades protein aggregates is known as aggrephagy. Recently, chronic blockade of the metabotropic glutamate receptor subtype 5 (mGluR5) in the zQ175 HD mouse model has been shown to cause an improvement in disease progression, which correlated with an activation of the GSK3β-mediated pathway of MA. A reduction in ZBTB16, a core component of the ZBTB16-Cullin3-Roc1 E3 ubiquitin ligase complex, and an increase in ATG14L, a key component of the vps34 complex responsible for autophagosome biogenesis, were evident following mGluR5 inhibition in zQ175 HD mice. In the present study, we have found that silencing of ATG14L using CRISPR Cas9 in STHdhQ7/Q7 striatal neurons causes an inhibition of MA, a unique post-translational modification on beclin-1, decreased mGluR5 expression, and the accumulation of Q138 (mHtt). We find that CRISPR-Cas9-induced silencing of ZBTB16 in STHdhQ7/Q7 striatal neurons causes an induction of MA, decreased mGluR5 expression, and the clearance of Q138 (mHtt). ZBTB16 likely exerts its effects on MA via regulation of ATG14L. These findings elucidate the important role of ATG14L and ZBTB16 in aggrephagy in STHdhQ7/Q7 striatal neurons, and suggest that the modulation of ATG14L and ZBTB16 may represent novel therapeutic approaches in the treatment of HD.

Acknowledgements

I would like to thank Dr. Ferguson for taking me on as an MSc student in his lab. I would also like to thank all of the members of the Ferguson lab for their support and friendship throughout my time in the lab. In particular, I would like to thank Dr. Khaled Abd-Elrahman and Dr. Ferguson for designing this project and allowing me to work on it. I would like to extend my deepest gratitude specifically to Dr. Alison Hamilton, Jessica Mabelle De Souza, and Dr. Lorena Bianchine Areal De Azevedo, for mentoring me and teaching me many techniques. I learned a great deal from them, and cannot thank them enough for all of their support and friendship. Whenever I was feeling dejected, they always encouraged me and helped me to get back on my feet again.

I would like to thank Dr. Ryan Russell and Zhihao Guo for teaching me the CRISPR Cas9 protocol used in this project. They taught me hands on in their own lab when they certainly did not have to. I am very grateful to them for their kindness and help.

I am extremely grateful to the assistant dean of graduate studies, Dr. Nadine Wiper-Bergeron for her unwavering support and kindness that she has shown me throughout my MSc. I was not one of her graduate students, yet she went out of her way to help me through some very difficult times, and I would not have made it through this without her. She has always believed in me and offered me every support, and I hope that someday I can pay her back for everything that she has done for me.

Lastly, I would like to thank my family for supporting me throughout my MSc. They were always interested in hearing about what I was working on, drove me to and from the lab on weekends, picked me up when I worked late, cooked me meals so I had one less thing to worry about, and were always available for fun activities to do as a break and opportunity to de-stress for me.

Table of Contents

List of Abbreviations

Aβ	Beta-amyloid
AC	Adenylate cyclase
AD	Alzheimer's disease
Akt	Protein kinase B
AMPA	α-amino-3-hydroxyl-5-methyl-4-isoxazole-propionate
AMPK	5'-AMP-activated protein kinase
ATG	Autophagy-related genes
ATG14L KO	ATG14L$^{-/-}$xSTHdHQ7/Q7
ATP	Adenosine triphosphate
BDNF	Brain derived neurotrophic factor
CAG	Cytosine-guanine-adenine
CaMKK2/CaMKKβ	Calcium/calmodulin dependent protein kinase kinase 2
cAMP	Cyclic AMP
CDPPB	3-Cyano-*N*-(1,3-diphenyl-1*H*-pyrazol-5-yl) benzamide
CMA	Chaperone-mediated autophagy
CNS	Central nervous system
CRISPR	Clustered regularly interspaced short palindromic repeats
CTEP	2-chloro-4-[2-[2,5-dimethyl-1-[4-(trifluoromethoxy)phenyl]imidazole-4-yl]ethynyl]pyridine
DAG	Diacylglycerol
DBZ	Deutetrabenazine
DFB	[(3-Fluorophenyl)methylene]hydrazine-3-fluorobenzaldehyde
DHPG	(*S*)-3,5-Dihydroxyphenylglycine
ER	Endoplasmic reticulum
FYCO1	FYVE and coiled-coil domain autophagy adaptor 1
GABA	γ-aminobutyric acid
GIRK	Inward rectifying potassium channels

GKAP	Guanylate kinase-associated protein
GPCR	G-protein coupled receptors
GSK3β	Glycogen synthase kinase 3 β
HBSS	Hank's Balanced Salt Solution
HD	Huntington's disease
HEAT	Huntingtin, Elongation factor 3 (EF3), protein phosphatase 2A (PP2A), and the yeast kinase TOR1
HSPA8/HSC70	Heat shock 70 kDA protein 8
HTT	Huntingtin gene
Htt	Wild type huntingtin protein
IP_3	Inositol-1,4,5-triphosphate
JHD	Juvenile Huntington's Disease
KO	Knockout
LAMP2A	Lysosomal-associated membrane protein 2A
LC3	Microtubule-associated protein 1A/1B
LIR	LC3-interacting region
MA	Macroautophagy
MAPK	Mitogen-activated protein kinase
MEK	Mitogen-activated protein kinase kinase
mGluR	Metabotropic glutamate receptor
mGluR5	Metabotropic glutamate receptor subtype 5
mHtt	Mutant huntingtin protein
MPEP	2-methyl-6-(phenylethynyl)-pyridine
MSN	Medium spiny neuron
mTORC1	Mechanistic target of rapamycin complex 1
NAM	Negative allosteric modulator
NMDA	N-methyl-D-aspartate
NMDAR	NMDA receptor
p62	SQSTM1/p62
PAM	Positive allosteric modulator
PD	Parkinson's disease
PE	Phosphatidylethanolamine
pGSK3β	S9 phosphorylated glycogen synthase kinase 3 β
PI3K	Phosphoinositide-3-kinase

PI3P	Phosphatidylinositol 3-phosphate
PIK3C3	Phosphatidylinositol 3-kinase catalytic subunit type 3
PIK3R4/vps34	Phosphatidylinositol 3-kinase regulatory subunit 4
PIKE	PI3K Enhancer
PIP_2	Phosphatidylinositol-4,5-bisphosphate
PKA	cAMP-dependent protein kinase A
PKC	Protein kinase C
PLA2	Phospholipase A2
$PLC_{\beta 1}$	Phospholipase Cβ1
polyQ	polyglutamine
PSD-95	Postsynaptic density protein 95
RB1CC1/FIP200	RB1-inducible coiled-coil
SHANK	SH_3 and multiple ankyrin repeat domains protein
SNAP29	Qbc-SNARE SNAP29
SNARE	N-ethylmaleimide-sensitive factor attachment protein receptors
STX17	Qa-SNARE syntaxin 17
TBZ	Tetrabenazine
TGFβ	Transforming growth factor β
ULK	Unc-51-like kinase family
UPS	Ubiquitin Proteasome System
UVRAG	UV radiation resistance associated gene protein
Vamp8	R-SNARE Vamp8
VU1545	*N*-[1-(2-Fluorophenyl)-3-phenyl-1H-pyrazol-5-yl]-4-nitrobenzamide
WIPI2	WD repeat domain, phosphoinositide interacting 2
WT	Wild type
ZBTB16	Phosphorylating zinc finger and BTB domain-containing protein 16
ZBTB16 KO	$ZBTB16^{-/-}$xSTHdhQ7/Q7

List of Figures

List of Tables

Chapter 1: Introduction

1.1 Huntington's Disease

Huntington's Disease (HD) is a devastating progressive neurodegenerative disease inherited in an autosomal dominant manner, and is characterized by a triad of motor, cognitive, and psychiatric symptoms (1-6). Like Alzheimer's Disease (AD) and Parkinson's Disease (PD), HD is classified as a neurodegenerative proteinopathy: the accumulation of misfolded protein aggregates (in the case of HD these are aggregates of mutant huntingtin protein) is correlated with the progressive degeneration of neurons (7-14). Patients with HD exhibit selective neurodegeneration, with the medium spiny neurons (MSN) of the caudate putamen of the striatum most heavily affected; however, as the disease progresses, degeneration is also observed in other areas of the brain, such as the cortex, cerebellum, and thalamus (15)(1, 16). Despite knowledge of the causative mutation (a trinucleotide repeat expansion in exon 1 of the huntingtin gene), to date there exist no disease modifying treatments, and treatment is largely palliative (1, 3).

Onset of HD typically occurs between 30 and 50 years of age, and is marked by the manifestation of motor symptoms consistent with HD, which cannot be explained by another condition (1)(17). Therefore, clinical diagnosis of HD is made by a confirmation of family history and/or a positive genetic test, coupled with the onset of motor symptoms indicative of HD (2). However, several years prior to official disease onset, subtle motor, cognitive, and psychiatric symptoms may be present (1, 2, 18, 19). HD is ultimately fatal. After disease onset, symptoms progress for approximately 15-20 years until death (1, 3, 17, 20, 21).

In typical adult onset HD, initial motor symptoms lead to a hyperkinetic phenotype, of which chorea is one of the most recognizable (2, 20, 22). This hyperkinetic phenotype results from the loss of MSNs of the indirect pathway (23). As the disease progresses, the hyperkinetic phenotype marked by chorea gives way to a hypokinetic phenotype which is caused by the loss of MSNs of the direct pathway (8). Motor symptoms of the hypokinetic phenotype include bradykinesia (slowness of movement),

akinesia, rigidity and ataxia, dystonia (abnormal postures), and problems with gait and balance (1, 2, 20). Currently, chorea is the only motor symptom which responds to drug therapy. Tetrabenazine (TBZ) and deutetrabenazine (DBZ) (both of which are vesicular monoamine transporter 2 inhibitors) are currently approved for treatment of chorea associated with HD (1, 3, 20, 24-26). TBZ has many undesirable side effects, including an increase in suicidality; DBZ, however, has fewer undesirable side effects (27-29).

Cognitive symptoms observed in HD include impaired visual attention, psychomotor speed, problems with visuomotor and spatial integration (1)(30). In more advanced stages of the disease, these symptoms can progress into dementia, where symptoms follow a subcortical pattern (2, 19). These subcortical symptoms include "impaired emotion recognition, processing speed, attention, memory retrieval, visuospatial and executive function" (2)(19, 20). Since dementia in HD is subcortical, its symptoms are different from those seen in cortical dementias such as AD (31). Therefore, current treatments used for AD, such as cholinesterase inhibitors or memantine, may not be as effective for the treatment of HD; there is little evidence supporting their use for treatment of HD (20).

Psychiatric symptoms present in HD include depression, anxiety, obsessive compulsive disorder, irritability, aggression, disinhibition and apathy (2, 20, 32-44). Psychosis can be seen in later stages, although it is quite rare with a prevalence of approximately 3-11% (2, 20, 32, 33). Apathy is characterized by behaviour which reflects a loss of interest (1), and is one of the most commonly occurring psychiatric symptoms; it worsens as HD progresses, and is most prevalent in advanced stages of HD (32, 33, 45). While other psychiatric symptoms of HD may be effectively managed with drug treatment (such as with serotonin reuptake inhibitors), apathy does not respond to drug therapy (20, 46).

In 1993, the causative genetic mutation for HD was identified (16, 17, 47). A cytosine-adenine-guanine (CAG) trinucleotide repeat expansion in exon 1 of the HTT gene (which encodes the huntingtin

protein (htt)), located on chromosome 4p16.3, leads to the production of a mutant huntingtin protein (mHtt) containing an expanded polyglutamine (polyQ) tract in the N-terminal region, which causes HD (2, 16, 47, 48). Fewer than 27 CAG repeats is considered normal, and HD will not develop (1, 49-51). CAG repeats of 27-35 are considered an intermediate allele, and repeat numbers within this range can lead to expansions into the pathogenic range or contractions during meiosis (1, 17, 49, 52). Hence, repeat numbers within this range can lead to the appearance of a seemingly sporadic case; a parent with a repeat number within this range would not develop HD, although they could have a child with HD. CAG repeat numbers between 36-39 cause reduced penetrance (1, 49, 53). Greater than 40 repeats is considered fully penetrant, and HD symptoms will definitely develop (1, 2, 49). Severity of disease and age at onset are correlated with the number of repeats, with a higher number of repeats being correlated with increased severity and decreased age of onset (1, 3, 17, 54, 55).

Patients with Juvenile HD (JHD), in which disease onset occurs at approximately less than or at 20 years of age, typically exhibit the greatest number of repeats and progress is much more rapid than typical adult onset HD (1, 17, 56-58). JHD usually presents with an akinetic-rigid variant version of HD, in which bradykinesia, rigidity, and akinesia are present right from the start, as opposed to developing later as in typical adult onset HD (17).

Htt is a protein of approximately 350 kDa containing HEAT (Huntingtin, Elongation factor 3 (EF3), protein phosphatase 2A (PP2A), and the yeast kinase TOR1) repeats found throughout unstructured regions (54). It contains sites for proteolytic cleavage by caspases, calpains, and endopeptidases, and sites for post-translational modifications (54, 59, 60). Htt is expressed throughout the cells of the body as a cytosolic protein (it is also found in the nucleus, axonal processes, and synapses), and it is expressed most highly in neurons, especially those found in the striatum, cerebellar cortex, hippocampus, and neocortex (15). Studies have shown that htt is important in embryonic and brain development, although its exact functions remain unclear. It is thought that htt is a scaffolding protein which plays a role in transcriptional regulation, vesicular trafficking, mitochondrial dynamics,

intracellular trafficking, nucleocytoplasmic shuttling, Brain derived neurotrophic factor (BDNF) production, synaptic transmission, cargo recognition in autophagy, and a variety of other protein-protein interactions (20, 54, 61-65).

The majority of patients suffering from HD are heterozygous, and the few who are homozygous do not enjoy any appreciably better health than those who are heterozygous (15). Therefore, it is thought that the polyQ expansion causing the formation of mHtt does not cause a complete loss of function, and many studies believe mHtt exhibits a toxic gain of function (14, 15, 20, 62-69). In support of this toxic gain of function hypothesis, mHtt has been shown to cause "transcriptional interference, cytoskeletal disruption, synaptic dysfunction, mitochondrial damage, excitotoxicity, accumulation of toxic aggregates, loss of BDNF, and changes in axonal transport" (20). Htt is cleaved into a variety of fragments, one of which is an N-terminal fragment containing exon 1, and this includes the polyQ region (70, 71). This exon 1 fragment has been shown to aggregate in various HD models (72, 73) and is thought to play a role in disease pathology, although this does not exclude a role for other fragments and full length mHtt in disease pathology. However, despite extensive research, it is still not fully understood exactly how mHtt leads to progressive, selective neurodegeneration. Pathological hallmarks of HD include intranuclear and cytoplasmic inclusions containing mHtt, ubiquitin, and components of the Ubiquitin Proteasome System (UPS) (7, 54, 74).

Despite the identification of the causative mutation, there is currently no cure for HD, and treatments are predominantly limited to symptom management. As such, research that expands our understanding of HD pathogenesis/disease mechanisms is desperately needed, in order that new, effective treatments, and eventually a cure, may be identified. To this end, mGluR5-mediated regulation of autophagy presents an interesting and novel avenue of research into HD pathogenesis, and may provide a successful approach to treatment.

1.2 Glutamate excitotoxicity in Huntington's Disease

Glutamate is the major excitatory neurotransmitter in the human brain (75). It is essential for many physiological processes, including learning, synaptic plasticity, and memory (75, 76). Despite its positive role in many vital physiological processes in the brain, glutamate can also cause/mediate neuronal cell death, known as glutamate excitotoxicity (77). Increased intracellular calcium levels are caused by excessive glutamate released from synapses, which leads to overstimulation of glutamate receptors, which in turn leads to neuronal cell death (4). Glutamate excitotoxicity is thought to play a role in the neuronal cell death that occurs in HD (75).

Two classes of receptors are activated by glutamate: ionotropic and metabotropic receptors. These receptors are found widely throughout the nervous system. Ionotropic receptors are ligand gated ion channels that produce fast excitatory neurotransmission, and include the N-methyl-D-aspartate (NMDA), α-amino-3-hydroxyl-5-methyl-4-isoxazole-propionate (AMPA), and kainite receptors (75, 78, 79). Metabotropic glutamate receptors (mGluR) are heterotrimeric, transmembrane G-protein coupled receptors (GPCR) belonging to the family C GPCRs, which, upon stimulation, lead to G protein-mediated second messenger signaling cascades, as well as G-protein independent signaling pathways (4, 75, 78, 80-85). All eight mGluRs are organized based on "sequence homology and G protein coupling specificity" (4) into three families: I (mGluR1 and mGluR5), II (mGluR2 and mGluR3), and III (mGluR4, mGluR6, mGluR7, and mGluR8) (4).

Activation of ionotropic glutamate receptors plays a role in glutamate excitotoxicity (4, 87, 88). Specifically, stimulation of NMDA receptors (NMDAR) leads to an influx of calcium through the open channel (78). Under conditions of glutamate excitotoxicity, this leads to an excessive influx of calcium, which ultimately leads to neuronal cell death (largely due to resulting mitochondrial dysfunction) (4, 89, 90). Supporting a role for altered NMDAR signaling contributing to HD pathogenesis is the finding that injection of the NMDAR agonist quinolinic acid into rat striatum

resulted in the neurodegeneration of MSNs (75, 86). This selective neurodegeneration mirrors the selective neurodegeneration of MSNs observed in HD. In addition, NMDARs containing the NR1A/NR2B subunits can be sensitized by mHtt, which contributes to an excessive influx of calcium (91, 92). NR2B subunits are thought to activate neurotoxic signaling pathways which contribute to neurodegeneration (75). Since NMDARs in MSNs of the striatum contain mainly this combination of subunits, this may provide an explanation for the selective neurodegeneration of striatal MSNs seen in HD (4, 75, 93). Taken together, it is clear that NMDAR signaling plays a critical role in neuronal cell death in HD.

The impact of the stimulation of mGluRs and their role in glutamate excitotoxicity in HD is more complex. However, the stimulation of group I mGluRs (mGluR1 and mGluR5) can lead to increased calcium release (83, 94, 95). While Group I mGluRs can lead to the activation of neurotoxic signaling pathways, they can also activate neuroprotective pathways (94, 96) (Figure 1.1). Group II and III mGluRs, on the other hand, may act to protect against excitotoxicity (94) (Figure 1.1).

Group II and III mGluRs are coupled to the G protein $G_{i/o}$. Upon stimulation of these receptors, the $G\alpha_{i/o}$ subunits uncouple from the Bγ subunits. The $G\alpha_{i/o}$ subunits act to inhibit adenylate cyclase (AC), preventing the conversion of adenosine triphosphate (ATP) into cyclic AMP (cAMP), thus resulting in decreased cAMP levels. This uncoupling also leads to the activation of neuroprotective pathways which promote cell survival and proliferation, including the phosphoinositide-3-kinase (PI3K)/protein kinase B (Akt) and mitogen-activated protein kinase (MAPK) pathways (94, 97, 98). Furthermore, the Bγ subunits inhibit voltage-gated calcium channels and activate inward rectifying potassium channels (GIRK), which contributes to an inhibition of presynaptic glutamate and γ-aminobutyric acid (GABA) release (94, 99, 100). Studies have shown that the activation of group II mGluRs in astrocytes leads to an increase in neurotrophic factors, including transforming growth

factor β (TGFβ), which promotes neuroprotection (94). Activation of group II mGluRs also results in an increase in neurotrophic factors produced by glial cells, such as BDNF (94).

Group I mGluRs are coupled to the heterotrimeric G protein G_{q11}. When stimulated, group I mGluRs promote the uncoupling of $G\alpha_{q/11}$ from Bγ. The $G\alpha_{q/11}$ subunits activate phospholipase Cβ1 ($PLC_{\beta1}$), which catalyzes the formation of diacylglycerol (DAG) and inositol-1,4,5-triphosphate (IP_3) from phosphatidylinositol-4,5-bisphosphate (PIP_2). IP_3 stimulates IP_3 receptors present on the endoplasmic reticulum (ER), thereby promoting intracellular calcium release. This increase in intracellular calcium release acts to increase neuronal excitability (however, studies have shown that the type/population of neuron determines whether this leads to excitability or inhibitory effects), but in excess can also act to promote excitotoxicity (78, 94). In the context of HD, the IP_3 receptor is sensitized by mHtt, and therefore stimulation of group 1 mGluRs can lead to excessive calcium release which in turn promotes neuronal excitotoxicity (101, 102). DAG and calcium released by stimulation of IP_3 receptors both activate protein kinase C (PKC), which in turn activates phospholipase A2 (PLA2), phospholipase D (PLD), and mitogen-activated protein kinase kinase (MEK). MEK activates the MAPK pathway, which ultimately leads to the production of transcription factors which lead to an increase in trophic factors (i.e. BDNF), and act to promote cell proliferation and survival (94). Homer proteins associate with group I mGluRs and shank proteins (103-105). This allows group I mGluRs, through the Homer-shank protein interaction, to activate the PI3K enhancer (PIKE), which in turn stimulates PI3K, which activates Akt to promote cell survival and neuroprotection (94, 106). In the context of HD, phosphorylation of mHtt by Akt results in a decrease in htt aggregates and neuronal cell loss (4, 107, 108). The interaction of group I mGluRs with Homer proteins also results in the activation of the MAPK pathway, thus further promoting neuroprotective signaling (94). NMDARs are believed to interact with a complex of scaffolding proteins, including postsynaptic density protein 95 (PSD-95), guanylate kinase-associated protein (GKAP), SH_3 and multiple ankyrin repeat domains protein (SHANK), and Homer proteins (78). The group I mGluRs are believed to be able to modulate

NMDAR signaling through their interaction with Homer. Homer connects group I mGluR signaling to NMDAR activity through its interaction with the PSD-95, GKAP, SHANK scaffolding complex associated with NMDARs (78, 104). Therefore, stimulation of group I mGluRs leads to an increased open channel probability of NMDARs, which results in an increase in intracellular calcium levels (78, 94). Therefore, activation of group I mGluRs can lead to both increased calcium release and neurotoxic effects and activation of neuroprotective pathways such as the PI3K/Akt and MAPK pathways. Modulation of group I mGluRs as a therapeutic approach to HD is therefore a complex task. In order to be most effective, it would likely need to involve selectively activating the neuroprotective pathways while inhibiting neurotoxic effects.

Recent studies have emerged supporting a role for the modulation of mGluR5 as a therapeutic approach to HD. mGluR5 is located in various brain regions, including, but not limited to, the cerebral cortex, the hippocampus, and the striatum (109-111). Interestingly, while mGluR5 is expressed highly in neurons of the striatum, the expression of mGluR1 in striatal neurons is negligible (112). Since the striatum is heavily affected in HD, modulation of mGluR5 signaling is an attractive therapeutic approach. The extent to which the modulation of mGluR5 would be most beneficial for the treatment of HD remains to be determined. Some studies provide evidence for the use of positive allosteric modulators (PAM), while others provide evidence for the use of negative allosteric modulators (NAM).

A study by Doria *et al.* demonstrated that the use of mGluR5 PAMs [(3-Fluorophenyl)methylene]hydrazine-3-fluorobenzaldehyde (DFB), *N*-[1-(2-Fluorophenyl)-3-phenyl-1H-pyrazol-5-yl]-4-nitrobenzamide (VU1545), and 3-Cyano-*N*-(1,3-diphenyl-1*H*-pyrazol-5-yl) benzamide (CDPPB) in *in vitro* striatal neuronal cultures led to the activation of neuroprotective pathways, such as the Akt pathway which promotes cell survival, without activating neurotoxic pathways which lead to increased intracellular calcium release (113). Conversely, the group I mGluR agonist (*S*)-3,5-Dihydroxyphenylglycine (DHPG) is also able to activate Akt, but, unlike the PAMs, its

use led to an increase in intracellular calcium levels. The mGluR PAMs were found to be neuroprotective under various conditions, such as with and without the presence of glutamate, and in the presence of NMDA, while DHPG was neuroprotective only with the presence of glutamate, but neurotoxic without it. This suggests that PAMs may be more therapeutically effective than agonists in the treatment of neurodegenerative diseases, as they do not activate neurotoxic signaling. The activation of Akt and prevention of an increase in intracellular calcium levels was found to be more pronounced in striatal neuronal cultures from BACHD mice (an HD mouse model) treated with the mGluR5 PAM VU1545 as opposed to those from WT mice treated with VU1545. In addition, the treatment of BACHD mice with CDPPB was found to improve the memory deficit present in these mice, demonstrating the potential therapeutic effectiveness of mGluR5 PAMs in the treatment of HD.

A follow-up study by Doria *et al.* further investigating the use of the mGluR5 PAM CDPPB *in vivo* provided more evidence supporting the potential use of mGluR5 PAMs in the treatment of HD (114). Treatment of BACHD mice with CDPPB was associated with the activation of the Akt and MAPK neuroprotective pathways, and with an increase in BDNF mRNA expression. BACHD mice develop htt aggregates and exhibit neuronal cell loss; treatment with CDPPB prevented this. Furthermore, CDPPB treatment was able to effectively rescue memory deficits and partially improve motor incoordination in BACHD mice. This study provides evidence for the correlation between activation of neuroprotective pathways and improvement of HD symptoms as a result of CDPPB treatment, supporting the potential for the use of CDPPB in the treatment of HD.

Conversely, a study by Abd-Elrahman *et al.* found that the mGluR5 NAM 2-chloro-4-[2-[2,5-dimethyl-1-[4-(trifluoromethoxy)phenyl]imidazole-4-yl]ethynyl]pyridine (CTEP) may be beneficial in the treatment of HD (115). In an *in vivo* mouse model of HD, the zQ175 model, the use of CTEP was associated with improved cognitive and motor function. This was correlated with the activation of the cellular clearance pathway autophagy, reduction of caspase-3 activity, reduced neuronal apoptosis, prevention of neuronal cell loss, and reduction of htt aggregates. Taken together, these results suggest

that CTEP may represent a novel therapeutic approach in the treatment of HD. Interestingly, similar results were observed in mouse models of AD treated with CTEP. Hamilton *et al.* have shown that chronic treatment of APPswe/PS1ΔE9 and 3xTg-AD male mice with CTEP caused a marked reduction in beta-amyloid (Aβ) plaque deposition and in levels of soluble Aβ oligomers (116). This was associated with an improvement in cognitive function. Lastly, treatment of the 6-OHDA-Toxicant PD model with CTEP promoted neurorecovery and thus may provide therapeutic benefit in PD (117). Taken together, these studies suggest that the mGluR5 NAM CTEP may be effective for the treatment of not only HD, but also AD and PD.

A study by Schiefer *et al.* investigated the effects of activation of mGluR2 (which acts to limit presynaptic glutamate release) and inhibition of mGluR5 (whose activation can lead to increased intracellular calcium levels) in the R6/2 transgenic mouse model of HD (118). Treatment with the mGluR2 agonist LY379268 or the mGluR5 antagonist 2-methyl-6-(phenylethynyl)-pyridine (MPEP) resulted in increased survival time; however, only MPEP treatment resulted in an improvement in motor deficits. This study suggests targeting of different mGluRs, perhaps even a combination therapy targeting multiple mGluRs, may improve HD symptoms.

Targeting glutamate excitotoxicity in HD is an attractive potential therapeutic approach for the treatment of HD. While activation of ionotropic glutamate receptors likely plays a critical role in HD neuronal cell loss, inhibition of these receptors also leads to many toxic effects (4, 139, 140). These toxic effects have led to the failure of agents which block these receptors in clinical trials (4, 139, 140). To this end, agents which modulate metabotropic glutamate receptor signaling may represent alternative therapeutic approaches. Group I mGluRs do not play an excitatory role in neurotransmission, rather, they play a modulatory role (4). Thus, their modulation represents an attractive therapeutic approach. Given that mGluR5 is highly expressed in the striatum, which is heavily affected in HD, and there is almost no mGluR1 expressed in the striatum, mGluR5 modulation

may be more therapeutically relevant than mGluR1 modulation for the treatment of HD (112). Several studies have investigated the modulation of the group I mGluR, mGluR5, in HD models. These studies have been somewhat conflicting, with some supporting the use of mGluR5 PAMs, and others supporting the use of mGluR5 NAMs for the treatment of HD. Therefore, the role of mGluR5 in HD pathogenesis and its potential as a therapeutic target is complex, and requires further investigation.

1.3 Autophagy

Autophagy is an evolutionarily conserved, intracellular, catabolic process responsible for the degradation of damaged organelles, misfolded protein aggregates, and other cellular debris (121). The end-products of autophagy can then be recycled and used in various biosynthetic pathways and to generate energy (122, 123). It is vital for the maintenance of proteostasis in the central nervous system (CNS) (7). Depending on cellular conditions, autophagy, which occurs in neurons at a basal homeostatic rate, can be upregulated (i.e. during times of cellular stress or nutrient starvation) or downregulated (i.e. when nutrients are abundant) (124).

Three types of mammalian autophagy have been identified/characterized to date: microautophagy, chaperone-mediated autophagy (CMA), and macroautophagy (MA). All three types of autophagy utilize the lysosome for degradation of autophagic cargo; however, they differ in terms of the cargo they are responsible for targeting to the lysosomes (125). Both microautophagy and MA can be non-specific, in that they simply take up cytoplasm (126), and they can be specific by targeting specific cargo for degradation. Conversely, CMA is always highly specific (127).

In microautophagy, cytosolic cargo is taken up directly into the lysosome via invaginations in the lysosomal membrane (126, 128). In CMA, proteins containing the pentapeptide sequence KFERQ are bound by the heat shock 70 kDA protein 8 (HSPA8/HSC70) and several co-chaperones and targeted to the lysosomal membrane, where they are unfolded (129, 130). The translocation complex required for the translocation of the cargo across the lysosomal membrane occurs when multimerization of the

lysosomal-associated membrane protein 2A (LAMP2A) is triggered by the binding of cargo to the monomeric form of LAMP2A (131, 132). After translocation of the cargo across the lysosomal membrane, the cargo is degraded and the translocation complex dissociates (132).

Upon induction of MA, a double membrane structure termed the phagophore begins to form (133). The phagophore expands and curves around the cargo until a closed spherical structure referred to as an autophagosome forms (126, 134). The autophagosome is trafficked towards a lysosome, which it then fuses with to form an autolysosome, which promotes the degradation of the cargo present in the autophagosome by lysosomal enzymes (126, 135, 136) (Figure 1.2). MA may also converge with the endolysosomal pathway – in this case, autophagosomes fuse with endolysosomes to form amphisomes, and amphisomes then fuse with lysosomes (126, 137, 138). A wide variety of proteins, many of which belong to the family of autophagy-related genes (ATG), are involved in the stages of MA.

In mammalian MA, the initiation of MA (in which the phagophore begins to form) is regulated by a group of proteins termed the induction complex (133). The induction complex is composed of the Unc-51-like kinase family (ULK1/ULK2), ATG13, C12orf44, and RB1-inducible coiled-coil (RB1CC1/FIP200) (126, 139-141). Once the induction complex has been recruited and activated, the vps34 complex, critical for autophagosome biogenesis, is recruited to the developing phagophore (142). This complex is composed of beclin-1, ATG14, phosphatidylinositol 3-kinase catalytic subunit type 3 (PIK3C3), and phosphatidylinositol 3-kinase regulatory subunit 4 (PIK3R4/vps34) (124, 126, 143-147). The vps34 complex is vital for autophagosome formation because it mediates the production of phosphatidylinositol 3-phophate (PI3P) lipids, which are crucial for phagophore formation (124, 126, 148, 149). ULK1 plays an important role in regulating the induction complex. It phosphorylates both beclin-1 and ATG14 to promote formation of the vps34 complexes (124). The phosphorylation of beclin-1 allows it to dissociate from Bc12, an antiapoptotic protein, thereby allowing it to interact with PIK3C3, promoting induction of autophagy (124, 150, 151). The

phosphorylation of ATG14 enhances its binding with beclin-1, further promoting formation of the vps34 complexes critical for autophagosome biogenesis and induction of autophagy. (124, 151).

The WD Repeat Domain Phosphoinositide Interacting 2 protein (WIPI2), bound to PI3P lipids, recruits the conjugation complex (composed of ATG5, ATG12, and ATG16), which is needed for elongation/expansion of the phagophore (124, 126, 152, 153). For expansion of the phagophore to occur, proteins belonging to the ATG8-like family of proteins are required (such as microtubule-associated protein 1A/1B-light chain 3 (LC3)) (126, 154). LC3 is processed at its C terminus by ATG14, resulting in the formation of cytosolic LC3-I (124, 126). This LC3-I form can then be converted into LC3-II, which is covalently conjugated with phosphatidylethanolamine (PE) on the expanding phagophore (it is also found on mature autophagosome membranes) (124, 126, 154). Conversion of LC3-I into LC3-II is increased during stressful conditions such as nutrient starvation (155). The conjugation complex and the ATG-8 like family of proteins function to allow for the full expansion of the developing phagophore into a mature autophagosome.

In neurons, autophagosomes are trafficked from neurites to the soma, where lysosomes typically reside (7). Therefore, microtubules are vital for the transportation/trafficking of the autophagosome and its fusion with the lysosome (156-158). Several proteins have been proposed to be critical for autophagosome-lysosome fusion. These include LC3, UV radiation resistance-associated gene protein (UVRAG), Rubicon, GTPase Rab7, and several soluble N-ethylmaleimide-sensitive factor attachment protein receptors (SNAREs). A study by Kimura *et al.* revealed that LC3 likely plays a key role in autophagosome trafficking, as inhibition of LC3 prevents this trafficking from occurring (159). UVRAG is believed to promote fusion of autophagosomes with lysosomes via the activation of GTPase Rab7 (present on lysosomes and, through an interaction with FYVE and Coiled-Coil Domain Autophagy Adaptor 1 (FYCO1), mediates trafficking of autophagosomes along microtubules) (160, 161), whereas Rubicon is believed to inhibit fusion by binding to UVRAG (162). However, while some studies support a role for UVRAG in fusion, others have reported that UVRAG is not involved

in fusion (163, 164). Further work will be needed to determine whether UVRAG is important in fusion. Lastly, several SNARE proteins have been identified as playing a role in fusion. The Qa-SNARE syntaxin 17 (STX17) and the Qbc-SNARE SNAP29 (SNAP29) form a complex that is bound by ATG14L to promote its interaction with R-SNARE Vamp8 (Vamp8) to promote autophagosome-lysosome fusion (160, 165). In addition to the ATG14L-STX17 interaction playing a role in fusion, their interaction also plays a role in initiation of MA (160). This supports a role for ATG14L in autophagosome-lysosome fusion, in addition to its role in autophagosome biogenesis.

MA is regulated by a variety of extracellular and intracellular conditions (167-174). Important regulators of MA include the mechanistic target of rapamycin complex 1 (mTORC1), 5'-AMP-activated protein kinase (AMPK), and cAMP-dependent protein kinase A (PKA). mTORC1, AMPK, and PKA all regulate MA in response to cellular conditions (124, 126). Under nutrient rich conditions, mTORC1 phosphorylates ULK1/2 and ATG13 of the induction complex, inactivating them and inhibiting induction of autophagy (124, 175, 176). Conversely, during nutrient starvation, hypoxia, and the absence of growth factors, mTORC1 dissociates from the induction complex, ULK1/2 and ATG13 are dephosphorylated, and induction of MA occurs (126, 177, 178). Also during nutrient rich conditions, PKA acts to inhibit induction of MA (126, 179). It is believed to do so by phosphorylating and activating MTORC1, by phosphorylating and inhibiting LC3, and by inhibiting AMPK. (126, 179-181). The major energy sensing kinase of the cell is AMPK – it is sensitive to AMP/ATP levels in the cell (182, 183). When energy levels in the cell are low, as marked by an increase in AMP levels, AMPK is activated, and phosphorylates and activates the TSC1/2 complex which inhibits mTORC1, and directly inhibits mTORC1, thereby activating induction of MA (125, 184-186). When energy levels in the cell are high, as marked by an increase in ATP levels, AMPK is inactivated, and induction of MA is inhibited (185). AMPK also responds to glucose levels and, in times of glucose starvation, it phosphorylates ULK1/2 (an activating phosphorylation) and inhibits mTORC1 both directly and indirectly via chaperones to activate induction of MA (176, 187). AMPK can also be activated by

Calcium/Calmodulin Dependent Protein Kinase Kinase 2 (CaMKK2/CaMKKβ) in response to ER stress (results in an increase in cytosolic calcium levels) in order to activate the induction of MA (188). Therefore, it is clear that MA is regulated by many proteins which in turn are regulated by a myriad of cellular conditions.

MA can be non-specific in its degradative role (i.e. bulk degradation induced by certain cellular conditions) (166). In addition, it can also be highly selective whereby specific cargo is targeted for degradation (166). Selective MA is critical for cellular homeostasis. Selective MA which degrades misfolded protein aggregates is known as aggrephagy (15, 166). In mammalian MA, selectivity is mediated by the binding of cargo receptors to specific cargo (either directly or to polyubiquitin chains present on cargo) and to LC3 via LC3-interacting region(s) (LIR) (166, 172, 189). Examples of cargo receptors containing LIR domains include, but are not limited to, SQSTM1/p62, optineurin, and ATG19. Discovered in 2007, p62 is a widely used marker of MA (189, 190). In the case of p62, it binds to ubiquitinated cargo, such as misfolded protein aggregates, and it targets this cargo to the autophagosome via an interaction between its LIR domain and LC3-II present on autophagosome membranes (189, 190). When autophagy is active, p62 is degraded along with its cargo, and when autophagy is inactive, p62 levels remain high, thus allowing the use of p62 as a marker of MA activation (191). Aggrephagy is critical for the maintenance of proteostasis, as it is critical for the degradation of misfolded protein aggregates (15, 171, 189, 192-194).

Recently, a novel pathway of MA regulation dependent on glycogen synthase kinase 3 beta (GSK3β) has been identified and described (115, 195). Briefly, stimulation of GPCRs results in an inhibitory phosphorylation at the serine 9 (S9) site in glycogen synthase kinase 3 beta (GSK3β) (195). This inhibitory phosphorylation prevents GSK3β from phosphorylating zinc finger and BTB domain-containing protein 16 (ZBTB16), a component of the ZBTB16-Cullin3-Roc1 E3 ubiquitin ligase complex, at the S184 and T282 sites (195). This allows ZBTB16 to interact with ATG14L, a

component of the vps34 complex responsible for autophagosome formation, and to ubiquitinate it (195, 196). This ubiquitination of ATG14L leads to its degradation, thus leading to the inhibition of autophagy (195). When GSK3β is not phosphorylated at the S9 site, it is able to phosphorylate ZBTB16 at the S184 and T282 sites and prevent it from interacting with ATG14L. This inhibitory phosphorylation of ZBTB16 leads to the auto-ubiquitination and degradation of ZBTB16, meaning ATG14L will not be degraded and will form vps34 complexes, and autophagy will be induced (195).

Given the role of MA in maintaining cellular homeostasis, and its regulation by various extracellular and intracellular conditions/signals, it is unsurprising that dysregulation of MA has been implicated in many human diseases, including various cancers, diabetes, heart disease, and neurodegenerative diseases (126, 189, 197). Therefore, selective targeting of MA may represent an attractive therapeutic approach to several human diseases in which its dysregulation is observed.

1.4 Macroautophagy in Huntington's Disease

Neurons are particularly sensitive to changes in the cellular environment, and tight regulation of cellular homeostasis is critical for their functioning and survival. Autophagy plays a critical role in cellular homeostasis (121). Since neurons are post-mitotic and non-dividing cells, they cannot simply use cell division to manage the accumulation of toxic protein aggregates and cellular debris; they rely on autophagy to tolerate this (7, 198). Hence, basal levels of autophagy are always present in healthy neurons, and can change depending on external conditions/signals, including neuronal excitotoxicity and nutrient starvation (7, 121, 123, 199-201). In HD, the accumulation of toxic misfolded Htt aggregates is associated with the degeneration of neurons. Several deficits in aggrephagy have been observed in HD, preventing the clearance of these aggregates and allowing their accumulation (200, 202-204).

There are two major degradative pathways in neurons – the UPS and autophagy (189, 205). Of the three types of autophagy (MA, CMA, and microautophagy), MA and CMA are active in neurons; however, it remains to be seen whether microautophagy is active in neurons (7, 189). Poly-ubiquitinated proteins can be targeted to the UPS for degradation. These soluble ubiquitinated proteins are unfolded in order to pass through the proteasome structure (189). Similar to the UPS, CMA requires proteins that can be unfolded for degradation (126, 189, 206). Therefore, both the UPS and CMA are restricted to proteins which can be unfolded, thereby hindering their abilities to degrade aggregated proteins like those found in HD (126, 189, 206). Aggrephagy (MA), however, does not require protein unfolding for degradation, and is therefore better able to handle misfolded aggregates (189, 207, 208). As such, in trying to maintain proteostasis, neurons may try to compensate for defective UPS by upregulating MA (189, 207, 208).

WT Htt has been proposed to play a role as a scaffold protein in selective MA (15, 54, 64, 65, 209). Essentially, Htt is believed to play a role in MA initiation and cargo recognition by mediating binding between p62 and ULK1 (15, 65, 2010). ULK1 phosphorylation of p62 promotes MA and clearance of mHtt (210, 211). Further supporting a role for Htt in MA, are the findings that the accumulation of protein (impaired proteostasis) correlated with the loss of Htt in the mouse CNS, and the loss of Htt function results in the accumulation of autophagosomes and impairment of retrograde transport of autophagosomes (15, 212-214). Therefore, mHtt may contribute to MA dysfunction in several manners: (i) impaired cargo recognition, possibly through an aberrant interaction with p62 (can lead to the production of empty autophagosomes), (ii) sequestering of mTORC1 and beclin-1 (inhibiting their activity), (iii) impaired autophagosome trafficking and fusion with lysosomes, and (iv) binding to ubiquitinated proteins and organelles to prevent their recognition and degradation by MA (in the case of impaired mitochondria recognition, this can result in metabolic deficits and reactive oxygen species production observed in HD) (7, 15, 54, 194, 215-219) (Figure 1.2).

Mitophagy is a special type of selective MA responsible for mitochondrial turnover. As neurons age, it has been posited that mitochondrial turnover becomes less efficient, causing an increase in oxidative stress, damaging lysosomes and leading to impaired MA and UPS function (220). At first, the UPS and MA can deal with this proteotoxic stress, and proteostasis remains intact in neurons. Eventually, the stress becomes too much for the UPS and MA to handle, and it is at this point that mHtt aggregates are believed to accumulate (7). Thus, less efficient mitophagy may contribute to deficits in aggrephagy, leading to the accumulation of mHtt aggregates. Therefore, deficits in MA may help to explain why HD onset is typically observed during midlife and not from birth (7).

HD mouse models have revealed deficits in proteostasis related to dysfunctional autophagy (215). For example, increased LC3-II and p62 have been observed in the striatum of HD transgenic mice (221). This suggests that selective regulation of aggrephagy may represent a beneficial therapeutic approach in the treatment of HD. Indeed, in *Drosophila*, cell, and mouse models of HD, mTOR inhibitors (which induce autophagy), have been shown to lead to clearance of mHtt fragments, decrease polyQ aggregate formation, and decrease cytotoxicity (15, 194, 222). In mouse models of HD, AMPK activators (induce autophagy), have shown similar beneficial effects as those listed for mTOR inhibitors (15, 223-226). Specifically, treatment of HD mouse models with the mTOR inhibitor CCI-779 (a rapamycin analog) and the AMPK activator trehalose, lead to a decrease in polyQ aggregates, and an improvement in motor function (7, 194, 226). This supports the notion of regulation of aggrephagy in the treatment of HD.

GPCRs respond to external signals and are responsible for the regulation of a large number of cellular processes, including autophagy (195, 227, 228). The relationship between GPCRs and aggrephagy may be of therapeutic significance. When a global inhibitor of GPCRs, ADM1300, was administered to a mouse model of HD, a decrease in the number of huntingtin aggregates was correlated with the activation of aggrephagy, as shown by a decrease in p62 levels (195). This activation of aggrephagy correlated with a decrease in ZBTB16, an increase in ATG14L, and an improvement in disease

symptoms (195). However, since GPCRs are important for the regulation of many cellular processes, global inhibition is not a viable therapeutic strategy. Identification of specific GPCRs involved in the regulation of aggrephagy remains critical. To this end, mGluR5, a member of the mGluR I family, has been identified.

A recent study by Abd-Elrahman *et al.* has revealed that chronic blockade of mGluR5 in the zQ175 mouse model of HD with CTEP (an mGluR5 NAM) is correlated with an increase in induction of the GSK3β-ZBTB16 pathway of MA (115). This correlated with a decrease in the size and number of huntingtin aggregates, and an improvement in HD-related symptoms (115). Inhibition of mGluR5 prevents the inhibitory phosphorylation of GSK3β, leading to the inhibitory phosphorylation of ZBTB16, resulting in the induction of aggrephagy (Figure 1.3). This increase in the induction of aggrephagy was correlated with improvements in cognitive and motor deficits in the HD mouse model (115). Similar results have also been observed in the APPsew/PS1ΔE9 and 3xTg-AD mouse model of AD. It has been found that in these mouse models of AD, there is an increase in the surface expression of mGluR5 which correlates with decreased induction of MA (229). When mGluR5 was inhibited by CTEP, the number of amyloid beta aggregates and the surface expression of mGluR5 decreased (229). This correlated with a loss of ZBTB16 expression and induction of aggrephagy, as indicated by a decrease in p62 levels (229). Taken together, the results of these studies indicate that mGluR5 plays a significant role in the regulation of the GSK3β-ZBTB16-Cullin3-Roc1 E3 ubiquitin ligase pathway of MA, and that targeting this pathway may be of therapeutic significance in not only HD, but also in AD (Figure 1.3).

It remains unknown whether ATG14L and ZBTB16 are direct effectors of mGluR5, and the specific identities and roles of all the proteins involved in this pathway require additional elucidation. The mechanism by which mGluR5 mediates this pathway of aggrephagy also needs further investigation. The mouse studies of chronic blockade of mGluR5 do not elucidate the mechanism by which mGluR5

regulates aggrephagy. These studies do not show a direct link between ATG14L and ZBTB16, and mGluR5 signaling (Figure 1.3). Understanding the mechanism by which mGluR5 regulates the GSK3β-ZBTB16-Cullin3-Roc1 E3 ubiquitin ligase pathway of autophagy is crucial in order to further our understanding of the role of aggrephagy in neurodegenerative diseases, and to determine whether targeting aggrephagy could represent a viable therapeutic approach.

Hypotheses

1. ATG14L is critical for the activation of aggrephagy. ZBTB16 is critical for the inhibition of aggrephagy.
2. ATG14L and ZBTB16 are direct effectors of mGluR5-mediated regulation of aggrephagy.

Objectives

1. Employ CRISPR Cas9 to knockout ATG14L and ZBTB16 in mouse striatal cells (STHdhQ7/Q7).
2. Explore the impact of an ATG14L knockout and a ZBTB16 knockout on mGluR5-mediated regulation of aggrephagy.

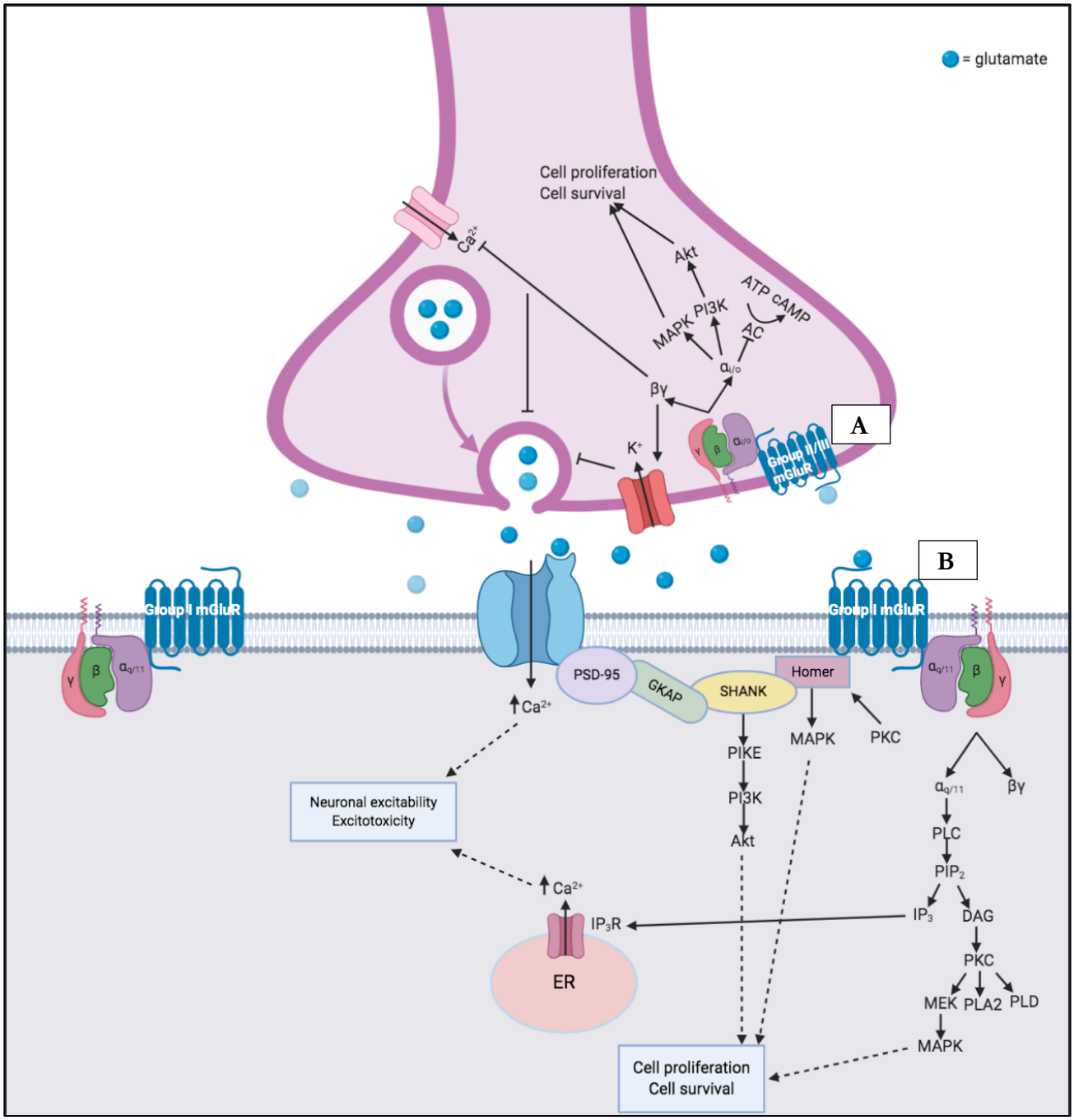
= glutamate
Cell proliferation
Cell survival
Akt
ATP cAMP
MAPK PI3K
AC
$\alpha_{i/o}$
βγ
Ca^{2+}
K^+
A
Group II/III mGluR
B
Group I mGluR
Group I mGluR
$\alpha_{q/11}$
β
γ
PSD-95
GKAP
SHANK
Homer
MAPK
PKC
PIKE
PI3K
Akt
Neuronal excitability
Excitotoxicity
Ca^{2+}
IP_3R
ER
$\alpha_{q/11}$
βγ
PLC
PIP_2
IP_3
DAG
PKC
MEK
PLA2
PLD
MAPK
Cell proliferation
Cell survival

Figure 1.1 Group I, II, and III mGluR signaling cascades.

A) Stimulation of group II/III mGluRs triggers the uncoupling of the $G\alpha_{i/o}$ subunit from the $\beta\gamma$ subunits. $G\alpha_{i/o}$ inhibits AC, preventing the conversion of ATP into cAMP. The PI3K/Akt and MAPK neuroprotective pathways are also activated by $G\alpha_{i/o}$ upon mGluR II/III stimulation. The $\beta\gamma$ subunits inhibit voltage-gated Ca^{2+} channels, thus decreasing intracellular calcium levels, and stimulates GIRK channels, promoting influx of K^+; these actions decrease presynaptic glutamate release. B) Stimulation of group I mGluRs triggers the uncoupling of the $G\alpha_{q/11}$ subunits from the $\beta\gamma$ subunits. The $G\alpha_{q/11}$ subunits activate PLC, which cleaves PIP_2 into DAG and IP_3. DAG activates PKC, which activates MEK, PLA2, and PLD. MEK activates MAPK, which promotes cell proliferation and survival. IP_3 sensitizes IP_3R on the ER, resulting in an increase in intracellular Ca^{2+} levels, which can increase neuronal excitability and promote neurotoxicity during excitotoxic conditions. Group I mGluRs associate with Homer proteins, which associate with SHANK proteins. The Homer-SHANK interaction allows group I mGluR stimulation to activate PIKE, which activates the PI3K/Akt neuroprotective pathway, and can activate the MAPK neuroprotective pathway. Homer proteins interact with a scaffolding complex composed of SHANK proteins, GKAP, and PSD-95 that associates with NMDARs. This allows group I mGluRs to modulate NMDARs. Thus activation of group I mGluRs promotes opening of NMDARs, resulting in an increase in intracellular Ca^{2+} levels, which can increase neuronal excitability and toxicity under excitotoxic conditions.

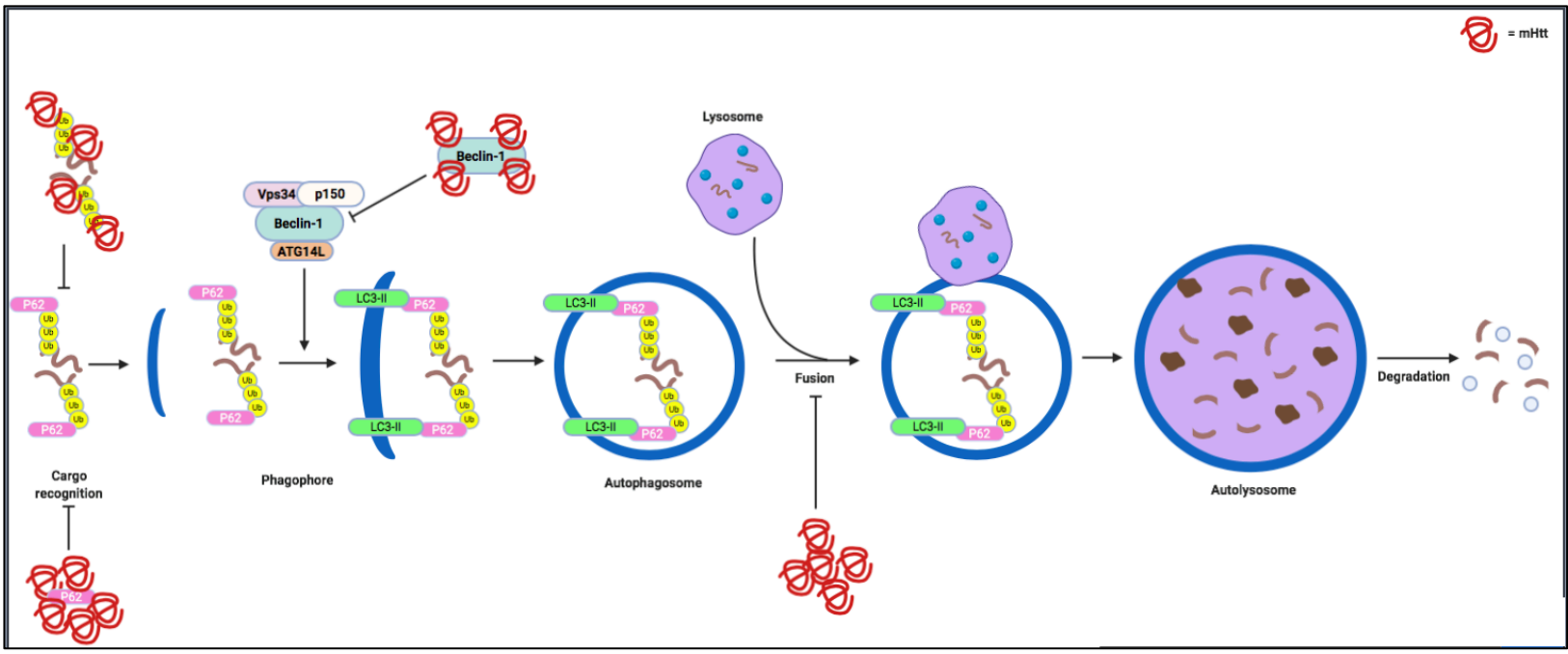
= mHtt
Lysosome
Beclin-1
Vps34
p150
Beclin-1
ATG14L
P62
Ub
LC3-II
Cargo recognition
Phagophore
Autophagosome
Fusion
Autolysosome
Degradation

Figure 1.2. Major steps of selective macroautophagy and the effects of mutant huntingtin.

A cargo receptor (p62 is used in this schematic) recognizes and binds to ubiquitinated cargo. Upon initiation of MA, the phagophore, a double membrane organelle, begins to form. The cargo receptor targets the ubiquitinated cargo to the phagophore via an interaction with LC3-II present on the phagophore membrane. The phagophore continues to elongate around the cargo until it forms a closed, spherical vesicle known as an autophagosome. The autophagosome is trafficked towards lysosomes, and fuses with lysosomes to form an autolysosome. This allows for the degradation, via lysosomal enzymes, of the cargo present in the autophagosome. The degradation products may be utilized to generate energy or recycled into various biosynthetic pathways. mHtt can interfere with MA in several manners: it can impair cargo recognition via an aberrant interaction with p62, it can interact with ubiquitinated proteins to prevent their recognition by cargo receptors, it can sequester beclin-1, a component of the vps34 complexes, and it can impair autophagosome trafficking and fusion with lysosomes.

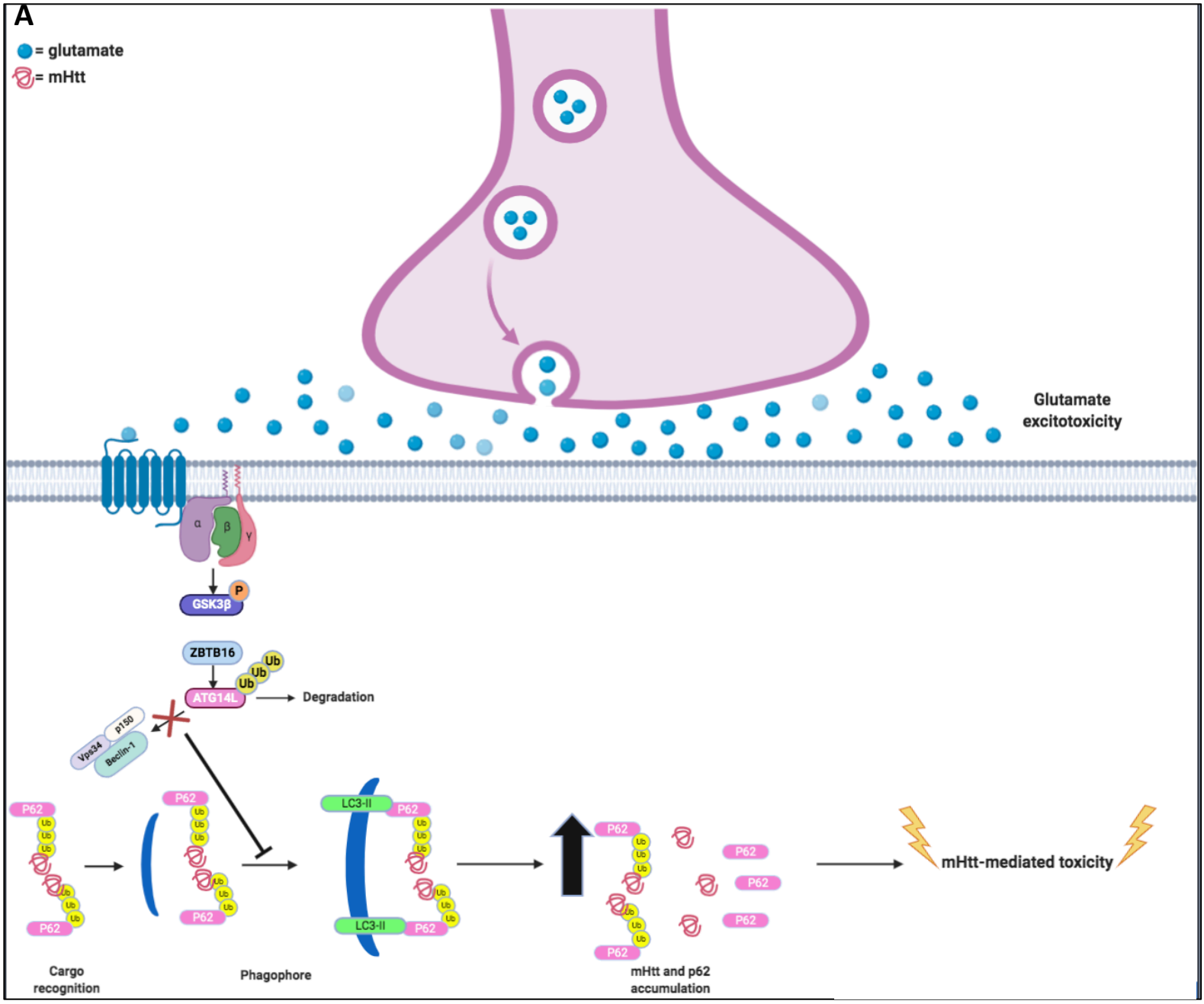
A
= glutamate
= mHtt
Glutamate excitotoxicity
α
β
γ
GSK3β
P
ZBTB16
Ub
ATG14L
Degradation
p150
Vps34
Beclin-1
P62
LC3-II
Cargo recognition
Phagophore
mHtt and p62 accumulation
mHtt-mediated toxicity

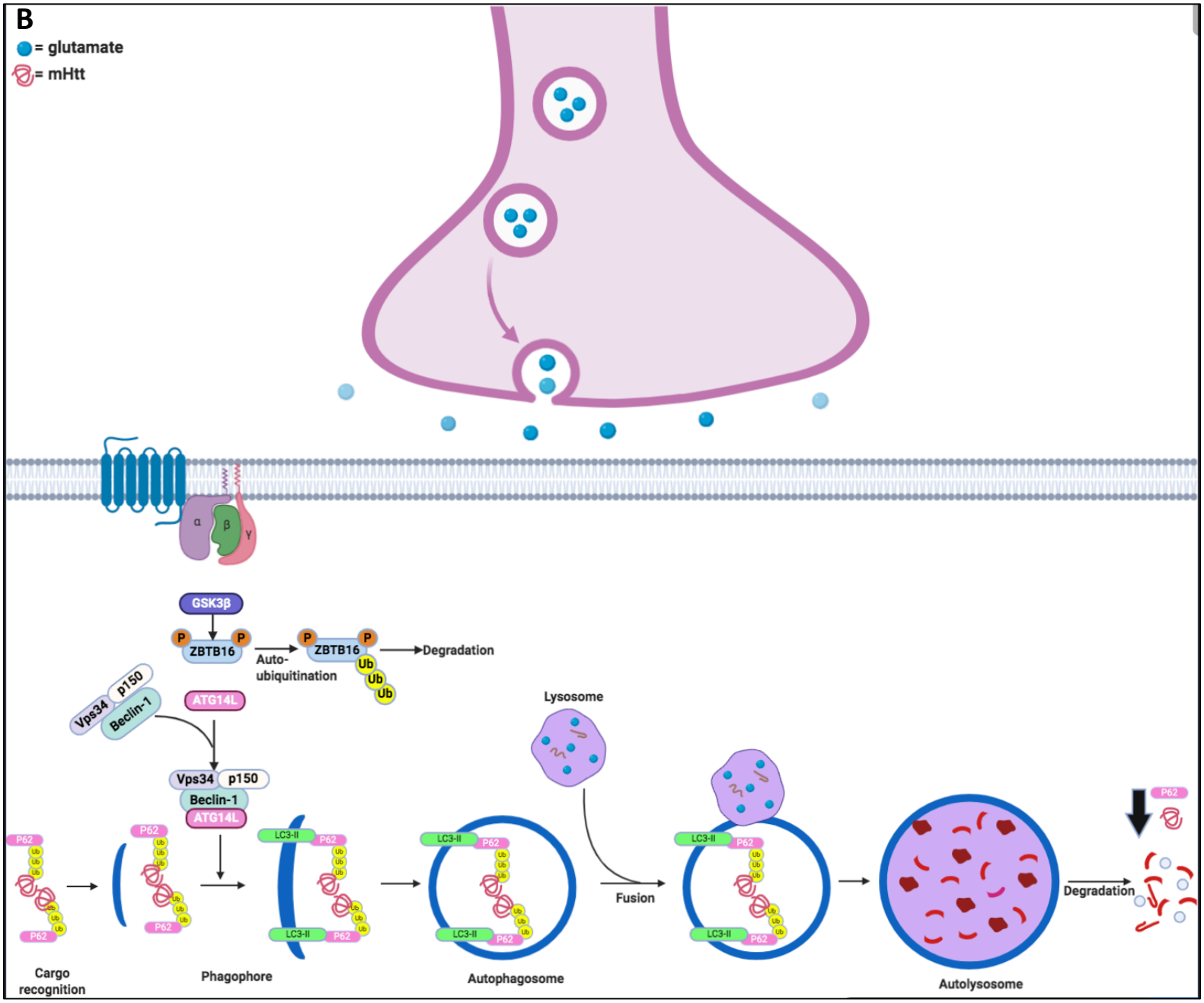
B
= glutamate
= mHtt
α
β
γ
GSK3β
P
ZBTB16
Auto-
ubiquitination
Ub
Degradation
Vps34
p150
Beclin-1
ATG14L
Lysosome
P62
LC3-II
Cargo
recognition
Phagophore
Autophagosome
Fusion
Autolysosome
Degradation

Figure 1.3. mGluR5-mediated regulation of aggrephagy in HD.

A) Stimulation of mGluR5 results in the inhibitory phosphorylation at the S9 site of GSK3β. This inhibitory phosphorylation of GSK3β prevents it from phosphorylating ZBTB16, a component of the ZBTB16-Cullin3-Roc1-E3 ubiquitin ligase complex, at the S184 and T282 sites. ZBTB16 is therefore able to interact with ATG14L and ubiquitinate it, leading to the degradation of ATG14L. Thus, ATG14L will not be present to form vps34 complexes needed for autophagosome formation. This results in the inhibition of MA, as shown by an increase in p62 (cargo receptor and a marker of autophagy) levels. This inhibition of aggrephagy is believed to result in the accumulation of mHtt aggregates. B) When mGluR5 is not stimulated (or inhibited by either an antagonist or a NAM), GSK3β remains unphosphorylated and active. GSK3β phosphorylates ZBTB16 at the S184 and T282 sites, preventing the interaction of ZBTB16 with ATG14L and leading to the auto-ubiquitination and subsequent degradation of ZBTB16. ATG14L is thus able to form vps34 complexes, and MA occurs, as marked by a decrease in p62 levels. This activation of aggrephagy is believed to play a role in the clearance of mHtt aggregates.

Chapter 2: Materials and Methods

2.1 Reagents

CRISPR Cas9 guide primers (Invitrogen), PCR primers (Invitrogen), DH5α Competent Cells, Subcloning Efficiency™, 40 (Invitrogen 18265017), and phire green hot start II PCR master mix (F126S) were obtained from Thermo Fisher Scientific. BBSI restriction enzyme (R0539L) and NEB Buffer 2.1 were obtained from New England Biolabs. T4 rapid DNA ligase and T4 rapid DNA ligase buffer (MRL-100) were obtained from Benchmark Bioscience. Polyethylenimine (PEI) was obtained from the laboratory of Dr. Ryan Russell (University of Ottawa). Ampicillin (AMP201.5) and kanamycin (KAN201.25) were obtained from Cedarlane Labs. QIAprep Spin Miniprep Kit (27106) was obtained from Qiagen. (S)-3,5-Dihydroxyphenylglycine (DHPG) (0805) was obtained from Cedarlane Labs (Tocris). 2-chloro-4-[2-[2,5-dimethyl-1-[4-(trifluoromethoxy)phenyl]imidazole-4-yl]ethynyl]pyridine (CTEP) (Axon 1972) was obtained from Axon Med Chem. Western blot reagents were obtained from Bio-rad. Antibodies and where they were obtained are listed in Table 2.1. All other biochemical reagents were obtained from sigma-aldrich.

Antibody	Catalogue Number	Company
Mouse anti-SQSTM1/p62	ab56416	Abcam
Rabbit anti-Plzf	ab39354	Abcam
Rabbit anti-Vinculin (EPR8185)	ab129002	Abcam
Rabbit anti-ATG14 (Human) pAb (MBL)	PD026	Cedarlane Labs
Mouse anti-polyQ specific Antibody, clone MW1	MABN2427	EMD Millipore
Rabbit anti-Metabotropic Glutamate Receptor 5	AB5675	MilliporeSigma
Rabbit anti-Beclin-1 [D40C5]	3495S	New England Biolabs
Rabbit anti-Phospho-Beclin-1 (Ser15)[D4B7R]	84966S	New England Biolabs
Rabbit anti-Phospho-GSK3β (Ser9) [5B3]	9323S	New England Biolabs
Mouse anti-GSK3β (3D10)	9832S	New England Biolabs
Rabbit anti-LC3B	NB100-2220	Novus Biologicals
Rabbit anti-GFP tag	A-6455	Thermo Fisher Scientific
Goat anti-mouse IgG (H+L), HRP (Invitrogen)	G21040	Thermo Fisher Scientific
Goat-anti-rabbit IgG (H+L) Cross-Adsorbed Secondary	G-21234	Thermo Fisher Scientific

Table 2.1. Antibodies used for western blot analysis

2.2 Plasmids and constructs

pSpCas9(BB)-2A-Puro (PX459) V2.0 (plasmid #62988) was obtained from addgene. Q15 and Q138 huntingtin constructs (both YFP tagged) were obtained from the laboratory of Dr. Ray Truant (McMaster University).

2.3 Cell culture

The immortalized mouse striatal neuron cell line STHdhQ7/Q7 was obtained from the laboratory of Dr. Ray Truant (McMaster University). Cells were cultured in Dulbecco's Modified Eagle Medium

(DMEM, 1x, 4.5g/L glucose, with L-glutamine, sodium) supplemented with 10% fetal bovine serum (FBS).

2.4 Transfection

For the CRISPR Cas9 plasmid transfection, cells were seeded into 10 cm dishes at approximately 40%-50% confluency 18 hours prior to transfection. For Q15 and Q138 experiments, cells were seeded into 6 well plates at approximately 30%-40% confluency 18 hours prior to transfection. All experiments were performed 48 hours post transfection. Transfections were carried out using the transfection reagent PEI. The protocol used was obtained from the laboratory of Dr. Ryan Russell (University of Ottawa). Briefly, for each well of a 6 well plate to be transfected, 200 μL of warm DMEM (no FBS added), 1 μg of DNA to be transfected, and PEI (used at a 1:4 ratio of DNA:PEI) are mixed and incubated for approximately 30 minutes at room temperature. The media in the 6 well plate was changed, and the transfection mixture was added to the appropriate well. Transfection was checked with the EVOS® FL Cell Imaging System.

2.5 Generation of CRISPR Cas9 guide RNAs

CRISPR Cas9 guides were designed using the crispr mit edu software (formerly http://crispr.mit.edu, no longer exists today) to target the first exon of the ATG14L gene and the ZBTB16 gene, respectively, in *Mus musculus*. The first exon was chosen as it is present in all known isoforms of the genes. Two pairs of guides with the highest efficiency and lowest probability of off-target effects were selected for each guide (sequences listed in table 2.2). In order to anneal the top and bottom strands of each set of guides, the top and bottom strands of each guide (10 μM/strand), T4 DNA ligase buffer (1X), and nuclease free water were mixed together and heated in a dry bath at 95°C for three minutes, at which point the heating blocks were removed from the dry bath and one block was placed on top of the block containing the tube with the annealing mixture and cooled at room temperature until reaching 50°C. To ligate the annealed guides into the pSpCas9(BB)-2A-Puro (PX459) V2.0 plasmid,

the pSpCas9(BB)-2A-Puro (PX459) V2.0 plasmid (200 ng/μL), the annealed guides (1:20 dilution), ATP (0.5 mM), NEB Buffer 2.1 (1X), Rapid T4 DNA ligase (1:40 dilution), BBSI restriction enzyme (1:20 dilution), and nuclease free water were placed in a thermocycler with the following conditions: 12X (37°C for five minutes, and 21°C for five minutes), and 21°C on hold. The pSpCas9(BB)-2A-Puro (PX459) V2.0 plasmid is ampicillin-resistant, and therefore DH5α competent *E. coli* cells were transformed with the ligation product and plated on an ampicillin-containing agar-plate. PCR was used to screen colonies for successful uptake of the plasmid, with each reaction containing 2X phire green hot start II PCR master mix, forward primer 68 (sequence TAAAATGGACTATCATATGC), the bottom strand of the guide, DNA from the transformation product (1 colony in 10 μL of nuclease free water), and nuclease free water. The thermocycle3r conditions for the colony screening PCR were 1X (98°C for five minutes), 27X (98°C for 10 seconds, 53°C for 15 seconds, and 72°C for 30 seconds), 1X (72°C for five minutes), and 4°C on hold. DNA from colonies identified as containing the plasmid containing the guides was collected and purified, and sent for DNA sequencing (primer p68 was used as the sequencing primer).

2.6 Generation of ATG14L and ZBTB16 Knockout cell lines

STHdhQ7/Q7 cells were split 18 hours before transfection into 10 cm dishes at between 40%-50% confluency. Plasmids containing each set of guides were co-transfected with GFP into the cells with the transfection reagent PEI. 24 hours post-transfection, the cells were rinsed with 1X PBS, trypsinized, and DMEM + 10% FBS was added. Cells were centrifuged at 1.2K for two minutes, the supernatant was aspirated, and cells were resuspended in PBS containing 0.2% BSA, and kept on ice. Two 96 well plates per guide were prepared with DMEM + 20% FBS in each well. Fluorescence activated cell sorting was performed by the University of Ottawa Flow Cytometry facility so that a single GFP expressing cell was seeded into each well of the 96 well plates. The 96 well plates were then placed in a 37°C incubator and the cells were left to grow for approximately 3 weeks, or until a colony of 90%-100% confluency had grown. Colonies were first maintained in 12 well plates, and then

6 well plates. Once colonies reached 80%-100% confluency in the 6 well plates, they were lysed with 1% RIPA buffer containing Protease Inhibitor Cocktail Set III (2 μL/1 μL RIPA), and the phosphatase inhibitors sodium orthovanadate (1 mM) and sodium fluoride (10 mM). Western blotting was performed to screen for successful knockouts. Colonies identified as knockouts from western blotting were then sent for DNA sequencing at the Ottawa Hospital Research Institute DNA Sequencing Facility (sequencing primers listed in table 2.2) to further confirm that a successful knockout was generated.

Guide	Primer sequence (5' to 3')	Forward or Reverse primer
ATG14L guide 1	TCAGATCATCATGGCGTCTC	Forward
ATG14L guide 2		
ZBTB16 guide 1	CCACCTTGCAGAGCAGAGAA	Forward
ZBTB16 guide 2		

Table 2.2. Sequences of primers used for DNA sequencing of potential CRISPR knockout cell lines

2.7 DHPG and CTEP treatment

Cells were rinsed once with Hank's Balanced Salt Solution (HBSS, 1X), and starved with HBSS for approximately two hours. DHPG (10μM) or CTEP (10 μM) was added to warmed HBSS (five minutes in a 37°C sterile water bath), and the solution was then added to the wells requiring treatment. HBSS containing neither DHPG nor CTEP was added to control wells. For DHPG treatment, after 10 minutes, wells were aspirated and rinsed with ice cold HBSS twice. For CTEP treatment, after 30 minutes, wells were aspirated and rinsed with ice cold HBSS twice. Cells were then lysed with 1% RIPA buffer containing Protease Inhibitor Cocktail Set III (2 μL/1 μL RIPA), and the phosphatase inhibitors sodium orthovanadate (1 mM) and sodium fluoride (10 mM), and lysates were collected.

2.8 Western Blot

A Bradford assay was performed with cell lysates, and samples were prepared accordingly using 1% RIPA buffer and sodium dodecyl sulphate (SDS) buffer. Samples were loaded into a SDS-polyacrylamide gel of the appropriate resolving gel percentage. The gel was placed in an electrophoresis unit and a constant voltage of 100V was applied. Separated proteins present in the gel were then transferred to a nitrocellulose membrane. The membranes were blocked with a 5% skim milk solution (in 1X TBS with 0.05% Tween 20 (TBST)) for one hour at room temperature. The membranes were then incubated with primary antibodies (1:1000) in 1% milk (in TBST) solution overnight at 4°C, washed three times with TBST at room temperature, incubated with secondary antibodies (1:5000) in a 1% milk (in TBST) solution for one hour at room temperature, and then washed three times with TBST at room temperature. Membranes were then incubated using western enhanced chemiluminescence clarity solutions, and visualized with a Bio-rad Chemidoc Imaging System.

2.9 Statistical Analysis

Western blots were analyzed using Image Lab software to obtain densitometric data. Protein expression was normalized to loading controls. Data was compared using a two-way analysis of variance test (ANOVA) and analyzed with the Fisher's LSD test to determine statistical significance. Data is represented as mean ± SEM.

Chapter 3: Results

3.1 Successful generation of ATG14L and ZBTB16 knockout cell lines using CRISPR Cas9

In order to knockout ATG14L and ZBTB16 in STHdhQ7/Q7 cells, we employed a clustered regularly interspaced short palindromic repeats (CRISPR) Cas9 approach. CRISPR Cas9 is a method for genome engineering that has emerged within recent years. Compared to other genome engineering methods, such as zinc finger nucleases (ZFN's) and transcription activator-like effector nucleases

(TALEN), it is highly efficient, cost effective, easily designed, and highly specific (230). CRISPR Cas9 has been characterized extensively in papers such as Jinek *et al.* 2012, and Ran *et al.* 2013 (230, 231). We utilized CRISPR Cas9 in lieu of RNA interference, as it leads to a permanent, rather than transient, silencing in gene expression (it acts at the DNA level rather than the mRNA level) that is transferable across generations (230, 232). This allows for the creation of specifically designed cell lines; in this case, it allowed for the generation of novel STHdhQ7/Q7 ATG14L and ZBTB16 knockout cell lines.

Two sets of guide RNA's (guides) were designed to target a 20 base pair sequence in exon one of the *mus musculus* gene to be knocked out (ATG14L in one cell line, ZBTB16 in the other cell line) (Figure 3.1A). These guides were specifically designed to target their respective sequences with high efficiency, while also having a very low probability of off-target binding elsewhere in the genome.

Once the targeted sequence is recognized, the Cas9 enzyme will cleave approximately 3 base pairs ahead of the PAM sequence located adjacent to the target sequence (230). This allows for generation of a double stranded break, which recruits the error-prone non-homologous end joining (NHEJ) pathway, which introduces an insertion/deletion mutation leading to a frameshift, and potentially a premature stop codon (230). This is what causes the knockout.

Once designed and produced, guides were ligated into the pSpCas9(BB)-2A-Puro (PX459) V2.0 plasmid, which contains the Cas9 enzyme. The plasmid containing the guides was co-transfected with GFP into STHdhQ7/Q7 cells, the assumption being that cells which successfully took up GFP also took up the plasmid (Figure 3.1A). Therefore, using fluorescence activated cell sorting, cells were sorted so that each well of a 96 well plate contained one GFP positive cell. This allowed us to grow potential knockout colonies without contamination from cells which did not successfully take up the Cas9 plasmid containing the guides.

Once colonies reached 90-100% confluency, the efficiency of the guides to generate a knockout was determined via western blot analysis. We found that both pairs of guides for both ATG14L and ZBTB16 led to the production of knockout colonies (Figure 3.1B). A single ATG14L and a single ZBTB16 knockout colony produced by guide one were utilized for all experiments (Figure 3.1B).

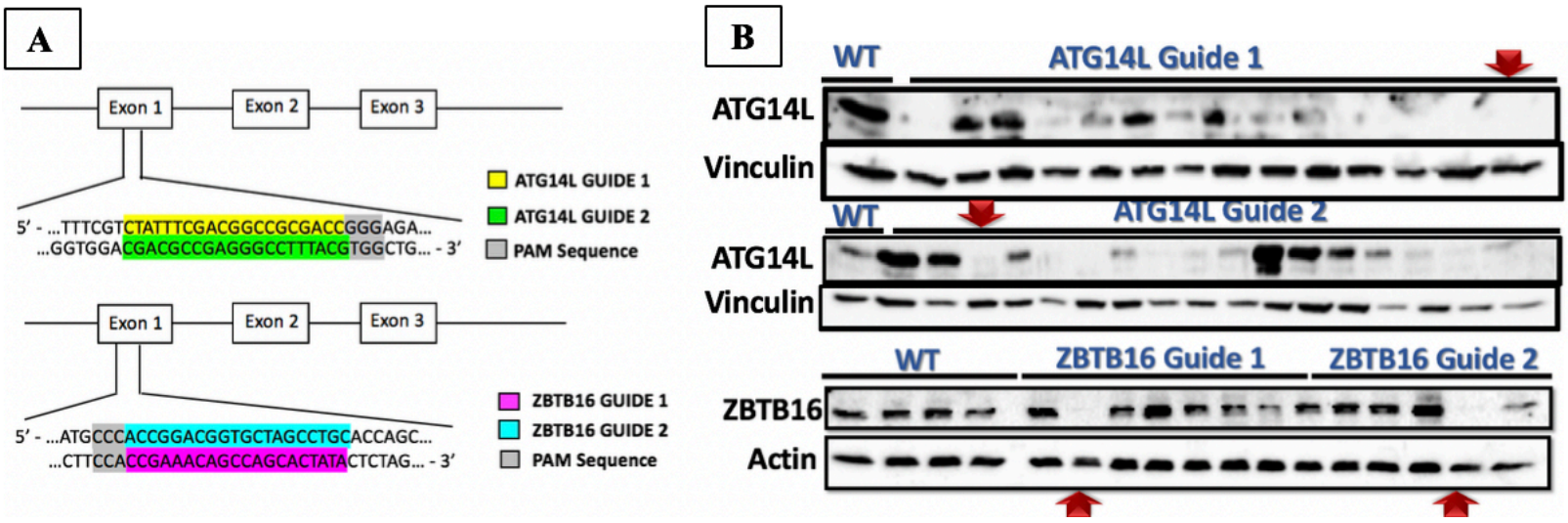

Figure 3.1. Generation of ATG14L and ZBTB16 knockouts in STHdhQ7/Q7 cells using CRISPR Cas9.

(A) Schematic representation of the region in exon 1 of ATG14L and ZBTB16 that guides were designed to target. **(B)** Representative western blots of STHdhQ7/Q7 (WT) cells co-transfected with GFP and the ATG14L or ZBTB16 CRISPR Cas9 plasmids. Arrows show the successful knockout colonies used for further experiments.

3.2 Silencing of ATG14L in STHdhQ7/Q7 cells results in inhibition of autophagy

ATG14L is a key component of vps34 complexes that mediate autophagosome formation during MA in mammalian cells (124, 126). Expression of ATG14L is known to correlate with an activation of aggrephagy and an improvement of HD symptoms in an HD mouse model (115). MA-related deficits are thought to play a role in the pathogenesis of HD and, since neurodegeneration is observed most heavily in the striatum, we first tested whether silencing of ATG14L in the STHdhQ7/Q7 striatal neuron cell line using a CRISPR Cas9 approach leads to an inhibition of MA (1, 15, 200, 202-204). We measured two things: (i) the expression levels of p62 (a marker of MA which associates with ubiquitinated cargo to target them to the autophagosome and is normally degraded during autophagy), and (ii) the ratio of LC3-II to LC3-I (LC3-II is the membrane bound form of the LC3 protein present on autophagosome membranes which interacts with the p62-cargo complex, while LC3-I is the cytosolic form of the LC3 protein) (191, 233, 234). An increase in p62 expression would indicate an inhibition of MA, while an increase in the ratio of LC3-II to LC3-I expression can indicate an inhibition of MA (191, 233, 234). We found that ATG14L$^{-/-}$xSTHdhQ7/Q7 cells (ATG14L KO) exhibited a significant increase in expression of p62 in comparison to STHdhQ7/Q7 cells (WT) (Figure 3.2E, K, 3.3D, I, and 3.4D, I)**.** This indicates that p62 is not being degraded in KO cells as it is in WT cells, suggesting that MA induction is inhibited in the ATG14L KO cells, while it is active in WT cells containing ATG14L. ATG14L KO cells also exhibited an abnormal accumulation of LC3-II compared to WT cells, as shown by an increase in LC3-II:LC3-I, which could indicate an inhibition of MA (Figure 3.2D, J). Taken together, the increase in p62 and LC3-II:LC3-I expression suggests that MA is inhibited in ATG14L KO cells.

3.3 Silencing of ATG14L in STHdhQ7/Q7 cells results in a beclin-1 modification

Beclin-1 is a member of vps34 complexes which are responsible for mediating the production of PI3P, which is critical for autophagosome formation (124, 126). Therefore, the regulation of beclin-1 by a variety of upstream signaling pathways regulates autophagosome formation, and thus MA as a whole (235). Regulation of beclin-1 occurs through a variety of post-translational modifications, some of

which serve to activate MA, and others which inhibit MA (235). These modifications include phosphorylation, ubiquitination, acetylation, and cleavage (235). For example, phosphorylation by ULK1 at the S15 site in beclin-1 leads to activation of MA, while phosphorylation at the S234 and S295 sites by AKT1 leads to inhibition of MA (235).

Since beclin-1 is a key player in MA, and is known to interact with ATG14L, we wanted to test whether CRISPR-Cas9 induced silencing of ATG14L would cause any changes in beclin-1 expression (124, 126). Western blot analysis of beclin-1 revealed a band directly above the band corresponding to unmodified beclin-1 in the ATG14L KO cells which was not present in WT cells (Figure 3.2C, H, I, 3.3C, G, H, and 3.4C, G, H). These double bands were observed under all experimental conditions in ATG14L KO cells, but no conditions were capable of causing the appearance of the second band in WT cells. Therefore, this second band likely represents a post translational modification of beclin-1 caused by the silencing of ATG14L.

Western blot analysis revealed that beclin-1 expression was significantly increased in ATG14L KO cells compared to WT cells (Figures 3.2C, H, I, 3.3C, G, H, 3.4C, G, H). Reduced beclin-1 expression is typically associated with an inhibition of autophagy, and therefore this increase in beclin-1 expression in ATG14L KO cells may represent an attempt by the cells to initiate autophagy in the absence of ATG14L (115, 236).

3.4 Silencing of ATG14L in STHdhQ7/Q7 cells has no impact on pGSK3β and ZBTB16

We have previously described a novel pathway of MA regulation which is dependent on GSK3β (115). In this proposed pathway, GSK3β regulates ZBTB16, which in turn regulates ATG14L (115). Briefly, when GSK3β is phosphorylated at the S9 site (pGSK3β), it is unable to interact with ZBTB16, allowing ZBTB16 to interact with and ubiquitinate ATG14L, leading to the degradation of ATG14L and the inhibition of MA (115, 195). Conversely, when GSK3β is not phosphorylated, it

phosphorylates ZBTB16 and prevents its interaction with ATG14L, thereby allowing MA to occur (115, 195). Given the novelty of this pathway, we wanted to test whether changes in ATG14L were able to cause changes in the upstream proteins of this pathway, GSK3β and ZBTB16, in a feedback manner. Specifically, we were interested in whether loss of ATG14L would result in a feedback inhibition of pGSK3β and ZBTB16 in an attempt by the cell to activate MA (i.e. result in changes in their expression consistent with activation of MA). We found that CRISPR Cas9-induced silencing of ATG14L in striatal neurons did not cause any significant changes in either pGSK3β levels or ZBTB16 levels (Figure 3.2A, B, F, G, 3.3A, B, E, F, 3.4A, B, E, F). Therefore, the loss of ATG14L does not cause changes in these upstream proteins of this pathway of MA.

3.5 Transfection of mutant huntingtin in STHdhQ7/Q7 and ATG14L$^{-/-}$xSTHdhQ7/Q7 cells has no impact on mGluR5, ZBTB16, beclin-1, and p62 expression

The accumulation of huntingtin aggregates has previously been shown to correlate with increased pGSK3β, ZBTB16, and p62 expression in zQ175 HD mice, which suggests that an inhibition of aggrephagy mediated by this novel GSK3β pathway may contribute to HD pathology (115). Since we found that transfection of Q138 in WT cells led to an increase in pGSK3β, we expected these cells to also exhibit corresponding changes in other components of the GSK3β-mediated pathway of MA consistent with an inhibition of MA. More specifically, we expected to see an increase in ZBTB16 expression, and an increase in p62 expression. Surprisingly, WT cells transfected with Q138 exhibited no significant changes in expression of ZBTB16 or p62 in comparison to non-transfected and Q15 transfected WT cells (Figure 3.4B, C, D, F, G, H, I, 3.6B, C, E, F). Additionally, we also observed no changes in beclin-1 expression between cells transfected with Q138, and non-transfected and Q15 transfected cells (Figure 3.4B, C, D, F, G, H, I, 3.6B, C, E, F). Taken together, these results seem to reject the notion of impaired MA in response to mutant huntingtin. They may also call into question the roles of each component of the GSK3β-mediated pathway of MA, at least in the context of HD (i.e. insofar as some portions of this pathway may not interact with each other in a way we would have

predicted); however, it is also possible that the experimental conditions could account for these observations.

Given that we also observed a greater increase in pGSK3β expression in ATG14L KO cells, we next tested whether any changes in ZBTB16, beclin-1, and p62 expression were caused in ATG14L KO cells due to the transfection of Q138. Since these cells lack ATG14L, which is necessary for MA to occur, we did not expect to see a change in p62 expression. Indeed, we observed no change in p62 expression in ATG14L KO cells transfected with Q138 compared to non-transfected and Q15 transfected ATG14L KO cells (Figure 3.4D, I). Additionally, we did not observe any changes in ZBTB16 and beclin-1 expression in ATG14L KO cells transfected with Q138 compared to non-transfected and Q15 transfected ATG14L KO cells (Figure 3.4B, C, F, G, H).

We have previously shown that mGluR5 may regulate the GSK3β-mediated pathway of MA (115). Given that mGluR5 has been implicated in HD pathology, we wanted to test whether transfection of Q138 caused any changes in mGluR5 expression in both WT and ATG14L KO cells. To this end, we observed no significant changes in mGluR5 expression between non-transfected, Q15 transfected, and Q138 transfected cells of both WT cells and ATG14L KO cells (Figure 3.8).

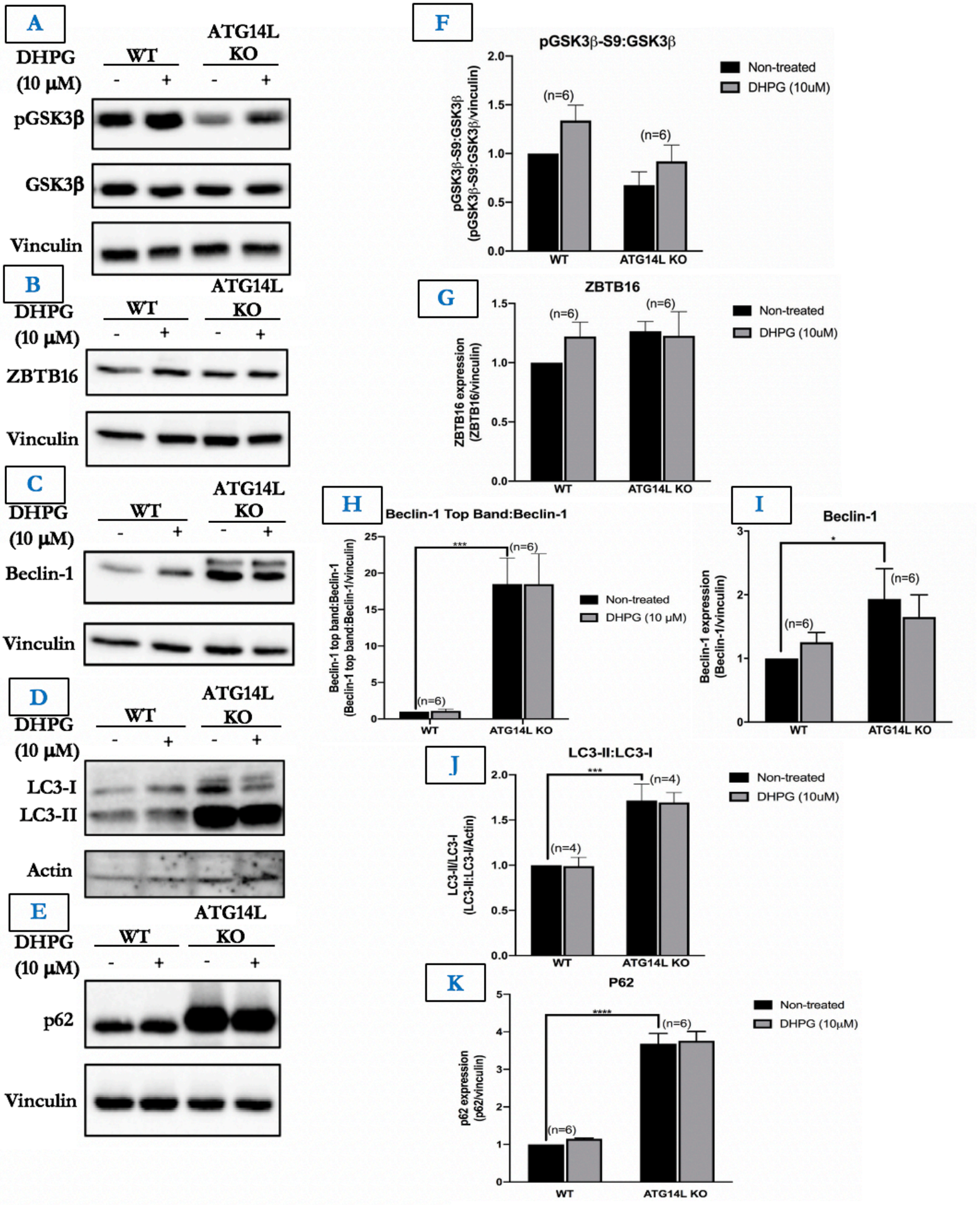
A
DHPG
(10 μM)
WT
ATG14L KO
- + - +
pGSK3β
GSK3β
Vinculin
B
DHPG
(10 μM)
WT
ATG14L KO
- + - +
ZBTB16
Vinculin
C
DHPG
(10 μM)
WT
ATG14L KO
- + - +
Beclin-1
Vinculin
D
DHPG
(10 μM)
WT
ATG14L KO
- + - +
LC3-I
LC3-II
Actin
E
DHPG
(10 μM)
WT
ATG14L KO
- + - +
p62
Vinculin
F
pGSK3β-S9:GSK3β
pGSK3β-S9:GSK3β (pGSK3β-S9:GSK3β/vinculin)
Non-treated
DHPG (10uM)
(n=6)
(n=6)
WT
ATG14L KO
G
ZBTB16
ZBTB16 expression (ZBTB16/vinculin)
Non-treated
DHPG (10uM)
(n=6)
(n=6)
WT
ATG14L KO
H
Beclin-1 Top Band:Beclin-1
Beclin-1 top band:Beclin-1 (Beclin-1 top band:Beclin-1/vinculin)
***
(n=6)
(n=6)
Non-treated
DHPG (10 μM)
WT
ATG14L KO
I
Beclin-1
Beclin-1 expression (Beclin-1/vinculin)
*
(n=6)
(n=6)
WT
ATG14L KO
J
LC3-II:LC3-I
LC3-II/LC3-I (LC3-II:LC3-I/Actin)
***
(n=4)
(n=4)
Non-treated
DHPG (10uM)
WT
ATG14L KO
K
P62
p62 expression (p62/vinculin)
****
(n=6)
(n=6)
Non-treated
DHPG (10μM)
WT
ATG14L KO

Figure 3.2. Effect of CRISPR Cas9 induced silencing of ATG14L in STHdhQ7/Q7 cells treated with the group I mGluR agonist DHPG. (A-E) Representative western blots for pGSK3β (n=6), ZBTB16 (n=6), Beclin-1 (n=6), Beclin-1 top band (n=6), LC3-II/LC3-I (n=4), and p62 (n=6) with the corresponding loading controls in cell lysates from STHdhQ7/Q7 wild type (WT) and ATG14L$^{-/-}$xSTHdhQ7/Q7 cells (ATG14L KO) after treatment with either DHPG (10 μM) or HBSS. **(F-K)** Quantification of blots represented in (A-E) shown as the mean ± SEM for fold change in protein expression relative to the loading control. * $p<0.05$, *** $p<0.001$, and **** $p<0.0001$ by two-way ANOVA and Fisher's LSD comparisons.

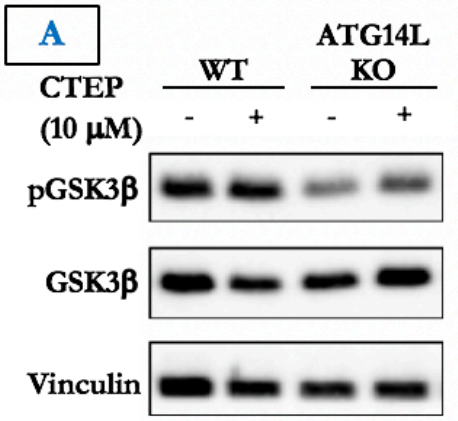
A
WT
ATG14L KO
CTEP (10 μM)
- + - +
pGSK3β
GSK3β
Vinculin

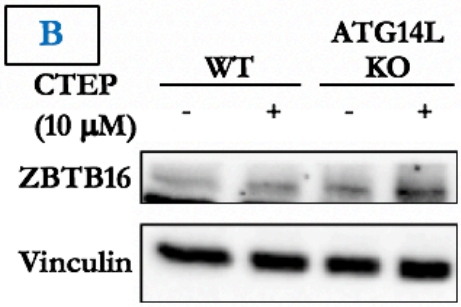
B
WT
ATG14L KO
CTEP (10 μM)
- + - +
ZBTB16
Vinculin

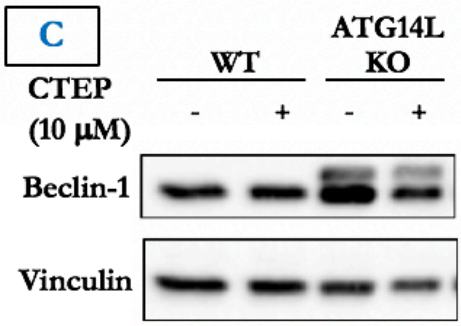
C
WT
ATG14L KO
CTEP (10 μM)
- + - +
Beclin-1
Vinculin

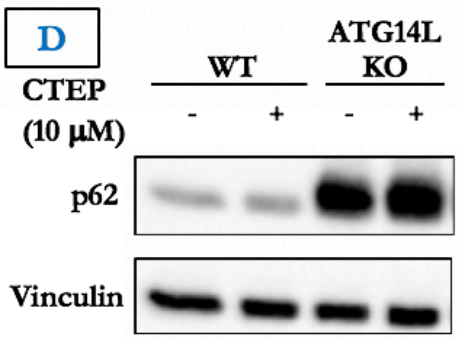
D
WT
ATG14L KO
CTEP (10 μM)
- + - +
p62
Vinculin

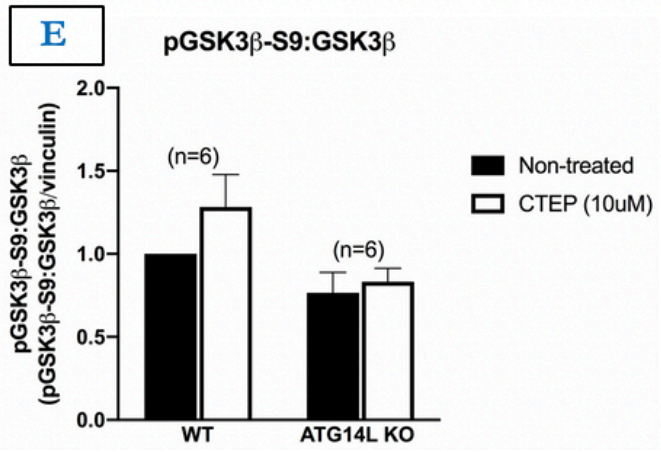
E
pGSK3β-S9:GSK3β
pGSK3β-S9:GSK3β (pGSK3β-S9:GSK3β/vinculin)
2.0
1.5
1.0
0.5
0.0
(n=6)
(n=6)
WT
ATG14L KO
Non-treated
CTEP (10uM)

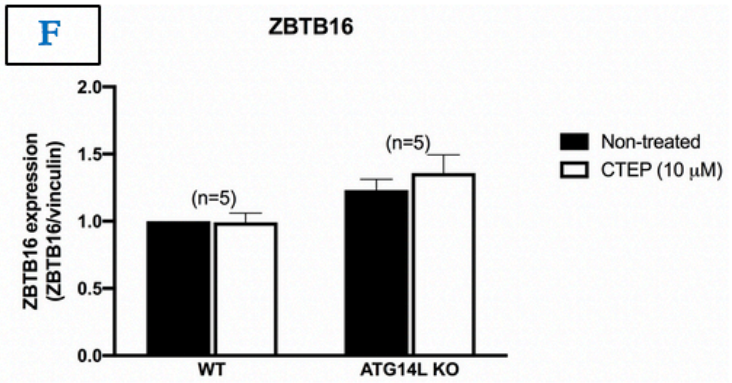
F
ZBTB16
ZBTB16 expression (ZBTB16/vinculin)
2.0
1.5
1.0
0.5
0.0
(n=5)
(n=5)
WT
ATG14L KO
Non-treated
CTEP (10 μM)

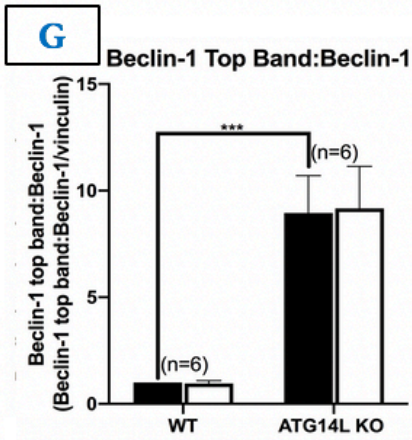
G
Beclin-1 Top Band:Beclin-1
Beclin-1 top band:Beclin-1 (Beclin-1 top band:Beclin-1/vinculin)
15
10
5
0
***
(n=6)
(n=6)
WT
ATG14L KO
Non-treated
CTEP (10uM)

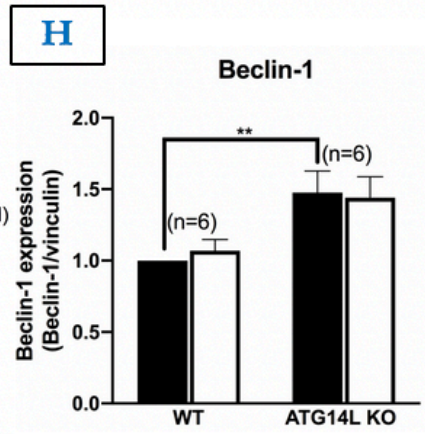
H
Beclin-1
Beclin-1 expression (Beclin-1/vinculin)
2.0
1.5
1.0
0.5
0.0
**
(n=6)
(n=6)
WT
ATG14L KO

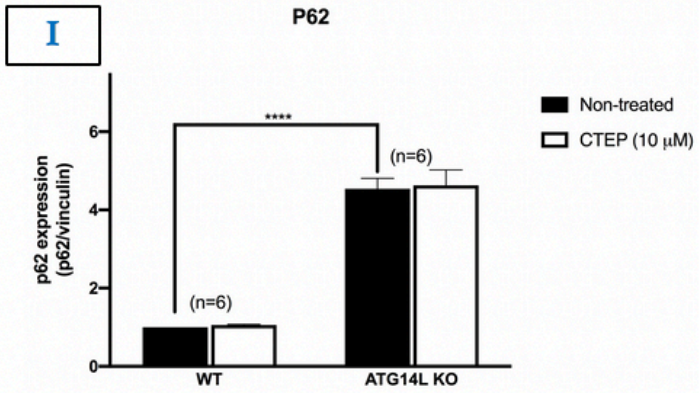
I
P62
p62 expression (p62/vinculin)
6
4
2
0
****
(n=6)
(n=6)
WT
ATG14L KO
Non-treated
CTEP (10 μM)

Figure 3.3. Effect of CRISPR Cas9 induced silencing of ATG14L in STHdhQ7/Q7 cells treated with the mGluR5 NAM CTEP. (A-D) Representative western blots for pGSK3β (n=6), ZBTB16 (n=5), Beclin-1 (n=6), Beclin-1 top band (n=6), and p62 (n=6) with the corresponding loading controls in cell lysates from STHdhQ7/Q7 wild type and ATG14L$^{-/-}$xSTHdhQ7/Q7 cells after treatment with either CTEP (10 μM) or HBSS. **(E-I)** Quantification of blots represented in (A-D) shown as the mean ± SEM for fold change in protein expression relative to the loading control. ** p<0.01, *** p<0.001, and **** p<0.0001 by two-way ANOVA and Fisher's LSD comparisons.

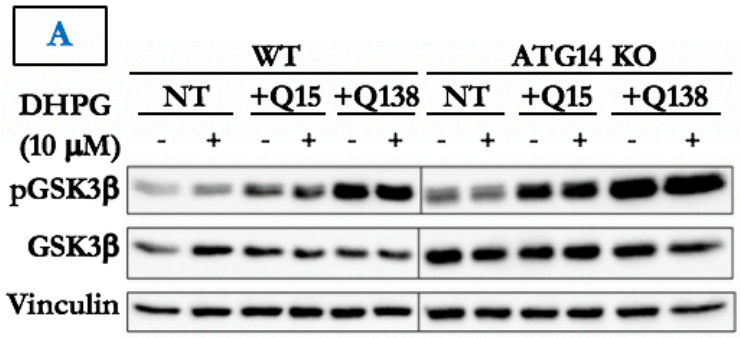
A
WT
ATG14 KO
DHPG
NT
+Q15
+Q138
NT
+Q15
+Q138
(10 μM)
- + - + - + - + - + - +
pGSK3β
GSK3β
Vinculin

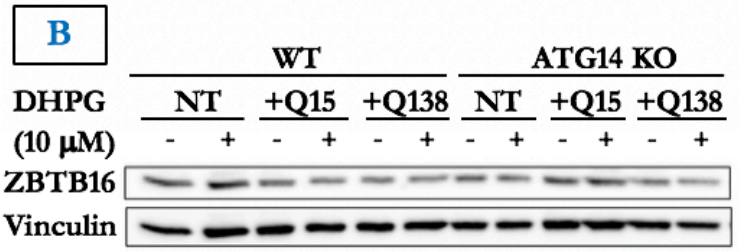
B
WT
ATG14 KO
DHPG
NT
+Q15
+Q138
NT
+Q15
+Q138
(10 μM)
- + - + - + - + - + - +
ZBTB16
Vinculin

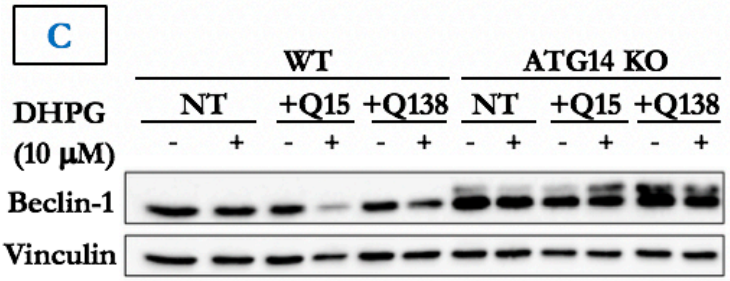
C
WT
ATG14 KO
DHPG
NT
+Q15
+Q138
NT
+Q15
+Q138
(10 μM)
- + - + - + - + - + - +
Beclin-1
Vinculin

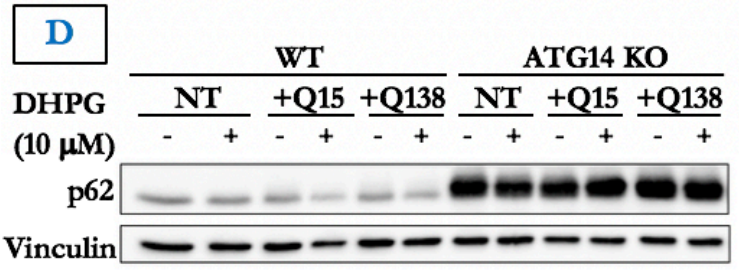
D
WT
ATG14 KO
DHPG
NT
+Q15
+Q138
NT
+Q15
+Q138
(10 μM)
- + - + - + - + - + - +
p62
Vinculin

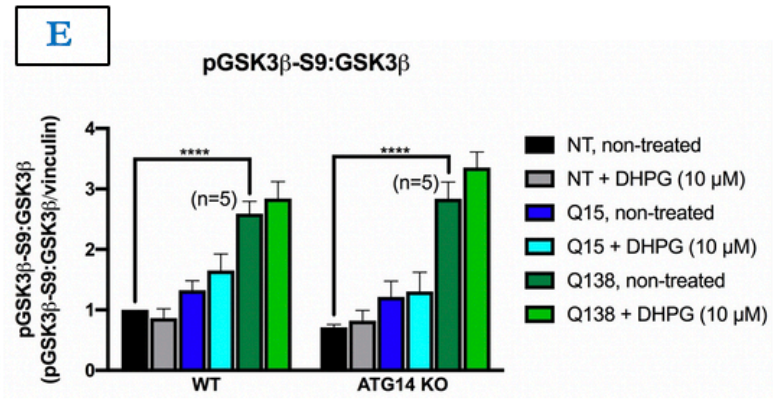
E
pGSK3β-S9:GSK3β
pGSK3β-S9:GSK3β (pGSK3β-S9:GSK3β/vinculin)
****
****
(n=5)
(n=5)
WT
ATG14 KO
NT, non-treated
NT + DHPG (10 μM)
Q15, non-treated
Q15 + DHPG (10 μM)
Q138, non-treated
Q138 + DHPG (10 μM)

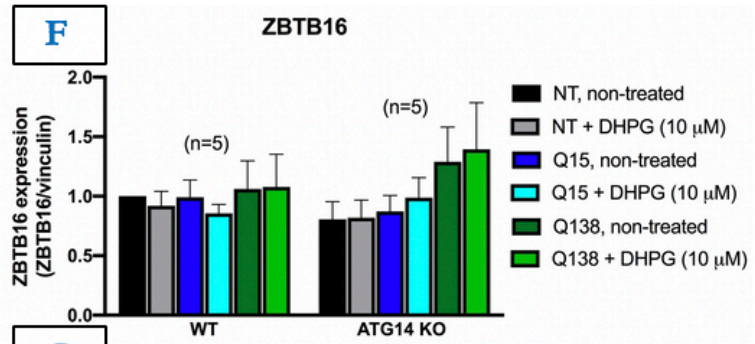
F
ZBTB16
ZBTB16 expression (ZBTB16/vinculin)
(n=5)
(n=5)
WT
ATG14 KO
NT, non-treated
NT + DHPG (10 μM)
Q15, non-treated
Q15 + DHPG (10 μM)
Q138, non-treated
Q138 + DHPG (10 μM)

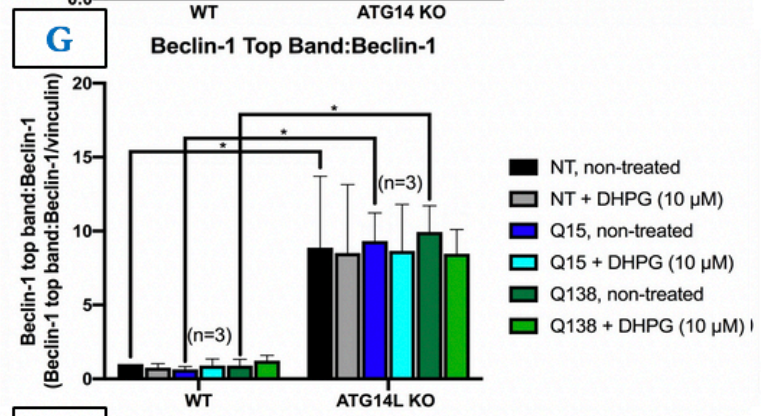
G
Beclin-1 Top Band:Beclin-1
Beclin-1 top band:Beclin-1 (Beclin-1 top band:Beclin-1/vinculin)
(n=3)
(n=3)
WT
ATG14L KO
NT, non-treated
NT + DHPG (10 μM)
Q15, non-treated
Q15 + DHPG (10 μM)
Q138, non-treated
Q138 + DHPG (10 μM)

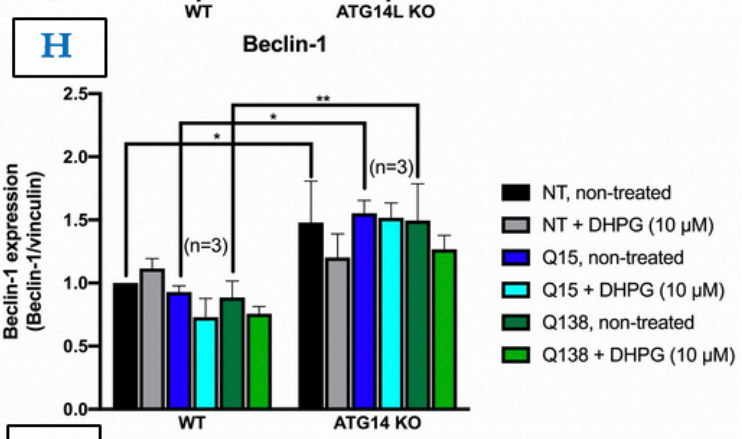
H
Beclin-1
Beclin-1 expression (Beclin-1/vinculin)
(n=3)
(n=3)
WT
ATG14 KO
NT, non-treated
NT + DHPG (10 μM)
Q15, non-treated
Q15 + DHPG (10 μM)
Q138, non-treated
Q138 + DHPG (10 μM)

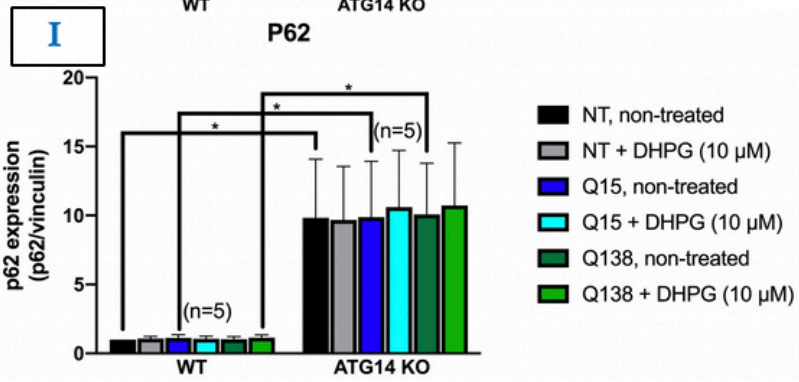
I
P62
p62 expression (p62/vinculin)
(n=5)
(n=5)
WT
ATG14 KO
NT, non-treated
NT + DHPG (10 μM)
Q15, non-treated
Q15 + DHPG (10 μM)
Q138, non-treated
Q138 + DHPG (10 μM)

Figure 3.4. Effect of mutant huntingtin transfection in STHdhQ7/Q7 wild type and ATG14L$^{-/-}$xSTHdhQ7/Q7 cells treated with the group I mGluR agonist DHPG. (A-D) Representative western blots for pGSK3β (n=5), ZBTB16 (n=5), Beclin-1 top band (n=3), Beclin-1 (n=3), and p62 (n=5) with the corresponding loading controls in cell lysates from STHdhQ7/Q7 wild type (WT) and ATG14L$^{-/-}$xSTHdhQ7/Q7 cells (ATG14L KO) with no transfection, transfection with Q15, and transfection with Q138, after treatment with either DHPG (10 μM) or HBSS. **(E-I)** Quantification of blots represented in (A-D) shown as the mean ± SEM for fold change in protein expression relative to the loading control. * $p<0.05$, ** $p<0.01$, and **** $p<0.0001$ by two-way ANOVA and Fisher's LSD comparisons.

3.6 Silencing of ZBTB16 in STHdhQ7/Q7 cells results in an increase in ATG14L expression and activation of autophagy

We have previously observed a correlation between increased ZBTB16 levels and decreased ATG14L levels in a zQ175 HD mouse model (115). Therefore, we wanted to test whether CRISPR Cas9-induced silencing of ZBTB16 was sufficient to cause an increase in ATG14L expression, and an activation of MA. As expected, we found that ZBTB16$^{-/-}$xSTHdhQ7/Q7 cells (ZBTB16 KO) exhibited a significant increase in ATG14L expression, and a significant decrease in p62 expression in comparison to WT cells (Figure 3.5, 3.6C, F). Since p62 is degraded when MA is active, and ATG14L is critical for autophagosome formation, these results indicate an activation of MA as a result of the genetic silencing of ZBTB16 in striatal neurons (124, 126).

3.7 Silencing of ZBTB16 in STHdhQ7/Q7 cells has no impact on pGSK3β and beclin-1 expression

It has previously been demonstrated that GSK3β regulates MA via regulation of ZBTB16 (115, 195). Given the novelty of this GSK3β-mediated pathway, we wanted to test whether changes in ZBTB16 were able to cause changes in the upstream GSK3β in a feedback manner. We found that CRISPR Cas9 induced silencing of ZBTB16 in STHdhQ7/Q7 striatal neurons did not cause any significant changes in p-GSK3β expression (Figure 3.6A, D). Therefore, loss of ZBTB16 does not cause any changes in expression of the upstream p-GSK3β.

We wanted to test whether the loss of ZBTB16 in STHdhQ7/Q7 cells would have any impact on levels of beclin-1, a key player in autophagosome biogenesis (124, 126, 235). We observed no significant changes in the expression of beclin-1 in ZBT16 KO cells in comparison to WT cells (Figure 3.6B, E). This suggests that while both ATG14L and beclin-1 are critical to autophagosome formation, ZBTB16 interacts with only ATG14L, and likely not with beclin-1.

3.8 Transfection of mutant huntingtin in ZBTB16$^{-/-}$xSTHdhQ7/Q7 cells has no impact on mGluR5, beclin-1, and p62 expression

Given that silencing of ZBTB16 in STHdhQ7/Q7 cells led to clearance of Q138, we wanted to test whether this correlated with changes in expression of members of the GSK3β-mediated pathway of MA upstream of ZBTB16, and in markers of MA. Since we have shown that loss of ZBTB16 expression results in an activation of autophagy, as shown by a decrease in expression of the marker of MA p62, we did not expect transfection of Q138 in ZBTB16 KO cells to cause any changes in p62 expression. Unsurprisingly, no significant changes in p62 expression in ZBTB16 KO cells were observed in response to transfection of Q138 (Figure 3.6C, F). Additionally, we did not observe any significant changes in beclin-1 expression between ZBTB16 KO cells transfected with Q138, and those non-transfected and Q15-transfected counterparts (Figure 3.6B, E).

Since no changes in expression of mGluR5 were observed in either WT or ATG14L KO cells as a result of Q15 or Q138 transfection, we did not expect to observe any changes in mGluR5 expression in Q15 and Q138 transfected ZBTB16 KO cells. Indeed, we did not observe any significant changes in mGluR5 expression between non-transfected, Q15 transfected, and Q138 transfected ZBTB16 KO cells (Figure 3.8B, D).

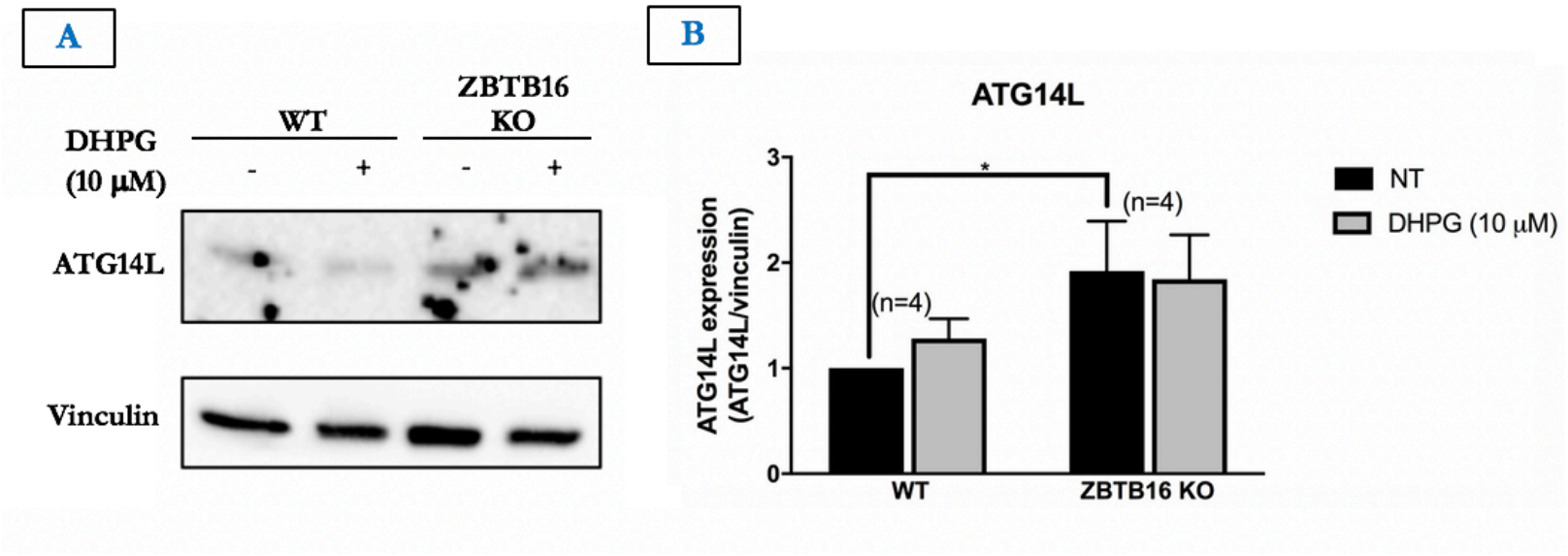

Figure 3.5. Effect of CRISPR Cas9 induced silencing of ZBTB16 in STHdhQ7/Q7 cells treated with the group I mGluR agonist DHPG on ATG14L expression. (A) Representative western blots for ATG14L (n=4) with the corresponding loading controls in cell lysates from STHdhQ7/Q7 wild type and ZBTB16$^{-/-}$xSTHdhQ7/Q7 cells after treatment with either DHPG (10 μM) or HBSS. **(B)** Quantification of blots represented in (A) shown as the mean ± SEM for fold change in ATG14L expression relative to the loading control. * $p<0.05$ by two-way ANOVA and Fisher's LSD comparisons.

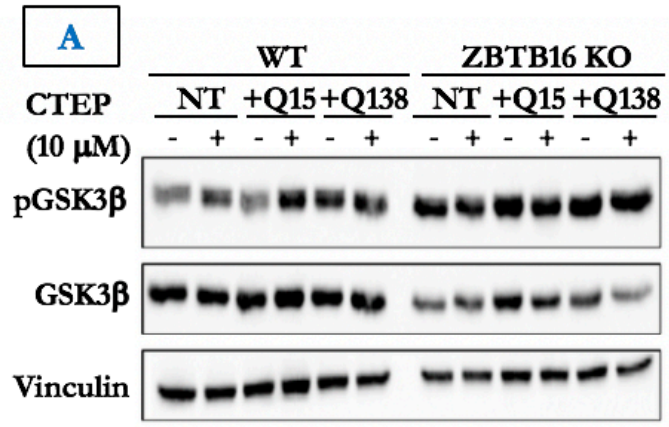
A
WT
ZBTB16 KO
CTEP
NT +Q15 +Q138 NT +Q15 +Q138
(10 µM)
- + - + - + - + - + - +
pGSK3β
GSK3β
Vinculin

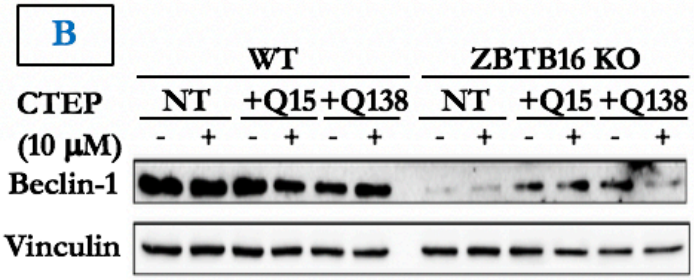
B
WT
ZBTB16 KO
CTEP
NT +Q15 +Q138 NT +Q15 +Q138
(10 µM)
- + - + - + - + - + - +
Beclin-1
Vinculin

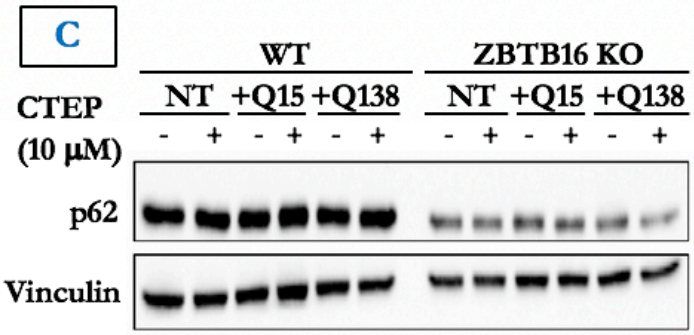
C
WT
ZBTB16 KO
CTEP
NT +Q15 +Q138 NT +Q15 +Q138
(10 µM)
- + - + - + - + - + - +
p62
Vinculin

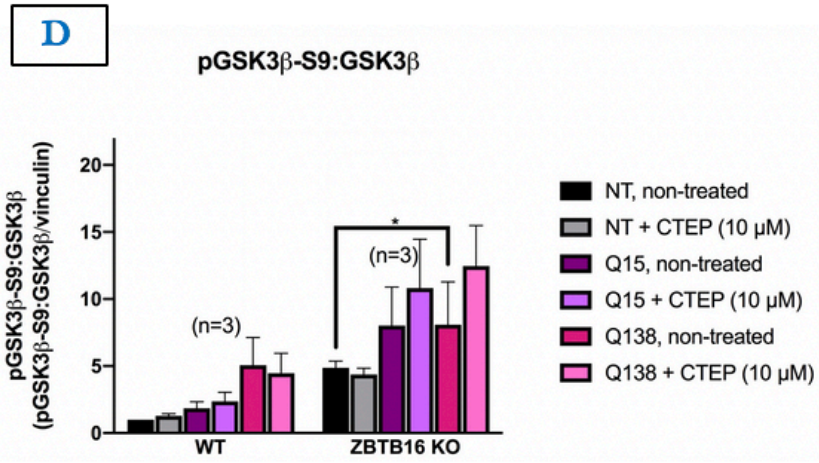
D
pGSK3β-S9:GSK3β
pGSK3β-S9:GSK3β
(pGSK3β-S9:GSK3β/vinculin)
20
15
10
5
0
(n=3)
(n=3)
*
WT
ZBTB16 KO
NT, non-treated
NT + CTEP (10 µM)
Q15, non-treated
Q15 + CTEP (10 µM)
Q138, non-treated
Q138 + CTEP (10 µM)

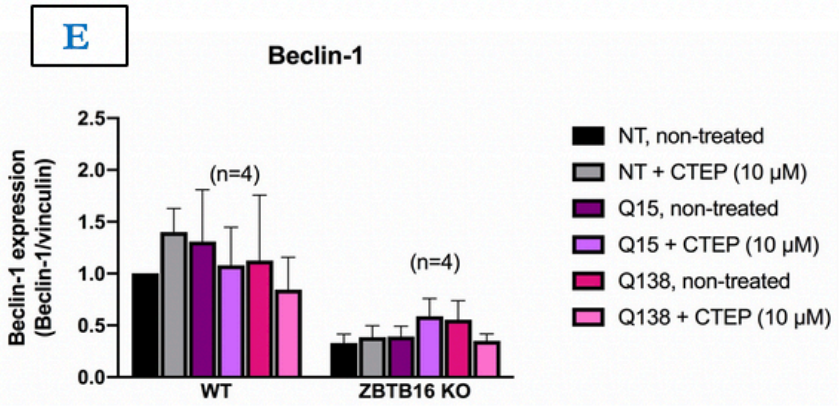
E
Beclin-1
Beclin-1 expression
(Beclin-1/vinculin)
2.5
2.0
1.5
1.0
0.5
0.0
(n=4)
(n=4)
WT
ZBTB16 KO
NT, non-treated
NT + CTEP (10 µM)
Q15, non-treated
Q15 + CTEP (10 µM)
Q138, non-treated
Q138 + CTEP (10 µM)

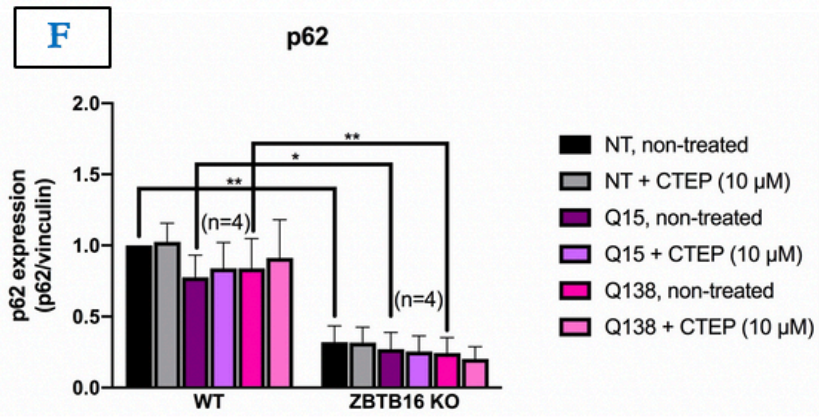
F
p62
p62 expression
(p62/vinculin)
2.0
1.5
1.0
0.5
0.0
**
*
**
(n=4)
(n=4)
WT
ZBTB16 KO
NT, non-treated
NT + CTEP (10 µM)
Q15, non-treated
Q15 + CTEP (10 µM)
Q138, non-treated
Q138 + CTEP (10 µM)

Figure 3.6. Effect of mutant huntingtin transfection in STHdhQ7/Q7 wild type and ZBTB16$^{-/-}$xSTHdhQ7/Q7 cells treated with the group I mGluR agonist DHPG. (A-D) Representative western blots for pGSK3β (n=5), ZBTB16 (n=5), Beclin-1 top band (n=3), Beclin-1 (n=3), and p62 (n=5) with the corresponding loading controls in cell lysates from STHdhQ7/Q7 wild type (WT) and ZBTB16$^{-/-}$xSTHdhQ7/Q7 cells (ZBTB16 KO) with no transfection, transfection with Q15, and transfection with Q138, after treatment with either DHPG (10 μM) or HBSS. **(E-I)** Quantification of blots represented in (A-D) shown as the mean ± SEM for fold change in protein expression relative to the loading control. * $p<0.05$, and ** $p<0.01$ by two-way ANOVA and Fisher's LSD comparisons.

3.9 Phosphorylation of the S9 site in GSK3β is increased in STHdhQ7/Q7 cells following transfection of mutant huntingtin

Phosphorylation at the S9 site in GSK3β was increased in the zQ175 HD mouse model in comparison to WT mice (115). Phosphorylation at this site is correlated with an inhibition of autophagy (115, 195). This increase in pGSK3β in zQ175 mice correlated with an inhibition of aggrephagy and the accumulation of huntingtin aggregates (115). Therefore, we wanted to test whether transfection of the Q138 mHtt construct, which contains 138 glutamine repeats, would cause an increase in pGSK3β expression in STHdhQ7/Q7 striatal neurons. We compared cells transfected with Q138, to cells transfected with Q15 (a WT Htt construct containing 15 glutamine repeats) and non-transfected cells. As expected, we found that pGSK3β expression was significantly increased in cells transfected with Q138 in comparison to non-transfected cells and cells transfected with Q15 (Figure 3.4A, E). In addition, cells transfected with Q15 exhibited no change in p-GSK3β expression in comparison to non-transfected cells (Figure 3.4A, E). Therefore, this increase in p-GSK3β expression is a result of mHtt, and not WT Htt.

Given that transfection of Q138 in WT cells causes an increase in pGSK3β expression, we wanted to test whether the transfection of Q138 in ATG14L KO cells and ZBTB16 KO cells would still cause an increase in pGSK3β expression. As expected, the transfection of Q138 did cause a significant increase in pGSK3β expression in ATG14L KO cells and ZBTB16 KO cells compared to non-transfected and Q15 transfected counterparts (Figure 3.4A, E, 3.6A, D). GSK3β is upstream of both ZBTB16 and ATG14L, and therefore the silencing of their expression was not expected to result in changes in pGSK3β compared to WT cells in response to the transfection of Q138.

3.10 Silencing of ATG14L expression in STHdhQ7/Q7 cells causes an accumulation of mutant huntingtin

We expected ATG14L KO cells to have greater levels of Q138 in comparison to WT cells, given that MA is impaired in the ATG14L KO cells. Increased accumulation of Q138 could indicate impaired aggrephagy. Indeed, we observed a significant increase in levels of Q138 in ATG14L KO cells compared to WT cells (Figure 3.7D, H). Since we have observed that zQ175 HD mice exhibit decreased ATG14L expression, impaired aggrephagy, and accumulation of huntingtin aggregates, this accumulation of Q138 in ATG14L KO cells gives support to the possibility that impaired aggrephagy is, at least in part, responsible for mHtt accumulation (115).

3.11 Silencing of ZBTB16 expression in STHdhQ7/Q7 cells leads to clearance of mutant huntingtin

We have previously shown that HD motor and cognitive symptoms and accumulation of huntingtin aggregates in zQ175 HD mice correlated with an increase in ZBTB16 expression and an inhibition of aggrephagy (115). Therefore, we were interested in whether CRISPR Cas9-induced silencing of ZBTB16 would result in a decrease in levels of Q138. Loss of ZBTB16 was expected to result in a clearance of Q138, as a result of activated aggrephagy. As expected, this is what we observed. We found a significant decrease in levels of Q138 in ZBTB16 KO compared to WT cells (Figure 3.7E, I). This supports our observations in zQ175 HD mice, as this confirms a role for ZBTB16 in aggrephagy in the context of HD, and underlines the potential therapeutic significance of silencing ZBTB16 for treatment of HD.

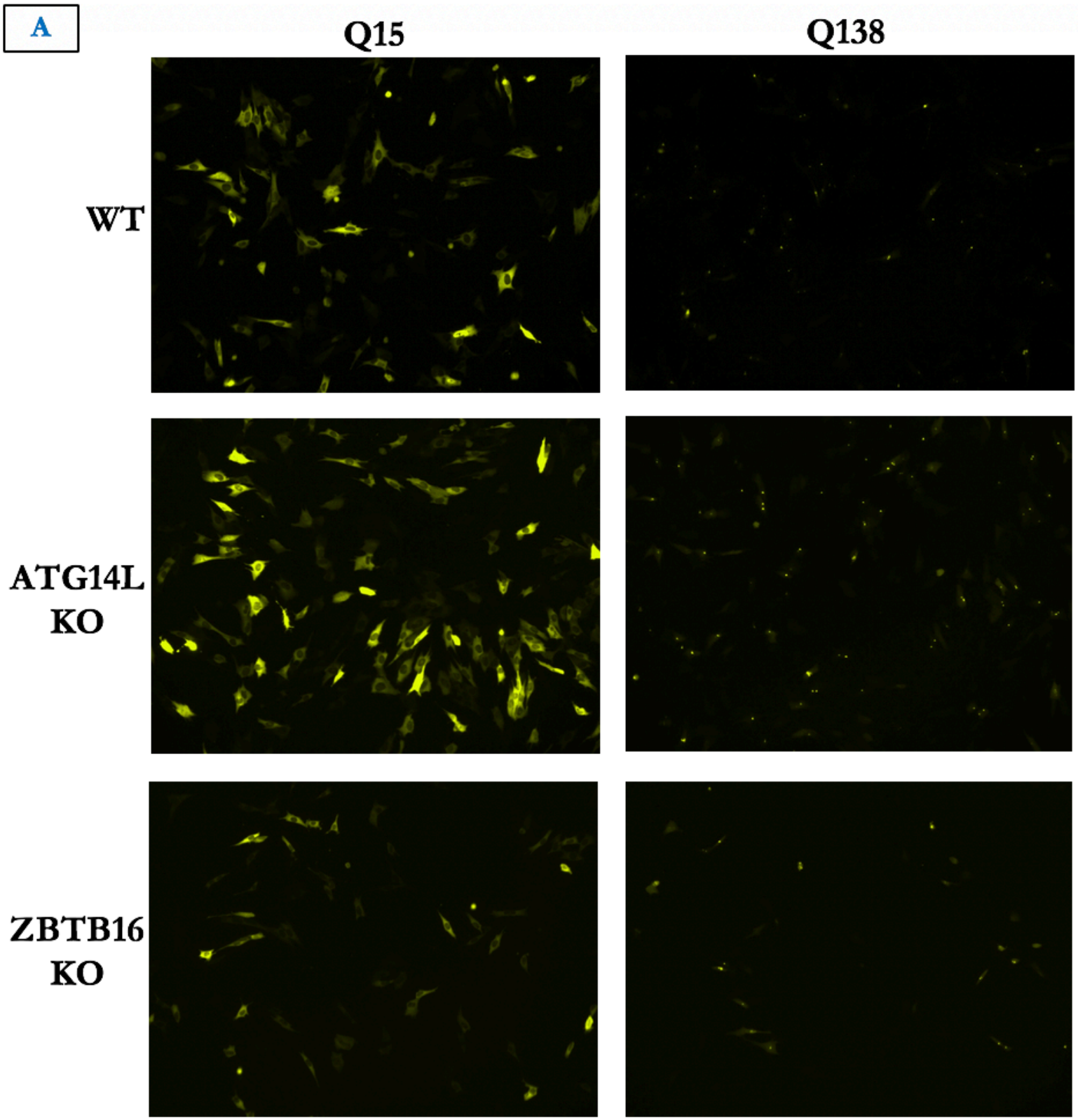
A
Q15
Q138
WT
ATG14L KO
ZBTB16 KO

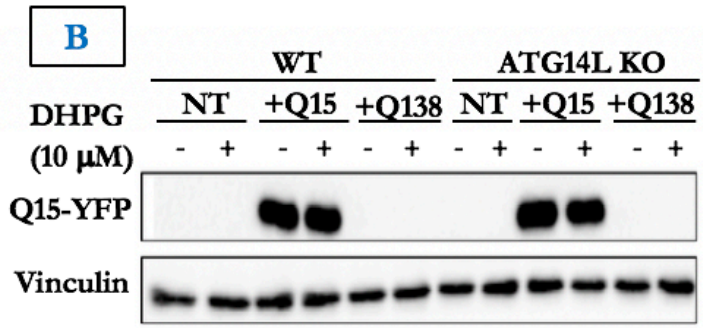
B
WT
ATG14L KO
DHPG
(10 µM)
NT
+Q15
+Q138
NT
+Q15
+Q138
- + - + - + - + - + - +
Q15-YFP
Vinculin

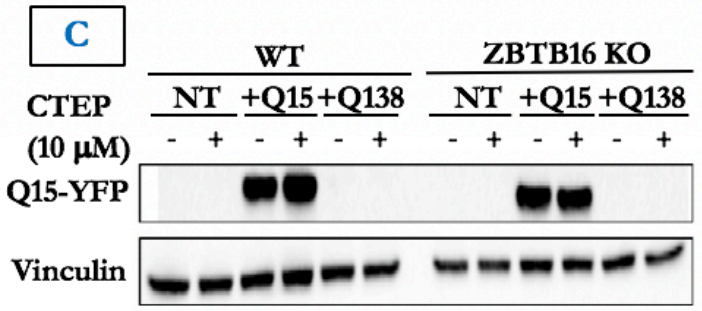
C
WT
ZBTB16 KO
CTEP
(10 µM)
NT
+Q15
+Q138
NT
+Q15
+Q138
- + - + - + - + - + - +
Q15-YFP
Vinculin

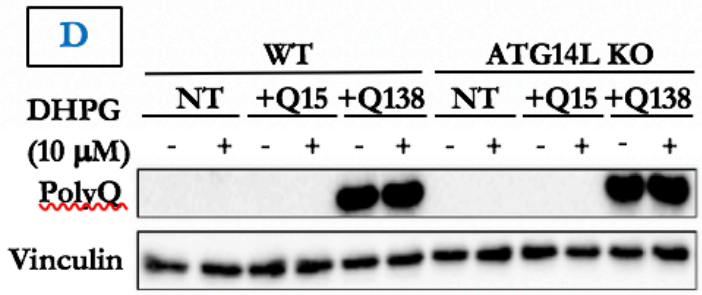
D
WT
ATG14L KO
DHPG
(10 µM)
NT
+Q15
+Q138
NT
+Q15
+Q138
- + - + - + - + - + - +
PolyQ
Vinculin

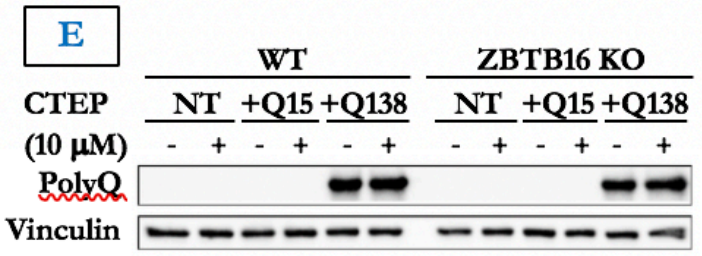
E
WT
ZBTB16 KO
CTEP
(10 µM)
NT
+Q15
+Q138
NT
+Q15
+Q138
- + - + - + - + - + - +
PolyQ
Vinculin

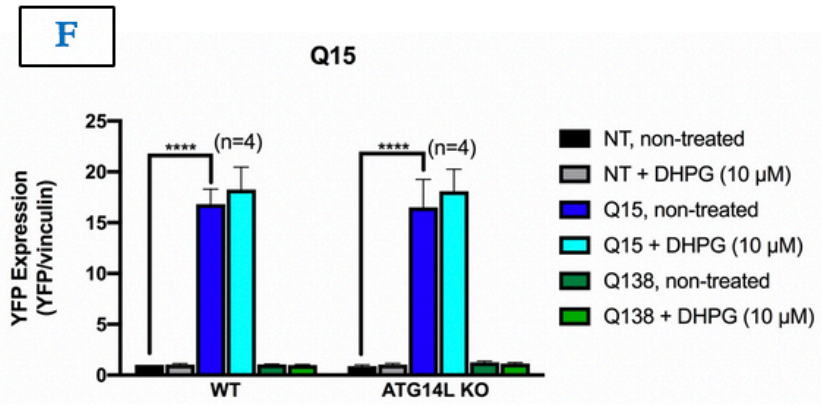
F
Q15
YFP Expression
(YFP/vinculin)
25
20
15
10
5
0
****
(n=4)
****
(n=4)
WT
ATG14L KO
NT, non-treated
NT + DHPG (10 µM)
Q15, non-treated
Q15 + DHPG (10 µM)
Q138, non-treated
Q138 + DHPG (10 µM)

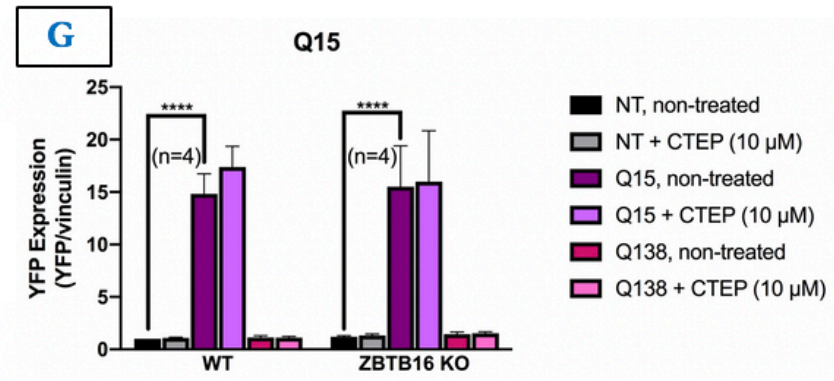
G
Q15
YFP Expression
(YFP/vinculin)
25
20
15
10
5
0
****
(n=4)
****
(n=4)
WT
ZBTB16 KO
NT, non-treated
NT + CTEP (10 µM)
Q15, non-treated
Q15 + CTEP (10 µM)
Q138, non-treated
Q138 + CTEP (10 µM)

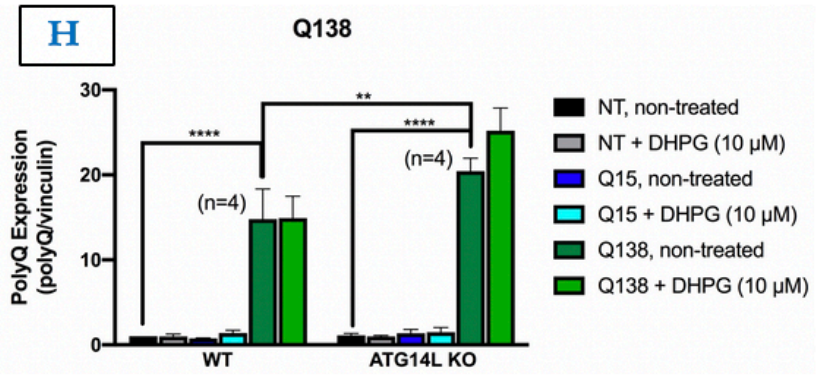
H
Q138
PolyQ Expression
(polyQ/vinculin)
30
20
10
0
**
****
****
(n=4)
(n=4)
WT
ATG14L KO
NT, non-treated
NT + DHPG (10 µM)
Q15, non-treated
Q15 + DHPG (10 µM)
Q138, non-treated
Q138 + DHPG (10 µM)

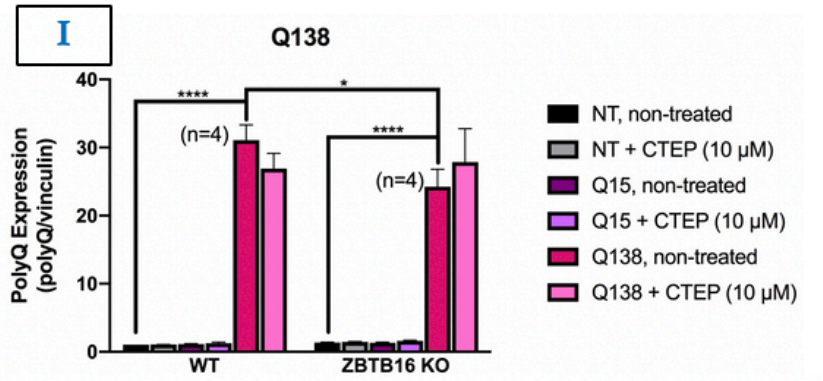
I
Q138
PolyQ Expression
(polyQ/vinculin)
40
30
20
10
0
*
****
****
(n=4)
(n=4)
WT
ZBTB16 KO
NT, non-treated
NT + CTEP (10 µM)
Q15, non-treated
Q15 + CTEP (10 µM)
Q138, non-treated
Q138 + CTEP (10 µM)

Figure 3.7. Silencing of ATG14L in STHdhQ7/Q7 cells results in accumulation of Q138, while silencing of ZBTB16 in STHdhQ7/Q7 cells results in clearance of Q138. (A) WT, ATG14L KO, and ZBTB16 KO cells transfected with either Q15 or Q138. **(B-E)** Representative western blots for Q15 (YFP antibody) (n=4), and Q138 (polyQ antibody) (n=4) with the corresponding loading controls in cell lysates from STHdhQ7/Q7 wild type (WT), $ATG14L^{-/-}$ xSTHdhQ7/Q7 cells (ATG14L KO), and $ZBTB16^{-/-}$xSTHdhQ7/Q7 cells (ZBTB16 KO) with no transfection, transfection with Q15, and transfection with Q138, after treatment with either DHPG (10 μM), CTEP (10 μM), or HBSS. **(F-I)** Quantification of blots represented in (B-E) shown as the mean ± SEM for fold change in protein expression relative to the loading control. * $p<0.05$, ** $p<0.01$, and **** $p<0.0001$ by two-way ANOVA and Fisher's LSD comparisons.

3.12 Silencing of ATG14L and ZBTB16 expression result in decreased mGluR5 expression

Both ATG14L and ZBTB16 are key components of the GSK3β-mediated pathway of MA (115, 195). We have previously shown that mGluR5 may regulate this pathway of MA, and therefore the expression of these proteins. However, it was unknown whether these proteins are able to in turn regulate mGluR5 expression. Therefore, we wanted to test whether silencing of ATG14L and ZBTB16 would result in any changes in mGluR5 expression. Interestingly, we found that CRISPR Cas9 induced silencing of both ATG14L and ZBTB16 in STHdhQ7/Q7 cells resulted in a significant decrease in mGluR5 expression compared to WT cells (Figures 3.8). This may indicate that both ATG14L and ZBTB16 play a role in the regulation of mGluR5 expression.

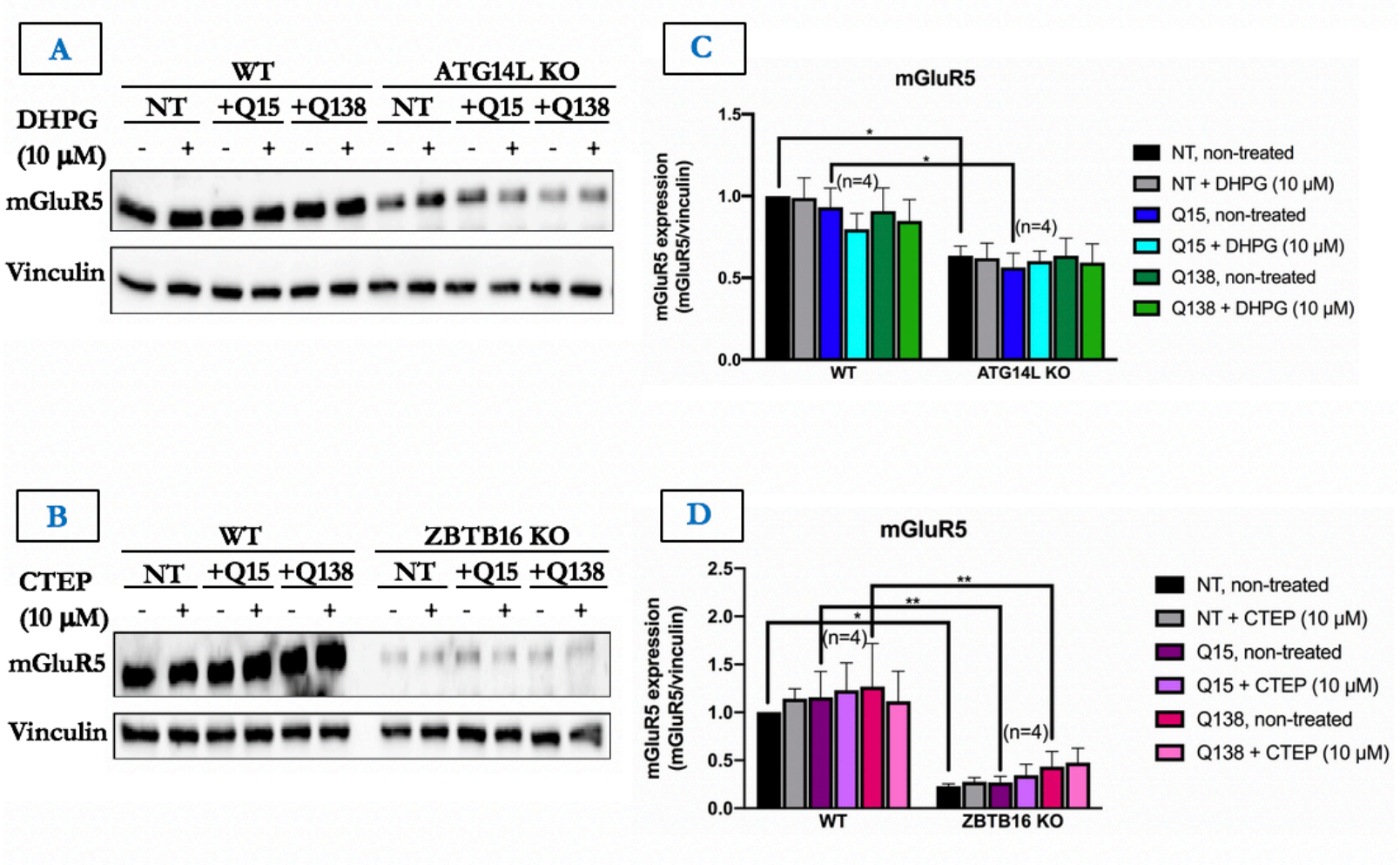

Figure 3.8. Silencing of ATG14L and of ZBTB16 in STHdhQ7/Q7 cells results in reduced mGluR5 expression. **(A-B)** Representative western blots for mGluR5 (n=4) with the corresponding loading controls in cell lysates from STHdhQ7/Q7 wild type (WT), ATG14L$^{-/-}$xSTHdhQ7/Q7 cells (ATG14L KO), and ZBTB16$^{-/-}$xSTHdhQ7/Q7 cells (ZBTB16 KO) with no transfection, transfection with Q15, and transfection with Q138, after treatment with either DHPG (10 μM), CTEP (10 μM), or HBSS. **(E-I)** Quantification of blots represented in (A-D) shown as the mean ± SEM for fold change in protein expression relative to the loading control. * $p<0.05$, and ** $p<0.01$ by two-way ANOVA and Fisher's LSD comparisons.

3.13 Treatment of STHdhQ7/Q7, ATG14L$^{-/-}$xSTHdhQ7/Q7, and ZBTB16$^{-/-}$xSTHdhQ7/Q7 cells with DHPG and CTEP was ineffective

We have previously shown that chronic blockade of mGluR5 with the NAM CTEP correlates with the activation of MA via regulation of several pathways of MA, one of which is the GSK3β-mediated pathway (115). Briefly, chronic blockade of mGluR5 in zQ175 HD mice resulted in a decrease in pGSK3β, which correlated with a decrease in ZBTB16, an increase in ATG14L, and a decrease in p62 (115). This correlated with an improvement of HD symptomology and a clearance of huntingtin aggregates (115). Therefore, it is likely that mGluR5 directly regulates the GSK3β-mediated pathway of aggrephagy, and that ZBTB16 and ATG14L are direct effectors of mGluR5. However, direct evidence supporting this hypothesis was lacking. In order to elucidate the role of ZBTB16 and ATG14L in mGluR5-mediated regulation of MA, we treated non-transfected, Q15 transfected, and Q138 transfected WT, ATG14L KO, and ZBTB16 KO cells with the group I mGluR agonist DHPG, or the mGluR5 NAM CTEP.

Prior to treatment with either DHPG or CTEP, we starved the cells for two hours with sterile HBSS (pH 7.4). We then treated cells with either 10 μM of DHPG for 10 minutes, or with 10 μM of CTEP for 30 minutes. The concentrations and treatment times were previously established by members of our laboratory. We used pGSK3β expression as a measure of whether the treatments were working: for DHPG, an increase in pGSK3β compared to non-treated conditions would signify that the treatment is working, while for CTEP, a decrease in pGSK3β compared to non-treated conditions would signify that the treatment is working. While DHPG treatments resulted in a trend of increasing pGSK3β expression, these increases were not statistically significant. Surprisingly, neither DHPG or CTEP resulted in any significant changes in expression of the members of the GSK3β-mediated pathway of MA, in markers of MA (p62 and LC3-II:LC3-I), or in Q138 levels in WT, ATG14L KO, and ZBTB16 KO cells (Figures 3.2, 3.3, 3.4, 3.5, 3.6, 3.7, 3.8). Therefore, we cannot draw any

conclusions on the role of mGluR5 in regulating the GSK3β-mediated pathway of aggrephagy. It remains unknown if ZBTB16 and ATG14L are indeed direct effectors of mGluR5. Additional experiments will be required to continue investigating this.

Chapter 4: Discussion

Treatment of HD is currently palliative, in that it largely focuses on symptom management; to date, there exist no disease-modifying treatments (1, 3). Therefore, furthering our understanding of HD pathology is critical in order to identify potential therapeutic approaches for the treatment of HD. The accumulation of misfolded aggregates of mHtt is a pathological hallmark of HD (7-10). MA is an important degradative pathway active in neurons, and is responsible for clearing misfolded protein aggregates (aggrephagy), among other constituents (7, 121). Impaired aggrephagy has been implicated in HD, and thus targeting aggrephagy may represent a promising therapeutic approach in treating HD (7, 200, 202-204). The present study confirms a key role for ATG14L in aggrephagy in striatal neurons, and identifies ZBTB16 as a key regulator of ATG14L, and of aggrephagy. Additionally, our data elucidates the relationship of both ATG14L and ZBTB16 with mHtt protein.

We have previously shown that ATG14L expression is decreased in a zQ175 HD mouse model, and this correlated with the accumulation of mHtt aggregates and worsening HD motor and cognitive symptoms (115). Therefore, we wanted to further explore the role of ATG14L as it relates to HD. Given that the striatum is the most severely impacted region of the brain in HD, we decided to use the STHdhQ7/Q7 striatal neuron model for our investigations (1, 15, 16). This model contains seven glutamine repeats, and thus encodes WT Htt protein.

In order to further characterize the role of ATG14L in aggrephagy in striatal neurons, we utilized a CRISPR Cas9 approach to silence (i.e. knockout) ATG14L expression. CRISPR Cas9 was utilized as opposed to other gene modification techniques such as TALEN, Zinc finger endonucleases as it is highly efficient, cheaper, and more straightforward than these other methods (230, 231). We opted out of using RNA interference, as CRISPR Cas9 allows the generation of a permanent genetic modification which can be passed on throughout generations (232). CRISPR is a cutting-edge technique, and is being used more and more in scientific endeavours (230, 231). Our utilization of CRISPR Cas9 was highly successful, and resulted in the generation of several ATG14L KO cell lines.

ATG14L plays a key role in both the induction of mammalian MA, and in the fusion of autophagosomes with lysosomes (124, 126, 160, 165). As a key component of vps34 complexes, which mediate the production of PI3P critical to developing autophagosomes, ATG14L is crucial for autophagosome formation (124, 126). In mediating the interaction of the STX17 and SNAP29 complex with Vamp8, ATG14L promotes autophagosome-lysosome fusion (160, 165). Therefore, ATG14L plays a key role in various steps of MA, and it is thus unsurprising that the loss of ATG14L expression is associated with impaired MA (115, 195).

Since ATG14L plays a major role in MA, it is unsurprising that our data indicate that silencing of ATG14L expression in STHdhQ7/Q7 striatal neurons resulted in an inhibition of MA. We have shown that ATG14L KO cells exhibit a large increase in expression of p62, and in LC3-II:LC3-I expression. p62 is a widely used marker of MA, as it binds ubiquitinated cargo and targets it to the autophagosome via an interaction with LC3-II (which is bound to the autophagosome membrane) and is degraded upon autophagosome-lysosome fusion with the contents of the autophagolysosome (189-191). Therefore, when MA is inhibited, p62 accumulates in the cytoplasm, and when MA is active, p62 is degraded and its cytoplasmic expression decreases (189-191). Therefore, the increase in p62 expression that we have observed in the ATG14L KO cells compared to WT STHdhQ7/Q7 cells represents an inhibition of MA, as expected, given that ATG14L is essential for autophagosome formation. During autophagosome membrane formation, the cytosolic form of LC3, LC3-I, is conjugated to PE, to form the membrane-bound form, LC3-II, which is present on both the outer and inner membranes of the developing autophagosome (234, 237). Upon maturation of the autophagosome, PE is removed from LC3-II by ATG4, thereby removing LC3-II from the outer membrane (234, 237). Thus, upon autophagosome maturation, LC3-II is removed from the outer membrane, but remains on the inner (luminal) membrane (237). LC3-II expression levels correlate with autophagosome numbers, and the ratio of LC3-II:LC3-I is often used as a marker of MA activity (234, 237, 238). Our data indicate an abnormal accumulation of LC3-II in ATG14L KO cells in comparison to WT STHdhQ7/Q7 cells, as shown by an increase in the LC3-II:LC3-I ratio. However,

while LC3-II is degraded during MA, interpreting LC3-II data can be difficult, as an increase in LC3-II:LC3-I can mean one of many possibilities: first, it may represent an increase in autophagosome formation (which could indicate an activation of MA), or second, it may represent a decrease in autophagosome fusion with lysosomes, and therefore a decrease in degradation of autophagic cargo (237, 238). However, because our data indicate that the ATG14L KO cells also exhibit an increase in p62, which indicates an inhibition of MA, and it is known that ATG14L plays a role in autophagosome and lysosome fusion, we believe this increase in LC3-II:LC3-I observed in the ATG14L KO cells represents an impairment in autophagosome-lysosome fusion and, in effect, degradation of autophagic cargo, resulting in an overall impairment of MA. However, use of more robust and sensitive LC3-II:LC3-I assays should be used in the future to confirm or deny this theory.

In addition to ATG14L, beclin-1 is a critically important component of vps34 complexes responsible for PI3P production, and is thus vital for autophagosome biogenesis (124, 126, 235). In addition to its role in vps34 complexes, beclin-1 also forms a complex with UVRAG (in place of ATG14L) important for autophagosome maturation and endocytosis, and with RUBICON, which promotes inhibition of MA (235). Beclin-1 contains many domains, allowing it to interact with many different proteins which act to regulate beclin-1 activity, and thereby MA as a whole (235). Therefore, beclin-1 is considered a platform by which many upstream signaling molecules interact to exert their effects on MA via regulation of beclin-1 (235). In MA, this regulation of beclin-1 occurs through post-translational modifications, including acetylation, phosphorylation, ubiquitination, etc. (235). Depending on the location and type of modification, MA may be either inhibited or activated.

In the present study, we have shown that beclin-1 expression is increased in ATG14L KO cells in comparison to WT STHdhQ7/Q7 cells. Increased beclin-1 expression indicates an activation of MA, while decreased beclin-1 expression indicates an inhibition of MA (236). Since we have shown that silencing of ATG14L expression in STHdhQ7/Q7 cells resulted in the inhibition of MA, we were expecting a decrease in beclin-1 expression that would be consistent with an inhibition of MA.

However, the increased beclin-1 expression that we have observed in ATG14L KO cells may indicate an attempt by the neurons to compensate for the inhibition of MA caused by loss of ATG14L by increasing beclin-1 levels. In addition, we consistently observed a band present above the band corresponding to beclin-1 on western blot membranes. This band is likely too large to be due to a phosphorylation event, and is more likely due to a ubiquitination event (ubiquitin groups are larger than phosphate groups). Several ubiquitination post-translational modifications of beclin-1 have been identified to date, some of which activate MA, and others which inhibit MA (235). Given that we have observed an increase in beclin-1 expression, and an increase in beclin-1 expression typically represents an activation of MA, we believe that this second band seen on the blots could represent an MA-activating ubiquitination, caused by the neurons attempting to trigger MA and compensate for the inhibition of MA due to loss of ATG14L expression. Future experiments using a pan-ubiquitin antibody on the western blots will be useful in confirming whether this band indeed represents a ubiquitination.

ZBTB16 is a core component of the ZBTB16-Cullin3-Roc1 E3 ubiquitin ligase recently identified as a key player in GSK3β-mediated regulation of MA (195). Zhang *et al* have previously shown that this GSK3β-mediated pathway of MA is under the regulation of GPCRs, and Abd-Elrahman *et al* have identified a specific GPCR, mGluR5, which may regulate this pathway (115, 195). Upon activation of mGluR5, GSK3β is phosphorylated at the S9 site, thus inhibiting the ability of GSK3β to phosphorylate and inhibit ZBTB16 (115). This leaves ZBTB16 free to interact with and ubiquitinate ATG14L, leading to the degradation of ATG14L (115). Given that ATG14L is essential for both autophagosome formation and autophagosome-lysosome fusion, it is no surprise that this leads to the inhibition of MA (115). Conversely, when mGluR5 is not activated, or is actively inhibited, GSK3β does not undergo the S9 inhibitory phosphorylation, and is able to phosphorylate ZBTB16 at the S184 and T282 sites, resulting in autoubiquitination of ZBTB16 and its degradation (115). This results in increased ATG14L, and therefore an activation of MA (115).

Since increased ZBTB16 expression was correlated with an inhibition of aggrephagy, the accumulation of huntingtin aggregates, and the worsening of HD motor and cognitive symptoms in the zQ175 HD mouse model, while decreased ZBTB16 expression was correlated with the opposite, we wanted to further investigate the role of ZBTB16 in the striatal neuron cell model, STHdhQ7/Q7 (115). As with the generation of our ATG14L KO cell line, we successfully utilized CRISPR to silence ZBTB16 expression in STHdhQ7/Q7 cells.

Our data indicate that silencing of ZBTB16 in STHdhQ7/Q7 striatal neurons results in an activation of MA, as shown by a decrease in the expression of p62, and an increase in the expression of ATG14L. As previously discussed, p62 is a widely used marker of autophagy, as it binds cargo and is degraded with it when MA is active (189-191). Therefore, the large decrease in expression of p62 in ZBTB16 KO cells is indicative of an activation of MA. Decreased ATG14L expression has previously been correlated with inhibition of MA, while increased ATG14L expression has been correlated with activation of MA (115, 195). Therefore, the increase in ATG14L expression observed in the ZBTB16 is indicative of activation of MA. Taken together, these results indicate that loss of ZBTB16 results in activation of MA, and that ZBTB16 likely regulates MA by modulating ATG14L levels.

Interestingly, silencing of ZBTB16 did not cause any significant changes in beclin-1. Since loss of ZBTB16 resulted in changes in both p62 and ATG14L consistent with an activation of MA, we expected to observe an increase in beclin-1 expression. Given that the sample size for beclin-1 western blot analysis was only three (n=3), it is possible that a larger sample size may reveal significant trends we were not able to observe due to a low sample size.

Homeostasis is critical in neurons, and MA plays a crucial role in maintaining neuronal homeostasis (7, 121, 198). In many important molecular signaling pathways, feedback mechanisms exist (both negative and positive) to maintain cellular homeostasis. Therefore, we believed that it was possible

that both ATG14L and ZBTB16 could exert effects on upstream proteins involved in the GSK3β-mediated pathway of MA. In the case of ATG14L, these upstream proteins include ZBTB16 and GSK3β, while for ZBTB16, GSK3β is the only known upstream protein. If ATG14L and ZBTB16 exert any effects on upstream proteins, we posited that the loss of their expression may result in changes in expression of the upstream proteins. However, no changes in ZBTB16 or pGSK3β were observed in ATG14L KO cells, and no changes in pGSK3β were observed in ZBTB16 KO cells. Therefore, the loss of ATG14L and ZBTB16 expression has no impact on upstream protein expression in the GSK3β-mediated pathway of MA. While this does provide some evidence that ATG14L and ZBTB16 do not exert any effects on upstream proteins in a feedback manner, it certainly does not rule out this possibility.

Many dysfunctions in aggrephagy have been identified in neurodegenerative disorders, including HD (121, 200, 202-204). Since aggrephagy is, to date, the only degradative pathway active in neurons capable of degrading large, toxic, misfolded protein aggregates, these deficits in aggrephagy are thought to result in devastating consequences (189). These consequences include the accumulation of aggregates, which is believed to contribute to HD symptomology (126, 189). Additionally, WT Htt is believed to play a role in selective MA (15, 54, 64, 65, 209). Loss of WT Htt function has previously been associated with the accumulation of protein and autophagosomes, and mHtt is capable of inhibiting normal MA via several mechanisms, including sequestering of the cargo receptor p62, sequestering of beclin-1, and impaired autophagosome-lysosome fusion (7, 15, 54, 194, 212-219).

As previously discussed, Abd-Elrahman *et al.* have also shown that the accumulation of Htt aggregates and worsening of HD symptoms in the zQ175 HD mouse model correlated with the inhibition of the GSK3β-mediated pathway of MA, of which ZBTB16 and ATG14L are key components (115). Therefore, we wanted to investigate the effect of both ATG14L and ZBTB16 KO's on the expression level of an mHtt fragment, Q138. In the present study, we demonstrate a clear link between

aggrephagy and both ATG14L and ZBTB16. The accumulation of mHtt aggregates is a pathological hallmark of HD. Previous studies have demonstrated a correlation between clearance of mHtt aggregates and improved HD symptomology in HD mouse models (115, 195). In addition, these studies support a role for GSK3β-mediated aggrephagy in clearing these toxic aggregates (115, 195). Here, our data show that the loss of ATG14L results in a significant accumulation of mHtt (Q138), while the loss of ZBTB16 results in a significant clearance of mHtt (Q138). This demonstrates a direct link between two key players of the GSK3β-mediated pathway of MA, and aggrephagy of mHtt. Our results show that aggrephagy is, at least in part, necessary for the clearance of mHtt. Since it is clear that both ATG14L and ZBTB16 play significant roles in mHtt aggrephagy, in the future it would be interesting to further investigate their impact on not only the number, but the size, of mHtt aggregates and inclusions characteristic of HD.

In addition to the accumulation of mHtt aggregates, neuronal cell death is a defining feature of HD pathology, especially of the MSN's of the striatum (15). Since ATG14L and ZBTB16 impact aggrephagy of mHtt, it would be interesting to investigate the results of silencing each of these proteins on cell death. Given that silencing of ATG14L causes the accumulation of mHtt aggregates in STHdhQ7/Q7 striatal neurons, it is reasonable to assume this accumulation of mHtt may lead to the activation of neurotoxic cell signaling pathways resulting in neuronal cell death. For example, mHtt is known to sensitize NMDARs containing NR1A/NR2B subunits, which can lead to an influx of calcium (91, 92). This influx of calcium can trigger apoptosis and contribute to mitochondrial dysfunction, both of which can contribute to the neuronal cell death observed in HD (4, 89, 90). On the other hand, since silencing of ZBTB16 leads to clearance of mHtt aggregates in STHdhQ7/Q7 cells, it is possible that fewer neurotoxic signaling pathways triggered by mHtt which contribute to neuronal cell death are activated. This would lead to a reduction in neuronal cell death associated with HD.

An increase in pGSK3β has previously been shown to correlate with an accumulation of Htt aggregates and worsening of HD symptoms, in addition to an inhibition of aggrephagy (115). This suggests a role for GSK3β in HD-related inhibition of aggrephagy. Our data confirm our previous findings, as we observed an increase in pGSK3β expression in WT STHdhQ7/Q7 cells transfected with the Q138. This increase in pGSK3β was also observed in both ATG14L and ZBTB16 KO cells. This indicates that the presence of mHtt (Q138) causes an increase in phosphorylation of GSK3β in STHdhQ7/Q7 striatal neurons.

While transfection of Q138 was not expected to impact the expression of p62 in either ATG14L or ZBTB16 KO cells, we did expect to observe changes in p62 in WT STHdhQ7/Q7 striatal neurons. Since the transfection of Q138 caused a significant increase in pGSK3β expression, and increased pGSK3β expression has previously been correlated with an increase in p62 expression, indicating an inhibition of MA, in zQ175 HD mice, we expected to observe a similar increase in p62 in WT STHdhQ7/Q7 cells transfected with Q138 (115). Surprisingly, we did not observe this. While this may indicate that pGSK3β does not directly regulate aggrephagy, we cannot completely rule out the possibility that it does, as our experimental design may not have been the most effective for observing sensitive changes in MA proteins. This is in part due to the challenges of attempting to study both glutamate signaling and MA simultaneously. However, the fact that we did not observe the expected increase in p62 expression in WT cells upon transfection of Q138, may be explained by the fact that mHtt is known to sequester p62, which may have resulted in there being no observable change in p62 expression between WT non-transfected and Q138 transfected counterparts (7). Unfortunately, we also did not observe any significant changes in beclin-1 or ZBTB16 expression upon transfection of Q138. An increase in pGSK3β was expected to result in an increase in ZBTB16 expression, and the fact that it did not may reflect a flaw in the experimental approach, or it may indicate that another protein regulates ZBTB16 levels in addition to GSK3β. No change in beclin-1 expression may have

been caused by the fact that the starvation reduced autophagic load in non-transfected WT cells, meaning MA would be occurring at a very low level and changes in MA proteins would have been difficult to observe. Since mHtt sequesters beclin-1, the levels of beclin-1 would have also been low in Q138 transfected WT cells (7). Therefore, beclin-1 expression would be low in both Q138 transfected and non-transfected WT cells, making it difficult to observe changes due to Q138 transfection on beclin-1 expression.

Our lab has previously shown that blocking mGluR5 signaling with the mGluR5 specific NAM CTEP, resulted in an activation of GSK3β-mediated aggrephagy (as shown by a decrease in p62, an increase in beclin-1, an increase in ATG14L, a decrease in ZBTB16, and a decrease in pGSK3β), which correlated with clearance of Htt aggregates and improvement of HD motor and cognitive symptoms (115). We therefore hypothesized that mGluR5 regulates the GSK3β-mediated regulation of aggrephagy. In this study, we attempted to confirm a direct link between mGluR5 and this pathway of MA, and to show that ZBTB16 and ATG14L are effectors of mGluR5. Unfortunately, neither treatment with the group I mGluR agonist DHPG, or CTEP was successful. DHPG and CTEP effectiveness was measured by pGSK3β expression in WT cells: DHPG should have caused an increase, while CTEP should have caused a decrease. However, neither DHPG or CTEP caused any significant changes in pGSK3β expression, in any other proteins believed to be part of the GSK3β-mediated pathway of MA, or in markers of MA. Both DHPG and CTEP have previously been used in our lab to investigate other signaling pathways regulated by mGluR5, but never in a study where aggrephagy was investigated. Perhaps the protocol we used was not the best in terms of investigating both glutamate signaling and MA. Changes in MA may have been difficult to observe upon treatment with CTEP as nutrient starvation (achieved by starvation with HBSS) is known to induce MA (167-174). Therefore, having already been induced by starvation conditions, treatment with CTEP, which was predicted to activate MA, would not have shown any significant changes to the non-treated cells. In addition, we wanted to observe changes in MA caused by DHPG and CTEP, not those caused by

nutrient starvation. Therefore, this long starvation step may have prevented us from successfully achieving this.

Alternatively, it is also possible that, because the long two-hour HBSS starvation would have resulted in the removal of culture medium containing cellular debris and waste products, then in cells without transfection of Q138 there would not have been a significant load/cargo for the cells to degrade via aggrephagy. Therefore, treatment with DHPG, which was predicted to inhibit MA, would not have shown any significant changes in comparison to non-treated cells. The same is true of treatment with CTEP. While that certainly may help to explain why the treatments appeared ineffective in non-Q138 transfected cells, it does not fully explain why DHPG and CTEP treatment had no impact on WT cells transfected with Q138. Q138 should have acted as autophagic cargo. Perhaps for the Q138 transfection experiments, since Q138 was expected to impact MA, a long starvation was not appropriate (as starvation affects MA, as previously discussed) as we did not want to observe starvation effects on MA, but the effects of DHPG and CTEP on aggrephagy related to Q138. This might also explain why Q138 transfection with no treatment also did not cause any changes in markers of MA, or in members of the GSK3β-mediated signaling pathway aside from pGSK3β. While HBSS starvation of the cells was necessary in order to ensure that the effects observed were due to mGluR5 activation or inhibition, perhaps the starvation was too long in order to efficiently evaluate aggrephagy of Q138. Another lab studying mGluR5 signaling with DHPG has used a starvation time of 20 minutes (113). To conclude, it would appear that our lab's protocol for DHPG and CTEP treatment requires modifications in terms of studying aggrephagy-related changes. As such, knowing whether mGluR5 regulates GSK3β-mediated regulation of aggrephagy, and whether ATG14L and ZBTB16 are direct effectors of mGluR5, remains unknown and requires further investigation.

While we could not provide evidence that ZBTB16 and ATG14L are direct effectors of mGluR5, our data do indicate that silencing of ZBTB16 and ATG14L in STHdhQ7/Q7 cells impacts mGluR5

expression. Surprisingly, both ZBTB16 KO and ATG14L KO cells demonstrate a significant decrease in mGluR5 expression compared to WT STHdhQ7/Q7 cells. ZBTB16 is a known transcription factor involved in immune responses, and in repression of cell cycle control (239, 240). Given that mGluR5 stimulation is associated with inhibition of aggrephagy, perhaps ZBTB16 acts as a transcription factor which upregulates mGluR5 to further exert its inhibitory effects on aggrephagy, in addition to decreasing ATG14L levels (115). If this is the case, loss of ZBTB16 could result in a reduction of mGluR5 expression, which would contribute to a greater increase in activation of aggrephagy observed in ZBTB16 KO cells. ATG14L KO cells exhibiting a decrease in mGluR5 is quite surprising, but perhaps the decrease in mGluR5 activation, which is correlated with inhibition of aggrephagy, is an attempt by the cell to compensate for the inhibition of aggrephagy caused by the loss of ATG14, as we theorized to explain the increase in beclin-1 expression. Nevertheless, it is clear that further studies investigating the relationship between mGluR5 and ZBTB16 and ATG14L, respectively, are necessary.

To conclude, we provide evidence that ATG14L is essential for aggrephagy in STHdhQ7/Q7 striatal neurons, and that ZBTB16 is a critical regulator of aggrephagy through the regulation of ATG14L. Specifically, we have shown that loss of ATG14L results in the accumulation of mHtt, while loss of ZBTB16 results in the clearance of mHtt, indicating an important role for both in the context of HD. However, whether they are direct effectors of mGluR5 remains elusive, and will require further investigation. Both ATG14L and ZBTB16 play important roles in aggrephagy in STHdhQ7/Q7 cells, and modulation of their expression represents an attractive potential therapeutic approach for the treatment of HD. Future studies will determine whether this is a viable, therapeutic approach in the effort to find novel and effective treatments for HD.

References

1. Ghosh, R., Tabrizi, S. J. (2018). Clinical Features of Huntington's Disease. *Advances in Experimental Medicine and Biology*, *1049*, 1–28. https://doi.org/10.1038/nprot.2013.143.Genome
2. McColgan, P., Tabrizi, J. (2018). Huntington's disease : a clinical review. *European Journal of Neurology*, *25*, 24–34. https://doi.org/10.1111/ene.13413
3. Kumar, A., Kumar, V., Singh, K., Kumar, S., & Kim, Y. (2020). Therapeutic Advances for Huntington's Disease. *Brain Sciences*, *10*(43). https://doi.org/10.3390/brainsci10010043
4. Ribeiro, F. M., Pires, R. G. W., Ferguson, S. S. G. (2011). Huntington's Disease and Group I Metabotropic Glutamate Receptors. *Molecular Neurobiology*, *43*, 1–11. https://doi.org/10.1007/s12035-010-8153-1
5. Li, S. H., Li, X. J. (2004). Huntingtin-protein interactions and the pathogenesis of Huntington's disease. *Trends in Genetics*, *20*, 146-154. https://doi.org/10.1016/j.tig.2004.01.008
6. Young, A. B. (2003). Huntingtin in health and disease. *Journal of Clinical Investigation, 111*, 299-302. https://doi.org/10.1172/JCI17742
7. Cortes, C. J., & La Spada, A. R. (2014). The many faces of autophagy dysfunction in Huntington's disease: From mechanism to therapy. *Drug Discovery Today*, *19*(7), 963–971. https://doi.org/10.1016/j.drudis.2014.02.014
8. Ross, C. A., & Poirier, M. A. (2004). Protein aggregation and neurodegenerative disease. *Nature Medicine*, *10*(7), S10. https://doi.org/10.1038/nm1066
9. Taylor, J. P. (2002). Toxic Proteins in Neurodegenerative Disease. *Science*, *296*(5575), 1991–1995. https://doi.org/10.1126/science.1067122
10. Vonsattel, J. P., Myers, R. H., Stevens, T. J., Ferrante, R. J., Bird, E. D., & Richardson, E. J. (1985). Neuropathological classification of Huntington's disease. *Journal of Neuropathology and Experimental Neurology*, *44*(6), 559–577. https://doi.org/10.1097/00005072-198511000-00003
11. Hardy, J., and Selkoe, D.J. (2002). The amyloid hypothesis of Alzheimer's disease: progress and problems on the road to therapeutics. *Science,* 297, 353–356. https://doi.org/10.1126/science.1072994
12. Forno, L.S. (1996). Neuropathology of Parkinson's disease. *Journal of Neuropathology and Experimental Neurology,* 55, 259–272. https://doi.org/10.1097/00005072-199603000-00001
13. Nussbaum, R.L., and Ellis, C.E. (2003). Alzheimer's disease and Parkinson's disease. *The New England Journal of Medicine,* 348, 1356–1364. https://doi.org/10.1056/NEJM2003ra020003
14. Paulson, H. L. (1999). HUMAN GENETICS '99 : TRINUCLEOTIDE REPEATS Protein Fate in Neurodegenerative Proteinopathies : Polyglutamine Diseases Join the (Mis)Fold. *American Journal of Human Genetics*, *64*, 339–345.
15. Croce, K. R., & Yamamoto, A. (2019). A role for autophagy in Huntington's disease. *Neurobiology of Disease*, *122*, 16–22. https://doi.org/10.1016/j.nbd.2018.08.010
16. Cepeda, C., Tong, X. (2018). Huntington's disease : From basic science to therapeutics. *CNS Neuroscience and Therapeutics*, *24*, 247–249. https://doi.org/10.1111/cns.12841
17. Sun, Y., Zhang, Y., & Wu, Z. (2017). Huntington's Disease : Relationship Between Phenotype and Genotype. *Molecular Neurobiology*, *54*, 342–348. https://doi.org/10.1007/s12035-015-9662-8
18. Tabrizi, S. J., Langbehn, D. R., Leavitt, B. R., *et al.* (2009). Biological and clinical manifestations of Huntington's disease in the longitudinal TRACK-HD study: cross-sectional analysis of baseline data. *The Lancet Neurology, 8*, 791-801. https://doi.org/10.1016/S1474-4422(09)70170-X
19. Papoutsi, M., Labuschagne, I., Tabrizi, S. J., Stout, J. C. (2014). The cognitive burden in Huntington's disease: pathology, phenotype, and mechanisms of compensation. *Movement Disorders, 29*, 673-683. https://doi.org/10.1002/mds.25864
20. Wyant, K. J., Ridder, A. J., & Dayalu, P. (2017). Huntington's Disease — Update on Treatments. *Current Neurology and Neuroscience Reports*, *17*(33). https://doi.org/10.1007/s11910-017-0739-9

21. Bates, G. P., Dorsey, R., Gusella, J. F., *et al.* (2015). Huntington disease. *Nature Reviews Disease Primers, 1*(15005). https://doi.org/10.1038/nrdp.2015.5
22. Dorsey, E. R., Beck, C. A., Darwin, K., *et al.* (2013). Natural history of Huntington disease. *JAMA Neurology, 70*, 1520-1530. https://doi.org/10.1001/jamaneurol.2013.4408
23. Plotkin, J. L., Surmeier, D. J. (2015). Corticostriatal synaptic adaptations in Huntington's disease. *Current Opinion in Neurobiology, 33C*, 53-62. https://doi.org/10.1016/j.conb.2015.01.020
24. Wang, H., Chen, X., Li, Y., Tang, T. S., Bezprozvanny, I. (2010). Tetrabenazine is neuroprotective in Huntington's disease mice. *Molecular Neurodegeneration, 5*(18). https://doi.org/10.1186/1750-1326-5-18
25. Coppen, E. M., Roos, R. A. (2017). Current Pharmacological Approaches to Reduce Chorea in Huntington's Disease. *Drugs, 77*, 29-46. https://doi.org/10.1007/s40265-016-0670-4
26. de Tommaso, M., Serpino, C., Sciruicchio, V. (2011). Management of Huntington's disease: Role of tetrabenazine. *Therapeutics and Clinical Risk Management, 7*, 123-129. https://doi.org/10.2147/TCRM.S17152
27. Claassen, D. O., Carroll, B., De Boer, L. M., Wu, E., Ayyagari, R., Candhi, S., Stamler, D. (2017). Indirect tolerability comparison of Deutetrabenazine and Tetrabenazine for Huntington disease. *Journal of Clinical Movement Disorders, 4*(3). https://doi.org/10.1186/s40734-017-0051-5
28. Group, H. S. (2006). Tetrabenazine as antichorea therapy in Huntington disease: a randomized controlled trial. *Neurology, 66*, 366-372. https://doi.org/10.1212/01.wnl.0000198586.85250.13
29. Group, H. S., Frank, S., Testa, C. M., Stamler, D., Kayson, E., *et al.* (2016). Effect of deutetrabenazine on chorea among patients with Huntington disease: a randomized clinical trial. *JAMA, 316*(1), 40-50. https://doi.org/10.1001/jama.2016.8655
30. Tabrizi, S. J., Scahill, R. I., Owen, G., *et al.* (2013). Predictors of phenotypic progression and disease onset in premanifest and early-stage Huntington's disease in the TRACK-HD study: analysis of 36-month observational data. *The Lancet Neurology, 12*(7), 637-649. https://doi.org/10.1016/S1474-4422(13)70088-7
31. Paulsen, J. S., Butters, N., Sadek, J. R., Johnson, S. A., Salmon, D. P., Swerdlow, N. R., & Swenson, M. R. (1995). Distinct cognitive profiles of cortical and subcortical dementia in advanced illness. *Neurology, 45*(5), 951-956. https://doi.org/10.1212/wnl.45.5.951
32. van Duijn, E., *et al.* (2014). Neuropsychiatric symptoms in a European Huntington's disease cohort (REGISTRY). *Journal of Neurology, Neurosurgery, and Psychiatry, 85*(12), 1411-1418. https://doi.org/10.1136/jnnp-2013-307343
33. van Duijn, E., Kingma, E. M., van der Mast, R. C. (2007). Psychopathology in verified Huntington's disease gene carriers. *The Journal of Neuropsychiatry and Clinical Neurosciences, 19*(4), 441-448. https://doi.org/10.1176/jnp.2007.19.4.441
34. Moulton, C. D., Hopkins, C. W., & Bevan-Jones, W. R. (2014). Systemic review of pharmacological treatments for depressive symptoms in Huntington's disease. *Movement Disorders, 29*(12), 1556-1561. https://doi.org/10.1002/mds.25980
35. Como, P. G., Rubin, A. J., O'Brien, C. F., Lawler, K., Jickey, C., Rubin, A. E., Henderson, R., McDermott, M. P., McDermott, M., Steinberg, K., & Shoulson, I. (1997). A controlled trial of fluoxetine in nondepressed patients with Huntington's disease. *Movement Disorders, 12*(3), 397-401. https://doi.org/10.1002/mds.870120319
36. Beglinger, L. J., Adams, W. H., Langbehn, D., Fiedorowicz, J. G., Jorge, R., Biglan, K., Caviness, J., Olson, B., Robinson, R. G., Kieburtz, K, & Paulsen, J. S. (2014). Results of the citalopram to enhance cognition in Huntington disease trial. *Movement Disorders, 29*(3), 401-405. https://doi.org/10.1002/mds.25750
37. Holl, A. K., Wilkinson, L., Painold, A., Holl, E. M., & Bonelli, R. M. (2010). Combating depression in Huntington's disease: effective antidepressant treatment with venlafaxine XR. *International Clinical Psychopharmacology, 25*(1), 46-50. https://doi.org/10.1097/YIC.0b013e3283348018
38. Duff, K., Beglinger, L. J., O'Rourke, M. E., Nopoulos, P., Paulson, H. L., & Paulsen, J. S. (2008). Risperidone and the treatment of psychiatric, motor, and cognitive symptoms in

Huntington's disease. *Annals of Clinical Psychiatry, 20*(1), 1-3. https://doi.org/10.1080/10401230701844802
39. Ciammola, A., Sassone, J., Colciago, C., Mencacci, N. E., Poletti, B., Ciarmiello, A., Squitieri, F., & Silani, V. (2009). Aripiprazole in the treatment of Huntington's disease: a case series. *Neuropsychiatric Disease and Treatment, 5*, 1-4.
40. Sajatovic, M., *et al.* (1991). Clozapine treatment of psychiatric symptoms resistant to neuroleptic treatment in patients with Huntington's chorea. *Neurology, 41*(1), 156. https://doi.org/10.1212/wnl.41.1.156
41. Paleacu, D., Anca, M., Giladi, N. (2002). Olanzapine in Huntington's disease. *Acta Neurologica Scandinavica, 105*(6), 441-444. https://doi.org/10.1034/j.1600-0404.2002.01197.x
42. Squitieri, F., Cannella, M., Porcellini, A., Brusa, L., Simonelli, M., & Ruggieri, S. (2001). Short-term effects of olanzapine in Huntington disease. *Neuropsychiatry, Neuropsychology, and Behavioral Neurology, 14*(1), 69-72.
43. Brusa, L., Orlacchio, A., Moschella, V., Iani, C., Bernardi, G., & Mercuri, N. B. (2009). Treatment of the symptoms of Huntington's disease: preliminary results comparing aripiprazole and tetrabenazine. *Movement Disorders, 24*(1), 126-129. https://doi.org/10.1002/mds.22376
44. Craufurd, D., Thompson, J. C., Snowden, J. S. (2001). Behavioral changes in Huntington disease. *Neuropsychiatry, Neuropsychology, and Behavioral Neurology, 14*, 219-226.
45. Paulsen, J. S., Ready, R. E., Hamilton, J. M., Mega, M. S., & Cummings, J. L. (2001). Neuropsychiatric aspects of Huntington's disease. *Journal of Neurology, Neurosurgery, and Psychiatry,71*(3), 310-314. https://doi.org/10.1136/jnnp.71.3.310
46. Krishnamoorthy, A., Craufurd, D. (2011). Treatment of apathy in Huntington's disease and other movement disorders. *Current Treatment Options in Neurology, 13*(5), 508-519. https://doi.org/10.1007/s11940-011-0140-y
47. The Huntington's Disease Collaborative Research Group. (1993). A novel gene containing a trinucleotide repeat that is expanded and unstable on Huntington's disease chromosomes. *Cell, 72*, 971-983. https://doi.org/10.1016/0092-8674(93)90585-e
48. Ambrose, C. M., Duyao, M. P., Barnes, G., *et al.* (1994). Structure and expression of the Huntington's disease gene: evidence against simple inactivation due to an expanded CAG repeat. *Somatic Cell and Molecular Genetics, 20,* 27-38. https://doi.org/10.1007/BF02257483
49. Nance, M. A. (2017). Genetics of Huntington disease. In *Handbook of Clinical Neurology: Huntington Disease* (1st ed., Vol. 144). https://doi.org/10.1016/B978-0-12-801893-4.00001-8
50. Kay, C., Fisher, E., Michael, H. (2014). Epidemiology. In: Tabrizi, S. J., Jones, L (eds)., Bates, G. Oxford University Press, Huntington's disease, pp131-164.
51. Snell, R. G., MacMillan, J. C., Cheadle, J. P., *et al.* (1993). Relationship between trinucleotide repeat expansion and phenotypic variation in Huntington's disease. *Nature Genetics, 4,* 393-397. https://doi.org/10.1038/ng0893-393
52. The American College of Medical Genetics/American Society of Human Genetics Huntington Disease Genetic Testing Working Group. (1998). ACMG/ASHG statement. Laboratory guidelines for Huntington disease genetic testing. *American Journal of Human Genetics, 62,* 1243-1247.
53. Rubinsztein, D. C., Leggo, J., Coles, R., *et al.* (1996). Phenotypic characterization of individuals with 30-40 CAG repeats in the Huntington disease (HD) gene reveals HD cases with 36 repeats and apparently normal elderly individuals with 36-39 repeats. *American Journal of Human Genetics, 59,* 16-22.
54. Harding, R. J., & Tong, Y. (2018). Proteostasis in Huntington's disease : disease mechanisms and therapeutic opportunities. *Acta Pharmacologica Sinica*, *39*, 754–769. https://doi.org/10.1038/aps.2018.11
55. Lee, J. M., Ramos, E. M., Lee, J. H., Gillis, T., Mysore, J. S., Hayden, M. R., *et al.* (2012). CAG repeat expansion in Huntington disease determines age at onset in a fully dominant fashion. *Neurology, 78,* 690-695. https://doi.org/10.1212/WNL.0b013e318249f683

56. Barbeau, A. (1970). Parental ascent in the juvenile form of Huntington's chorea. *The Lancet, 2,* 937. https://doi.org/10.1016/s0140-6736(70)92119-7
57. Gonzalez-Alegre, P., Afifi, A. K. (2006). Clinical characteristics of childhood-onset (juvenile) Huntington disease: report of 12 patients and review of the literature. *Journal of Child Neurology, 21,* 223-229. https://doi.org/10.2310/7010.2006.00055
58. Sequeiros, J., Ramos, E. M., Cerqueira, J., Costa, M. C., Sousa, A., Pinto-Basto, J., Alonso, I. (2010). Large normal and reduced penetrance alleles in Huntington disease: instability in families and frequency at the laboratory, at the clinic and in the population. *Clinical Genetics, 78,* 381-387. https://doi.org/10.1111/j.1399-0004.2010.01388.x
59. Saudou, F., Humbert, S. (2016). The Biology of Huntingtin. *Neuron, 89,* 910-926. https://doi.org/10.1016/j.neuron.2016.02.003
60. Ratovitski, T., O'Meally, R. N., Jiang, M., Chaerkady, R., Chighladze, E., Stewart, J. C., *et al.* (2017). Post-translational modifications (ptms), identified on endogenous Huntingtin, cluster within proteolytic domains between HEAT repeats. *Journal of Proteome Research, 16,* 2692-2708. https://doi.org/10.1021/acs.jproteome.6b00991
61. Godinho, B. M., *et al.* (2015). Delivering a disease-modifying treatment for Huntington's disease. *Drug Discovery Today, 20*(1), 50-64. https://doi.org/10.1016/j.drudis.2014.09.011
62. Shannon, K. M., Fraint, A. (2015). Therapeutic advances in Huntington's disease. *Movement Disorders, 30*(11), 1539-1546. https://doi.org/10.1002/mds.26331
63. Dayalu, P., Albin, R. L. (2015). Huntington disease: pathogenesis and treatment. *Neurologic Clinics, 33*(1), 101-114. https://doi.org/10.1016/j.ncl.2014.09.003
64. Zheng, Z., Diamond, M. I. (2012). Huntington disease and the huntingtin protein. *Progress in Molecular Biology and Translational Science, 107,* 189-214. https://doi.org/10.1016/B978-0-12-385883-2.00010-2
65. Rui, Y. N., Xu, Z., Patel, B., Chen, Z., Chen, D., Tito, A., *et al.* (2015). Huntingtin functions as a scaffold for selective macroautophagy. *Nature Cell Biology, 17,* 262-275. https://doi.org/10.1038/ncb3101
66. Kalathur, R. K. R., Pinto, J. P., Sahoo, B., Chaurasia, G., Futschik, M. E. (2017). HDNetDB: a molecular interaction database for network-oriented investigations into huntington's disease. *Scientific Reports, 7,* 5216. https://doi.org/10.1038/s41598-017-05224-0
67. Giorgini, F. (2013). A flexible polyglutamine hinge opens new doors for understanding huntingtin function. *Proceedings of the National Academy of Sciences of the United States of America, 110,* 14516-14517. https://doi.org/10.1073/pnas.1313668110
68. Myers, R. H., Leavitt, J., Farrer, L. A., Jagadeesh, J., McFarlane, H., Mastromauro, C. A., Mark, R. J., Gusella, J. F. (1989). Homozygote for Huntington disease. *American Journal of Human Genetics, 45*(4), 615-618.
69. Wexler, N. S., Young, A. B., Tanzi, R. E., Travers, H., Starosta-Rubinstein, S., Penney, J. B., Snodgrass, S. R., Shoulson, I., Gomez, F., Arroyo, M. A. R., *et al.* (1987). Homozygotes for Huntington's disease. *Nature, 326*(6109), 194-197. https://doi.org/10.1038/326194a0
70. Trepte, P., Strempel, N., Wanker, E. E. (2014). Spontaneous self-assembly of pathogenic huntingtin exon 1 protein into amyloid structures. *Essays in Biochemistry, 56,* 167-180. https://doi.org/10.1042/bse0560167
71. Thakur, A. K., Jayaraman, M., Mishra, R., Thakur, M., Chellgren, V. M., Byeon, I. J., *et al.* Polyglutamine disruption of the huntingtin exon-1 N-terminus triggers a complex aggregation mechanism. *Nature Structural and Molecular Biology, 16*, 380-389. https://doi.org/10.1038/nsmb.1570
72. Pieri, L., Madiona, K., Bousset, L., Melki, R. (2012). Fibrillar α-synuclein and Huntingtin exon 1 assemblies are toxic to the cells. *Biophysical Journal, 102,* 2894-2905. https://doi.org/10.1016/j.bpj.2012.04.050
73. Mangiarini, L., Sathasivam, K., Seller, M., Cozens, B., Harper, A., Hetherington, C., *et al.* (1996). Exon 1 of the HD gene with an expanded CAG repeat is sufficient to cause a progressive

neurological phenotype in transgenic mice. *Cell, 87,* 493-506. https://doi.org/10.1016/s0092-8674(00)81369-0
74. DiFiglia, M., Sapp, E., Chase, K. O., Davies, S. W., Bates, G. P., Vonsattel, J. P., & Aronin, N. (1997). Aggregation of huntingtin in neuronal intranuclear inclusions and dystrophic neurites in brain. *Science, 277,* 1990-1993. https://doi.org/10.1126/science.227.5334.1990
75. Lewerenz, J., Maher, P., & Maher, P. (2015). Chronic Glutamate Toxicity in Neurodegenerative Diseases — What is the Evidence ? *Frontiers in Neuroscience*, *9*(469). https://doi.org/10.3389/fnins.2015.00469
76. Miyamoto, E. (2006). Molecular mechanism of neuronal plasticity: induction and maintenance of long-term potentiation in the hippocampus. *Journal of Pharmaceutical Sciences, 100,* 433-442. https://doi.org/10.1254/jphs.CPJ06007X
77. Olney, J. W. (1986). Inciting excitotoxic cytocide among central neurons. *Advances in Experimental Medicine and Biology, 203,* 631-645. https://doi.org/10.1007/978-1-4684-7971-3_48
78. Reiner, A., & Levitz, J. (2018). HHS Public Access. *Neuron*, *98*(6), 1080–1098. https://doi.org/10.1016/j.neuron.2018.05.018.Glutamatergic
79. Lodge, D. (2009). The history of the pharmacology and cloning of ionotropic glutamate receptors and the development of idiosyncratic nomenclature. *Neuropharmacology, 56,* 6-21. https://doi.org/10.1016/j.neuropharm.2008.08.006
80. Spooren, W., Lesage, A., Lavreysen, H., Gasparini, F., & Steckler, T. (2010). Metabotropic glutamate receptors: their therapeutic potential in anxiety. *Current Topics in Behavioural Neurosciences, 2,* 391-413. https://doi.org/10.1007/7854_2010_36
81. Dhami, G. K., & Ferguson, S. S. (2006). Regulation of metabotropic glutamate receptor signalling, desensitization, and endocytosis. *Pharmacology and Therapeutics, 111,* 260-271. https://doi.org/10.1016/j.pharmthera.2005.01.008
82. Olney, J. W. (1994). New mechanisms of excitatory transmitter neurotoxicity. *Journal of Neural Transmission. Supplementum, 43,* 47-51.
83. Dingledine, R., Borges, K., Bowie, D., & Traynelis, S. F. (1999). The glutamate receptor ion channels. *Pharmacological Reviews, 51,* 7-61.
84. Pin, J. P., Galvez, T., & Prezeau, L. (2003). Evolution, structure, and activation mechanism of family 3/C G-protein-coupled receptors. *Pharmacology and Therapeutics, 98,* 325-354. https://doi.org/10.1016/s0163-7258(03)00038-x
85. Ribeiro, F. M., Paquet, M., Cregan, S. P., & Ferguson, S. S. (2010). Group I metabotropic glutamate receptor signalling and its implication in neurological disease. *CNS & Neurological Disorders-Drug Targets, 9*(5), 574-595. https://doi.org/10.2174/187152710793361612
86. Beal, M. F., Kowall, N. W., Ellison, D. W., Mazurek, M. F., Swartz, K. J., & Martin, J. B. (1986). Replication of the neurochemical characteristics of Huntington's disease by quinolinic acid. *Nature, 321,* 168-171. https://doi.org/10.1038/321168a0
87. DiFiglia, M. (1990). Excitotoxic injury of the neostriatum: a model for Huntington's disease. *Trends in Neurosciences, 13,* 286-289. https://doi.org/10.1016/0166-2236(90)90111-m
88. Zeron, M. M., Hansson, O., Chen, N., Wellington, C. L., Leavitt, B. R., Brundin, P., Hayden, M. R., & Raymond, L. A. (2002). Increased sensitivity to *N*-methyl-D-aspartate receptor-mediated excitotoxicity in a mouse model of Huntington's disease. *Neuron, 33,* 849-860. https://doi.org/10.1016/s0896-6273(02)00615-3
89. Turley, K. R., Toledo-Pereyra, L. H., & Kothari, R. U. (2005). Molecular mechanisms in the pathogenesis and treatment of acute ischemic stroke. *Journal of Investigative Surgery, 18,* 207-218. https://doi.org/10.1080/08941930591004449
90. Sims, N. R., & Muyderman, H. (2010). Mitochondria, oxidative metabolism and cell death in stroke. *Biochimica et Biophysica Acta, 1802*(1), 80-91. https://doi.org/10.1016/j.bbadis.2009.09.003
91. Chen, N., Luo, T., Wellington, C., Metzler, M., McCutcheon, K., Hayden, M. R., & Raymond, L. A. (1999). Subtype-specific enhancement of NMDA receptor currents by mutant huntingtin. *Journal of Neurochemistry, 72,* 1890-1898. https://doi.org/10.1046/j.1471-4159.1999.0721890.x

92. Zeron, M. M., Chen, N., Moshaver, A., Lee, A. T., Wellington, C. L., Hayden, M. R., & Raymond, L. A. (2001). Mutant huntingtin enhances excitotoxic cell death. *Molecular and Cellular Neuroscience, 17,* 41-53. https://doi.org/10.1006/mcne.2000.0909
93. Landwehrmeyer, G. B., Standaert, D. G., Testa, C. M., Penney, J. B. Jr., & Young, A. B. (1995). NMDA receptor subunit mRNA expression by projection neurons and interneurons in rat striatum. *The Journal of Neuroscience, 15,* 5297-5307.
94. Ribeiro, F. M., Vieira, L. B., Pires, R. G. W., Olmo, R. P., & Ferguson, S. S. G. (2017). Metabotropic glutamate receptors and neurodegenerative diseases. *Pharmacological Research*, *115*, 179–191. https://doi.org/10.1016/j.phrs.2016.11.013
95. Conn, P. J., & Pin, J. P. (1997). Pharmacology and functions of metabotropic glutamate receptors. *Annual Review of Pharmacology and Toxicology, 37,* 205-237. https://doi.org/10.1146/annurev.pharmtox.37.1.205
96. Bruno, V., Battaglia, G., Copani, A., Cespedes, V. M., Galindo, M. F., Cena, V., Sanchez-Prieto, J., Gasparini, F., Kuhn, R., Flor, P. J., & Nicoletti, F. (2001). An activity-dependent switch from facilitation to inhibition in the control of excitotoxicity by group I metabotropic glutamate receptors. *European Journal of Neuroscience, 13*(8), 1469-1478. https://doi.org/10.1046/j.0953-816x.2001.01541.x
97. Iacovelli, L., Bruno, V., Salvatore, L., Melchiorri, D., Gradini, R., Caricasole, A., Barletta, E., De Blasi, A., & Nicoletti, F. (2002). Native group-III metabotropic glutamate receptors are coupled to the mitogen-activated protein kinase/phosphatidylinositol-3-kinase pathways. *Journal of Neurochemistry, 82*(2), 216-223. https://doi.org/10.1046/j.1471-4159.2002.00929.x
98. Ferraguti, F., Baldani-Guerra, B., Corsi, M., Nakanishi, S., & Corti, C. (1999). Activation of the extracellular signal-regulated kinase 2 by metabotropic glutamate receptors. *European Journal of Neuroscience, 11*(6), 2073-2082. https://doi.org/10.1046/j.1460-9568.1999.00626.x
99. Schoepp, D. D. (2001). Unveiling the functions of presynaptic metabotropic glutamate receptors in the central nervous system. *Journal of Pharmacology and Experimental Therapeutics, 299*(1), 12-20.
100. Sharon, D., Vorobiov, D., & Dascal, N. (1997). Positive and negative coupling of the metabotropic glutamate receptors to a G protein-activated K^+ channel, GIRK, in Xenopus oocytes. *Journal of General Physiology, 109*(4), 477-490. https://doi.org/10.1085/jgp.109.4.477
101. Tang, T. S., Tu, H., Chan, E. Y., Maximov, A., Wang, Z., Wellington, C. L., Hayden, M. R., & Bezprozvanny, I. (2003). Huntingtin and huntingtin-associated protein 1 influence neuronal calcium signaling mediated by inositol-(1,4,5)-triphosphate receptor type 1. *Neuron, 39*(2), 227-239. https://doi.org/10.1016/s0896-6273(03)00366-0
102. Tang, T. S., Slow, E., Lupu, V., Stavrovskaya, I. G., Sugimori, M., Llinas, R., Kristal, B. S., Hayden, M. R., & Bezprozvanny, I. (2005). Disturbed Ca^{2+} signaling and apoptosis of medium spiny neurons in Huntington's disease. *Proceedings of the National Academy of Sciences of the United States of America, 102*(7), 2602-2607. https://doi.org/10.1073/pnas.0409402102
103. Tu, J. C., Xiao, B., Yuan, J. P., Lanahan, A. A., Leoffert, K., Li, M., Linden, D. J., & Worley, P. F. (1998). Homer binds a novel proline-rich motif and links group 1 metabotropic glutamate receptors with IP_3 receptors. *Neuron, 21*(4), 717-726. https://doi.org/10.1016/s0896-6273(00)80589-9
104. Tu, J. C., Xiao, B., Naisbitt, S., Yuan, J. P., Petralia, R. S., Brakeman, P., Doan, A., Aakalu, V. K., Lanahan, A. A., Sheng, M., & Worley, P. F. (1999). Coupling of mGluR/Homer and PSD-95 complexes by the Shank family of postsynaptic density proteins. *Neuron, 23*(3), 583-592. https://doi.org/10.1016/s0896-6273(00)80810-7
105. Husi, H., Ward, M. A., Choudhary, J. S., Blackstock, W. P., & Grant, S. G. (2000). Proteomic analysis of NMDA receptor-adhesion protein signaling complexes. *Nature Neuroscience, 3*(7), 661-669. https://doi.org/10.1038/76615
106. Rong, R., Ahn, J. Y., Huanh, H., Nagata, E., Kalman, D., Kapp, J. A., Tu, J., Worley, P. F., Snyder, S. H., & Ye, K. (2003). PI3 kinase enhancer-Homer complex couples mGluR1 to PI3 kinase, preventing neuronal apoptosis. *Nature Neuroscience, 6*(11), 1153-1161.

107. Humbert, S., Bryson, E. A., Cordelieres, F. P., Connors, N. C., Datta, S. R., Finkbeiner, S., Greenberg, M. E., & Saudou, F. (2002). The IGF-1/Akt pathway is neuroprotective in Huntington's disease and involves Huntingtin phosphorylation by Akt. *Developmental Cell, 2,* 831-837. https://doi.org/10.1016/s1534-5807(02)00188-0
108. Warby, S. C., Doty, C. N., Graham, R. K., Shively, J., Singaraja, R. R., & Hayden, M. R. (2009). Phosphorylation of huntingtin reduces the accumulation of its nuclear fragments. *Molecular and Cellular Neuroscience, 40,* 121-127. https://doi.org/10.1016/j.mcn.2008.09.007
109. Shigemoto, R., Nomura, S., Ohishi, H., Sugihara, H., Nakanishi, S, & Mizuno, N. (1993). Immunohistochemical localization of a metabotropic glutamate receptor, mGluR5, in the rat brain. *Neuroscience Letters, 163*(1), 53-57. https://doi.org/10.1016/0304-3940(93)90227-c
110. Abe, T., Sugihara, H., Nawa, H., Shigemoto, R., Mizuno, N., & Nakanishi, S. (1992). Molecular characterization of a novel metabotropic glutamate receptor mGluR5 coupled to inositol phosphate/Ca^{2+} signal transduction. *Journal of Biological Chemistry, 267*(19), 13361-13368.
111. Romano, C., Sesma, M. A., McDonald, C. T., O'Malley, K., Van den Pol, A. N., & Olney, J. W. (1995). Distribution of metabotropic glutamate receptor mGluR5 immunoreactivity in rat brain. *The Journal of Comparative Neurology, 355*(3), 455-469. https://doi.org/10.1002/cne.903550310
112. Ribeiro, F. M., Ferreira, L. T., Paquet, M., Cregan, T., Ding, Q., Gros, R., & Ferguson, S. S. G. (2009). Phosphorylation-independent regulation of metabotropic glutamate receptor 5 desensitization and internalization by G protein-coupled receptor kinase 2 in neurons. *Journal of Biological Chemistry, 284*(35), 23444–23453. https://doi.org/10.1074/jbc.M109.000778
113. Doria, J. G., Silva, F. R., Souza, J. M. De, Vieira, L. B., Carvalho, T. G., & Reis, H. J. (2013). Metabotropic glutamate receptor 5 positive allosteric modulators are neuroprotective in a mouse model of Huntington ' s disease. *British Journal of Pharmacology*, *169*, 909–921. https://doi.org/10.1111/bph.12164
114. Doria, J. G., Souza, J. M. De, Andrade, J. N., Rodrigues, H. A., Guimaraes, I. M., Carvalho, T. G., *et al.* (2015). The mGluR5 positive allosteric modulator , CDPPB , ameliorates pathology and phenotypic signs of a mouse model of Huntington ' s disease. *Neurobiology of Disease*, *73*, 163–173. https://doi.org/10.1016/j.nbd.2014.08.021
115. Abd-Elrahman, K. S., Hamilton, A., Hutchinson, S. R., Liu, F., Russell, R. C., & Ferguson, S. S. G. (2017). mGluR5 antagonism increases autophagy and prevents disease progression in the zQ175 mouse model of Huntington's disease. *Science Signaling*, *10*(510), 1–12. https://doi.org/10.1126/scisignal.aan6387
116. Hamilton, A., Vasefi, M., Tuin, C. Vander, Mcquaid, R. J., Anisman, H., & Ferguson, S. S. G. (2016). Chronic Pharmacological mGluR5 Inhibition Prevents Cognitive Impairment and Reduces Pathogenesis in an Alzheimer Disease Mouse Model. *Cell Reports*, *15*(9), 1859–1865. https://doi.org/10.1016/j.celrep.2016.04.077
117. Farmer, K., Abd-Elrahman, K. S., Derksen, A., Rowe, E. M., Thompson, A. M., Rudyk, C. A., Prowse, N. A., Dwyer, Z., Bureau, S. C., Fortin, T., Ferguson, S. S. G., & Hayley, S. (2020). mGluR5 Allosteric Modulation Promotes Neurorecovery in a 6-OHDA-Toxicant Model of Parkinson's Disease. *Molecular Neurobiology*, 1418–1431. https://doi.org/10.1007/s12035-019-01818-z
118. Schiefer, J., Spru, A., Puls, C., Lu, H., Milkereit, A., Milkereit, E., Johann, V., & Kosinski, C. M. (2004). The metabotropic glutamate receptor 5 antagonist MPEP and the mGluR2 agonist LY379268 modify disease progression in a transgenic mouse model of Huntington's disease. *Brain Research*, *1019*, 246–254. https://doi.org/10.1016/j.brainres.2004.06.005
119. Gerber, A. M., & Vallano, M. L. (2006). Structural properties of the NMDA receptor and the design of neuroprotective therapies. *Mini-Reviews in Medicinal Chemistry, 6,* 805-815. https://doi.org/10.2174/138955706777698651
120. Ikonomidou, C., & Turski, L. (2002). Why did NMDA receptor antagonists fail clinical trials for stroke and traumatic brain injury? *The Lancet Neurology, 1,* 383-386. https://doi.org/10.1016/s1474-4422(02)00164-3

121. Zare-shahabadi, A., Masliah, E., Johnson, G.V.W., & Rezaei, N. (2016). Autophagy in Alzheimer's Disease. *Reviews in the Neurosciences, 16*(3), 338–348. https://doi.org/10.1037/emo0000122.Do
122. Uddin, M. S., Stachowiak, A., Al Mamun, A., Tzvetkov, N. T., Takeda, S., Atanasov, A. G., Bergantin, L.B., Abdel-Daim, M.M., & Stankiewicz, A. M. (2018). Autophagy and Alzheimer's disease: From molecular mechanisms to therapeutic implications. *Frontiers in Aging Neuroscience, 10*(JAN), 1–18. https://doi.org/10.3389/fnagi.2018.00004
123. Schläfli, A. M., Berezowska, S., Adams, O., Langer, R., & Tschan, M. P. (2015). Reliable LC3 and p62 autophagy marker detection in formalin fixed paraffin embedded human tissue by immunohistochemistry. *European Journal of Histochemistry, 59*(2), 137–144. https://doi.org/10.4081/ejh.2015.2481
124. Velazquez, A. F. C., & Jackson, W. T. (2018). So Many Roads : the Multifaceted Regulation of Autophagy Induction. *Molecular and Cellular Biology*, *38*(21), e00303-318. https://doi.org/10.1128/MCB.00303-18
125. Yang, Z., & Klionsky, D. J. (2010). Mammalian autophagy: core molecular machinery and signaling regulation. *Current Opinion in Cell Biology, 22*, 124–131. https://doi.org/10.1016/j.ceb.2009.11.014
126. Parzych, K. R., & Klionsky, D. J. (2014). An Overview of Autophagy: Morphology, Mechanism, and Regulation. *Antioxidants and Redox Signaling*, *20*(3), 460–473. https://doi.org/10.1089/ars.2013.5371
127. Dice, J. F. (1990). Peptide sequences that target cytosolic proteins for lysosomal proteolysis. *Trends in Biochemical Sciences, 15*, 305–309. https://doi.org/10.1016/0968-0004(90)90019-8
128. Mijaljica, D., Prescott, M., & Devenish, R. J. (2011). Microautophagy in mammalian cells: revisiting a 40-year-old conundrum. *Autophagy, 7*, 673–682. https://doi.org/10.4161/auto.7.7.14733
129. Chiang, H-L., Terlecky, S. R., Plant, C. P., & Dice, J. F. (1989). A role for a 70-kilodalton heat shock protein in lysosomal degradation of intracellular proteins. *Science, 246*, 382–385. https://doi.org/10.1126/science.2799391
130. Agarraberes, F. A., & Dice, J. F. (2001). A molecular chaperone complex at the lysosomal membrane is required for protein translocation. *Journal of Cell Science, 114*, 2491–2499.
131. Cuervo, A. M., & Dice, J. F. (1996). A receptor for the selective uptake and degradation of proteins by lysosomes. *Science, 273*, 501–503. https://doi.org/10.1126/science.273.5274.501
132. Bandyopadhyay, U., Kaushik, S., Varticovski, L., & Cuervo, A. M. (2008). The chaperone-mediated autophagy receptor organizes in dynamic protein complexes at the lysosomal membrane. *Molecular and Cellular Biology, 28*, 5747–5763. https://doi.org/10.1128/MCB.02070-07
133. He, C., & Klionsky, D. J. (2009). Regulation mechanisms and signaling pathways of autophagy. *Annual Review of Genetics, 43*, 67–93. https://doi.org/10.1146/annurev-genet-102808-114910
134. Mijaljica, D., Prescott, M., & Devenish, R. J. (2012). The intriguing life of autophagosomes. *International Journal of Molecular Sciences, 13*, 3618–3635. https://doi.org/10.3390/ijms13033618
135. Yorimitsu, T., & Klionsky, D. J. (2005). Autophagy: molecular machinery for self-eating. *Cell Death and Differentiation, 12*, 1542–1552. https://doi.org/10.1038/sj.cdd.4401765
136. Yang, Z., & Klionsky, D. J. (2009). An overview of the molecular mechanism of autophagy. *Current Topics in Microbiology and Immunology, 335*, 1–32. https://doi.org/10.1007/978-3-642-00302-8_1
137. Tooze, J., Hollinshead, M., Ludwig, T., Howell, K., Hoflack, B., & Kern, H. (1990). In exocrine pancreas, the basolateral endocytic pathway converges with the autophagic pathway immediately after the early endosome. *Journal of Cell Biology, 111*, 329–345. https://doi.org/10.1083/jcb.111.2.239

138. Berg, T. O., Fengsrud, M., Stromhaug, P. E., Berg, T., & Seglen, P. O. (1998). Isolation and characterization of rat liver amphisomes. Evidence for fusion of autophagosomes with both early and late endosomes. *Journal of Biological Chemistry, 273*, 21883–21892. https://doi.org/10.1074/jbc.273.34.21883
139. Hara, T., Takamura, A., Kishi, C., Iemura, S., Natsume, T., Guan, J-L., & Mizushima, N. (2008). FIP200, a ULK-interacting protein, is required for autophagosome formation in mammalian cells. *Journal of Cell Biology, 181*, 497–510. https://doi.org/10.1083/jcb.200712064
140. Ganley, I. G., Lam du, H., Wang, J., Ding, X., Chen, S., & Jiang, X. (2009). ULK1·ATG13·FIP200 complex mediates mTOR signaling and is essential for autophagy. *Journal of Biological Chemistry, 284*, 12297–12305. https://doi.org/10.1074/jbc.M900573200
141. Hosokawa, N., Hara, T., Kaizuka, T., Kishi, C., Takamura, A., Miura, Y., Iemura, S., Natsume, T., Takehana, K., Yamada, N., Guan, J-L., Oshiro, N., & Mizushima, N. (2009). Nutrient-dependent mTORC1 association with the ULK1-Atg13-FIP200 complex required for autophagy. *Molecular Biology of the Cell, 20*, 1981–1991. https://doi.org/10.1091/mbc.E08-12-1248
142. Itakura, E., & Mizushima, N. (2010). Characterization of autophagosome formation site by a hierarchical analysis of mammalian Atg proteins. *Autophagy, 6*, 764–776. https://doi.org/10.4161/auto.6.6.12709
143. Itakura, E., Kishi, C., Inoue, K., & Mizushima, N. (2008). Beclin 1 forms two distinct phosphatidylinositol 3-kinase complexes with mammalian Atg14 and UVRAG. *Molecular Biology of the Cell, 19*, 5360–5372. https://doi.org/10.1091/mbc.E08-01-0080
144. Liang, X. H., Jackson, S., Seaman, M., Brown, K., Kempkes, B., Hibshoosh, H., & Levine, B. (1999). Induction of autophagy and inhibition of tumorigenesis by *beclin 1*. *Nature, 402*, 672–676. https://doi.org/10.1038/45257
145. Kihara, A., Noda, T., Ishihara, N., & Ohsumi, Y. (2001). Two distinct Vps34 phosphatidylinositol 3-kinase complexes function in autophagy and carboxypeptidase Y sorting in *Saccharomyces cerevisiae*. *Journal of Cell Biology, 152*, 519–530. https://doi.org/10.1083/jcb.152.3.519
146. Furuya, N., Yu, J., Byfield, M., Pattingre, S., & Levine, B. (2005). The evolutionarily conserved domain of Beclin 1 is required for Vps34 binding, autophagy and tumor suppressor function. *Autophagy, 1*, 46–52. https://doi.org/10.4161/auto.1.1.1542
147. Yan, Y., Flinn, R. J., Wu, H., Schnur, R. S., & Backer, J. M. (2009). hVps15, but not Ca^{2+}/CaM, is required for the activity and regulation of hVps34 in mammalian cells. *Biochemical Journal, 417*, 747–755. https://doi.org/10.1042/BJ20081865
148. Burman, C., & Ktistakis, N. T. (2010). Regulation of autophagy by phosphatidylinositol 3-phosphate. *FEBS Letters, 584*, 1302–1312. https://doi.org/10.1016/j.febslet.2010.01.011
149. Tanida, I. (2011). Autophagy basics. *Microbiology and Immunology, 55,* 1-11. https://doi.org/10.1111/j.1348-0421.2010.00271.x.
150. Russell, R. C., Tian, Y., Yuan, H., Park, H. W., Chang, Y-Y., Kim, J., Kim, H., Neufeld, T. P., Dillin, A., & Guan, K-L. (2013). ULK1 induces autophagy by phosphorylating Beclin-1 and activating VPS34 lipid kinase. *Nature Cell Biology, 15,* 741-750. https://doi.org/10.1038/ncb2757
151. Park, J-M., Seo, M., Jung, C. H., Grunwald, D., Stone, M., Otto, N. M., Toso, E., Ahn, Y., Kyba, M., Griffin, T. J., & Higgins, L., Kim, D-H. (2018). ULK1 phosphorylates Ser30 of BECN1 in association with ATG14 to stimulate autophagy induction. *Autophagy, 14,* 584-597. https://doi.org/10.1080/15548627.2017.1422851
152. Dooley, H. C., Razi, M., Polson, H. E. J., Girardin, S. E., Wilson, M. I., & Tooze, S. A. (2014). WIPI2 links LC3 conjugation with PI3P, autophagosome formation, and pathogen clearance by recruiting Atg12-5-16L1. *Molecular Cell, 55,* 238-252. https://doi.org/10.1016/j.molcel.2014.05.021
153. Ohsumi, Y. (2001). Molecular dissection of autophagy: two ubiquitin-like systems. *Nature Reviews Molecular Cell Biology, 2*, 211–216. https://doi.org/10.1038/35056522

154. Geng, J., & Klionsky, D. J. (2008). The Atg8 and Atg12 ubiquitin-like conjugation systems in macroautophagy. *EMBO Reports, 9*, 859–864. https://doi.org/10.1038/embor.2008.163
155. Kabeya, Y., Mizushima, N., Ueno, T., Yamamoto, A., Kirisako, T., Noda, T., Kominami, E., Ohsumi, Y., & Yoshimori, T. (2000). LC3, a mammalian homologue of yeast Apg8p, is localized in autophagosome membranes after processing. *The EMBO Journal, 19*, 5720–5728. https://doi.org/10.1093/emboj/19.21.5720
156. Aplin, A., Jasionowski, T., Tuttle, D. L., Lenk, S. E., & Dunn, W. A., Jr. (1992). Cytoskeletal elements are required for the formation and maturation of autophagic vacuoles. *Journal of Cellular Physiology, 152,* 458-466. https://doi.org/10.1002/jcp.1041520304
157. Monastyrska, I., Rieter, E., Klionsky, D. J., & Reggiori, F. (2009). Multiple roles of the cytoskeleton in autophagy. *Biological Reviews of the Cambridge Philosophical Society, 84,* 431-448. https://doi.org/10.1111/j.1469-185X.2009.00082.x
158. Köchl, R., Hu, X. W., Chan, E. Y. W., & Tooze, S. A. (2006). Microtubules facilitate autophagosome formation and fusion of autophagosomes with endosomes. *Traffic, 7*, 129-145. https://doi.org/10.1111/j.1600-0854.2005.00368.x
159. Kimura, S., Noda, T., & Yoshimori, T. (2008). Dynein-dependent movement of autophagosomes mediates efficient encounters with lysosomes. *Cell Structure and Function, 33,* 109-122. https://doi.org/10.1247/csf.08005
160. Nakamura, S., & Yoshimori, T. (2017). New insights into autophagosome – lysosome fusion. *Journal of Cell Science*, *130*, 1209–1216. https://doi.org/10.1242/jcs.196352
161. Liang, C., Lee, J. S., Inn, K. S., Gack, M. U., Li, Q., Roberts, E. A., Vergne, I., Deretic, V., Feng, P., Akazawa, C., *et al.* (2008). Beclin1-binding UVRAG targets the class C Vps complex to coordinate autophagosome maturation and endocytic trafficking. *Nature Cell Biology, 10,* 776-787. https://doi.org/10.1038/ncb1740
162. Sun, Q., Zhang, J., Fan, W., Wong, K. N., Ding, X., Chen, S., & Zhong, Q. (2011). The RUN domain of rubicon is important for hVps34 binding, lipid kinase inhibition, and autophagy suppression. *Journal of Biological Chemistry, 286,* 185-191. https://doi.org/10.1074/jbc.M110.126425
163. Takáts, S., Pircs, K., Nagy, P., Varga, Á., Kárpáti, M., Hegedüs, K., Kramer, H., Kovács, A. L., Sass, M., & Juhász, G. (2014). Interaction of the HOPS complex with Syntaxin 17 mediates autophagosome clearance in Drosophila. *Molecular Biology of the Cell, 25,* 1338-1354. https://doi.org/10.1091/mbc.E13-08-0449
164. Jiang, P., Nishimura, T., Sakamaki, Y., Itakura, E., Hatta, T., Natsume, T., & Mizushima, N. (2014). The HOPS complex mediates autophagosome-lysosome fusion through interaction with syntaxin 17. *Molecular Biology of the Cell, 25,* 1327-1337. https://doi.org/10.1091/mbc.E13-08-0447.
165. Diao, J. J., Liu, R., Rong, Y. G., Zhao, M. L., Zhang, J., Lai, Y., Zhou, Q. J., Wilz, L. M., Li, J. X., Vivona, S., *et al.* (2015). ATG14 promotes membrane tethering and fusion of autophagosomes to endolysosomes. *Nature, 520,* 563-566. https://doi.org/10.1038/nature14147
166. Zaffagnini, G., & Martens, S. (2016). Mechanisms of Selective Autophagy. *Journal of Molecular Biology, 428*(9Part A), 1714-1724. https://doi.org/10.1016/j.jmb.2016.02.004
167. Takeshige, K. (1992). Autophagy in yeast demonstrated with proteinase-deficient mutants and conditions for its induction. *Journal of Cell Biology, 119*(2), 301–311. https://doi.org/10.1083/jcb.119.2.301
168. Novikoff, A. B., & Essner, E. (1962). Cytolysomes and mitochondrial degeneration. *Journal of Cell Biology, 15*,140–146. https://doi.org/10.1083/jcb.15.1.140
169. Mortimore, G. E., & Schworer, C. M. (1977). Induction of autophagy by amino-acid deprivation in perfused rat liver. *Nature, 270*(5633), 174–176. https://doi.org/10.1038/270174a0
170. Kraft, C., Reggiori, F., & Peter, M. (2009). Selective types of autophagy in yeast. *Biochimica et Biophysica Acta, 1793*(9), 1404–1412. https://doi.org/10.1016/j.bbamcr.2009.02.006

171. Ashford, T. P., & Porter, K. R. (1962). Cytoplasmic components in hepatic cell lysosomes. *Journal of Cell Biology, 12*, 198–202. https://doi.org/10.1083/jcb.12.1.198
172. Khaminets, A., Behl, C., & Dikic, I. (2015). Ubiquitin-dependent and independent signals in selective autophagy. *Trends in Cell Biology, 26*(1), 6-16. https://doi.org/10.1016/j.tcb.2015.08.010
173. De Duve, C., & Wattiaux, R. (1966). Functions of lysosomes. *Annual Review of Physiology, 28*, 435–492. https://doi.org/10.1146/annurev.ph.28.030166.002251
174. Rogov, V., Dötsch, V., Johansen, T., & Kirkin, V. (2014). Interactions between autophagy receptors and ubiquitin-like proteins form the molecular basis for selective autophagy. Molecular Cell, 53(2), 167–178. https://doi.org/10.1016/j.molcel.2013.12.014
175. Puente, C., Hendrickson, R. C., & Jiang, X. (2016). Nutrient-regulated phosphorylation of ATG13 inhibits starvation-induced autophagy. *Journal of Biological Chemistry, 291,* 6026-6035. https://doi.org/10.1074/jbc.M115.689646
176. Kim, J., Kundu, M., Viollet, B., & Guan, K-L. (2011). AMPK and mTOR regulate autophagy through direct phosphorylation of Ulk1. *Nature Cell Biology, 13,* 132-141. https://doi.org/10.1038/ncb2152
177. Jung, C. H., Jun, C. B., Ro, S. H., Kim, Y. M., Otto, N. M., Cao, J., Kundu, M., & Kim, D. H. (2009). ULK-Atg13-FIP200 complexes mediate mTOR signaling to the autophagy machinery. *Molecular Biology of the Cell, 20*, 1992–2003. https://doi.org/10.1091/mbc.E08-12-1249
178. Hosokawa, N., Hara, T., Kaizuka, T., Kishi, C., Takamura, A., Miura, Y., Iemura, S., Natsume, T., Takehana, K., Yamada, N., Guan, J-L., Oshiro, N., & Mizushima, N. (2009). Nutrient-dependent mTORC1 association with the ULK1-Atg13-FIP200 complex required for autophagy. *Molecular Biology of the Cell, 20*, 1981–1991. https://doi.org/10.1091/mbc.e08-12-1248
179. Cherra, S. J., III., Kulich, S. M., Uechi, G., Balasubramani, M., Mountzouris, J., Day, B. W., & Chu, C. T. (2010). Regulation of the autophagy protein LC3 by phosphorylation. *Journal of Cell Biology, 190*, 533–539. https://doi.org/10.1083/jcb.201002108
180. Blancquaert, S., Wang, L., Paternot, S., Coulonval, K., Dumont, J. E., Harris, T. E., & Roger, P. P. cAMP-dependent activation of mammalian target of rapamycin (mTOR) in thyroid cells. Implication in mitogenesis and activation of CDK4. *Molecular Endocrinology, 24*, 1453–1468. https://doi.org/10.1210/me.2010-0087
181. Mavrakis, M., Lippincott-Schwartz, J., Stratakis, C. A., & Bossis, I. (2006) Depletion of type IA regulatory subunit (RIα) of protein kinase A (PKA) in mammalian cells and tissues activates mTOR and causes autophagic deficiency. *Human Molecular Genetics, 15*, 2962–2971. https://doi.org/10.1093/hmg/ddl239
182. Meley, D., Bauvy, C., Houben-Weerts, J. H., Dubbelhuis, P. F., Helmond, M. T., Codogno, P., & Meijer, A. J. (2006). AMP-activated protein kinase and the regulation of autophagic proteolysis. *Journal of Biological Chemistry, 281*, 34870–34879. https://doi.org/10.1074/jbc.M605488200
183. Alers, S., Loffler, A. S., Wesselborg, S., & Stork, B. (2012). Role of AMPK-mTOR-Ulk1/2 in the regulation of autophagy: cross talk, shortcuts, and feedbacks. *Molecular and Cellular Biology, 32*, 2–11. https://doi.org/10.1128/MCB.06159-11
184. Gwinn, D. M., Shackelford, D. B., Egan, D. F., Mihaylova, M. M., Mery, A., Vasquez, D. S., Turk, B. E., & Shaw, R. J. (2008). AMPK phosphorylation of raptor mediates a metabolic checkpoint. *Molecular Cell, 30*, 214–226. https://doi.org/10.1016/j.molcel.2008.03.003
185. Hardie, D. G. (2007). AMP-activated/SNF1 protein kinases: conserved guardians of cellular energy. *Nature Reviews Molecular Cell Biology, 8*, 774–785. https://doi.org/10.1038/nrm2249
186. Inoki, K., Zhu, T., & Guan, K-L. (2003). TSC2 mediates cellular energy response to control cell growth and survival. *Cell, 115*, 577–590. https://doi.org/10.1016/s0092-8674(03)00929-2
187. Lee, J. W., Park, S., Takahashi, Y., & Wang, H-G. (2010). The association of AMPK with ULK1 regulates autophagy. *PLOS One, 5*(11), e15394. https://doi.org/10.1371/journal.pone.0015394

188. Høyer-Hansen, M., Bastholm, L., Szyniarowski, P., Campanella, M., Szabadkai, G., Farkas, T., Bianchi, K., Fehrenbacher, N., Elling, F., Rizzuto, R., Mathiasen, I. S., & Jäättelä, M. (2007). Control of macroautophagy by calcium, calmodulin-dependent kinase kinase-β, and Bcl-2. *Molecular Cell, 25*, 193–205. https://doi.org/10.1016/j.molcel.2006.12.009
189. Chu, C. T. (2019). Mechanisms of selective autophagy and mitophagy: Implications for neurodegenerative diseases. *Neurobiology of Disease*, *122*, 23–34. https://doi.org/10.1016/j.nbd.2018.07.015
190. Pankiv, S., Clausen, T. H., Lamark, T., Brech, A., Bruun, J. A., Outzen, H., Øvervatn, A., Bjørkøy, G., & Johansen, T. (2007). P62/SQSTM1 binds directly to Atg8/LC3 to facilitate degradation of ubiquitinated protein aggregates by autophagy. *The Journal of Biological Chemistry, 282*(33), 24131-24145. https://doi.org/10.1074/jbc.M702824200
191. Bjørkøy, G., Lamark, T., Pankiv, S., Øvervatn, A., Brech, A., & Johansen, T. (2009). Chapter 12 Monitoring Autophagic Degradation of p62/SQSTM1. *Methods in Enzymology, 451*(C), 181-197. http://doi.org/10.1016/S0076-6879(08)03612-4
192. Fortun, J., Dunn, W. A. Jr., Joy, S., Li, J., & Notterpek, L. (2003). Emerging role for autophagy in the removal of aggresomes in Schwann cells. *Journal of Neuroscience, 23*(33), 10672-10680. https://doi.org/10.1523/JNEUROSCI.23-33-10672.2003
193. Rideout, H. J., Lang-Rollin, I., & Stefanis, L. (2004). Involvement of macroautophagy in the dissolution of neuronal inclusions. *The International Journal of Biochemistry and Cell Biology, 36*(12), 2551-2562. https://doi.org/10.1016/j.biocel.2004.05.008
194. Ravikumar, B., Duden, R., & Rubinsztein, D. C. (2002). Aggregate-prone proteins with polyglutamine and polyalanine expansions are degraded by autophagy. *Human Molecular Genetics, 11,* 1107-1117. https://doi.org/10.1093/hmg/11.9.1107
195. Zhang, T., Dong, K., Liang, W., Xu, D., Xia, H., Geng, J., Najafov, A., Liu, M., Li, Y., Han, X., Xiao, J., Jin, Z., Peng, T., Gao, Y., Cai, Y., Qi, C., Zhang, Q., Sun, A., Lipinski, M., Zhu, H., Xiong, Y., Pandolfi, P. P., Li, H., Yu, Q., & Yuan, J. (2015). G-protein Coupled Receptors Regulate Autophagy by ZBTB16-mediated Ubiquitination and Proteasomal Degradation of Adaptor Protein Atg14L. *ELife*, *2015*(4), 1–19. https://doi.org/10.7554/eLife.06734
196. Obara, K., & Ohsumi, Y. (2011). Atg14: A key player in orchestrating autophagy. *International Journal of Cell Biology, 2011,* 713435. https://doi.org/10.1155/2011/713435
197. Wirawan, E., Vanden Berghe, T., Lippens, S., Agostinis, P., & Vandenabeele P. (2012). Autophagy: for better or for worse. *Cell Research, 22*, 43–61. https://doi.org/10.1038/cr.2011.152
198. Wong, E., & Cuervo, A. M. (2010). Autophagy gone awry in neurodegenerative diseases. *Nature Neuroscience, 13*(7), 805-811. https://doi.org/10.1038/nn.2575
199. Ravikumar, B., Futter, M., Jahreiss, L., Korolchuk, V. I., Lichtenberg, M., Luo, S., Massey, D. C. O., Menzies, F. M., Narayanan, U., Renna, M., Jimenez-Sanchez, M., Sarkar, S., Underwood, B., Winslow, A., & Rubinsztein, D. C. (2009). Mammalian macroautophagy at a glance. *Journal of Cell Science, 122*(11), 1707-1711. https://doi.org/10.1242/jcs.031773
200. Hara, T., Nakamura, K., Matsui, M., Yamamoto, A., Nakahara, Y., Suzuki-Migishima, R., Yokoyama, M., Mishima, K., Saito, I., Okano, H., & Mizushima, N. (2006). Suppression of basal autophagy in neural cells causes neurodegenerative disease in mice. *Nature, 441*(7095), 885-889. https://doi.org/10.1038/nature04724
201. Stavoe, A. K. H., & Holzbaur, E. L. F. (2018). Axonal autophagy: Mini-review for autophagy in the CNS. *Neuroscience Letters, 697,* 17-23. https://doi.org/10.1016/j.neulet.2018.03.025
202. Nixon, R. A. (2013). The role of autophagy in neurodegenerative disease. *Nature Medicine, 19*(8), 983-997. https://doi.org/10.1038/nm.3232
203. Komatsu, M., Waguri, S., Chiba, T., Murata, S., Iwata, J. I., Tanida, I., Ueno, T., Koike, M., Uchiyama, Y., Kominami, E., & Tanaka, K. (2006). Loss of autophagy in the central nervous system causes neurodegeneration in mice. *Nature, 441*(7095), 880-884. https://doi.org/10.1038/nature04723
204. Ntsapi, C., Lumkwana, D., Swart, C., du Toit, A., & Loos, B. (2017). New Insights Into Autophagy Dysfunction Related to Amyloid Beta Toxicity and Neuropathology in Alzheimer's

Disease. *International Review of Cell and Molecular Biology, 336,* 321-361. https://doi.org/10.1016/bs.ircmb.2017.07.002

205. Sweeney, P., Park, H., Baumann, M., Dunlop, J., Frydman, J., Kopito, R., McCampbell, A., Leblanc, G., Venkateswaran, A., Nurmi, A., & Hodgson, R. (2017). Protein misfolding in neurodegenerative diseases: implications and strategies. *Translational Neurodegeneration, 6*, 6. https://doi.org/10.1186/s40035-017-0077-5
206. Massey, A., Kiffin, R., & Cuervo, A. M. (2004). Pathophysiology of chaperone-mediated autophagy. The International Journal of Biochemistry and Cell Biology, 36(12), 2420–2434. https://doi.org/10.1016/j.biocel.2004.04.010
207. Ding, Q., Dimayuga, E., Martin, S., Bruce-Keller, A. J., Nukala, V., Cuervo, A. M., & Keller, J. N. (2003). Characterization of chronic low-level proteasome inhibition on neural homeostasis. *Journal of Neurochemistry, 86*(2), 489-497. https://doi.org/10.1046/j.1471-4159.2003.01885.x
208. Xilouri, M., Vogiatzi, T., Vekrellis, K., Park, D., & Stefanis, L. (2009). Abberant alpha-synuclein confers toxicity to neurons in part through inhibition of chaperone-mediated autophagy. *PLOS One, 4*(5), e5515. https://doi.org/10.1371/journal.pone.0005515
209. Guo, Q., Bin, H., Cheng, J., Seefelder, M., Engler, T., Pfeifer, G., Oeckl, P., Otto, M., Moser, F., Maurer, M., Pautsch, A., Baumeister, W., Fernandez-Busnadiego, R., Kochanek, S. (2018). The cryo-electron microscopy structure of huntingtin. *Nature, 555*(7694), 117-120. https://doi.org/10.1038/nature25502
210. Wold, M. S., Lim, J., Lachance, V., Deng, Z., & Yue, Z. (2016). ULK1-mediated phosphorylation of ATG14 promotes autophagy and is impaired in Huntington ' s disease models. *Molecular Neurodegeneration*, *11*(76). https://doi.org/10.1186/s13024-016-0141-0
211. Lim, J., Lachenmayer, M. L., Wu, S., Liu, W., Kundu, M., Wang, R., Komatsu, M., Oh, Y. J., Zhao, Y., & Yue, Z. (2015). Proteotoxic stress induces phosphorylation of p62/SQSTM1 by ULK1 to regulate selective autophagic clearance of protein aggregates. *PLOS Genetics, 11*(2), e1004987. https://doi.org/10.1371/journal.pgen.1004987
212. Wong, Y. C., Holzbaur, E. I. (2014). The regulation of autophagosome dynamics by huntingtin and HAP1 is disrupted by expression of mutant huntingtin, leading to defective cargo degradation. *Journal of Neuroscience, 34*(4), 1293-1305. https://doi.org/10.1523/JNEUROSCI.1870-13.2014
213. Ochaba, J., Lukacsovich, T., Csikos, G., Zheng, S., Margulis, J., Salazar, L., Mao, K., Lau, A. L., Yeung, S. Y., Humbert, S., Saudou, F., Klionsky, D. J., Finkbeiner, S., Zeitlin, S. O., Marsh, J. L., Housman, D. E., Thompson, L. M., & Steffan, J. S. (2014). Potential function for the Huntingtin protein as a scaffold for selective autophagy. *Proceedings of the National Academy of Sciences of the United States of America, 111*(47), 16889-16894. https://doi.org/10.1073/pnas.1420103111
214. Steffan, J. S. (2010). Does Huntingtin play a role in selective macroautophagy? *Cell Cycle, 9*(17), 3401-3413. https://doi.org/10.4161/cc.9.17.12718
215. Martinez-Vicente, M., Talloczy, Z., Wong, E., Tang, G., Koga, H., Kaushik, S., de Vries, R., Arias, E., Harris, S., Sulzer, D, & Cuervo, A. M. (2010). Cargo recognition failure is responsible for inefficient autophagy in Huntington's disease. *Nature Neuroscience, 13*(5), 567-576. https://doi.org/10.1038/nn.2528
216. Ravikumar, B., Vacher, C., Berger, Z., Davies, J. E., Luo, S., Oroz, L. G. (2004). Inhibition of mTOR induces autophagy and reduces toxicity of polyglutamine expansions in fly and mouse models of Huntington disease. *Nature Genetics, 36*(6), 585-595. https://doi.org/10.1038/ng1362
217. Shibata, M., Lu, T., Furuya, T., Degterev, A., Mizushima, N., Yoshimori, T., MacDonald, M., Yanker, B., & Yuan, J. (2006). Regulation of intracellular accumulation of mutant Huntingtin by Beclin 1. *Journal of Biological Chemistry, 281*(20), 14474-14485. https://doi.org/10.1074/jbc.M600364200
218. Kegel, K. B., Kim, M., Sapp, E., McIntyre, C., Castaño, J. G., Aronin, N., & DiFiglia, M. (2000). Huntingtin expression stimulates endosomal-lysosomal activity, endosome tabulation,

and autophagy. *Journal of Neuroscience, 20*(19), 7268-7278. https://doi.org/10.1523/JNEUROSCI.20-19-07268.2000
219. Atwal, R. S., Xia, J., Pinchev, D., Taylor, J., Epand, R. M., Truant, R. (2007). Huntingtin has a membrane association signal that can modulate huntingtin aggregation, nuclear entry and toxicity. *Human Molecular Genetics, 16*(21), 2600-2615. https://doi.org/10.1093/hmg/ddm217
220. Terman, A., Kurz, T., Navratil, M., Arriage, E. A., & Brunk, U. T. (2010). Mitochondrial turnover and aging of long-lived postmitotic cells: the mitochondrial-lysosomal axis theory of aging. *Antioxidants and Redox Signaling, 12*(4), 503-535. https://doi.org/10.1089/ars.2009.2598
221. Lee, H., Noh, J. Y., Oh, Y., Kim, Y., Chang, J. W., Chung, C. W., Lee, S. T., Kim, M., Ryu, H. & Jung, Y. K. (2012). IRE1 plays an essential role in ER stress-mediated aggregation of mutant huntingtin via the inhibition of autophagy flux. *Human Molecular Genetics, 21*(1), 101-114. https://doi.org/10.1093/hmg/ddr445
222. Berger, Z., Ravikumar, B., Menzies, F. M., Oroz, L. G., Underwood, B. R., Pangalos, M. N., Schmitt, I., Wullner, U., Evert, B. O., O'Kane, C. J., & Rubinsztein, D. C. (2006). Rapamycin alleviates toxicity of different aggregate-prone proteins. *Human Molecular Genetics, 15*(3), 433-442. https://doi.org/10.1093/hmg/ddi458
223. Ma, T. C., Buescher, J. L., Oatis, B., Funk, J. A., Nash, A. J., Carrier, R. L., & Hoyt, K. R. (2007). Metformin therapy in a transgenic mouse model of Huntington's disease. *Neuroscience Letters, 411*(2), 98-103. https://doi.org/10.1016/j.neulet.2006.10.039
224. Jiang, W., Wei, W., Gaertig, M. A., Li, S., & Li, X. J. (2015). Therapeutic Effect of Berberine on Huntington's Disease Transgenic Mouse Model. *PLOS One, 10*(7), e0134142. https://doi.org/10.1371/journal.pone.0134142
225. Sarkar, S., Davies, J. E., Huang, Z., Tunnacliffe, A., & Rubinsztein, D. C. (2007). Trehalose, a novel mTOR-independent autophagy enhancer, accelerates the clearance of mutant huntingtin and alpha-synuclein. *Journal of Biological Chemistry, 282*(8), 5641-5652. https://doi.org/10.1074/jbc.M609532200
226. Tanaka, M., Machida, Y., Niu, S., Ikeda, T., Jana, N. R., Doi, H., Kurosawa, M., Nekooki, M., & Nukina, N. (2004). Trehalose alleviates polyglutamine-mediated pathology in a mouse model of Huntington disease. *Nature Medicine, 10*(2), 148-154. https://doi.org/10.1038/nm985
227. Rosenbaum, D. M., Rasmussen, S. G., & Kobilka, B. (2009). The structure and function of G-protein-coupled receptors. *Nature, 459*(7245), 356-363. https://doi.org/10.1038/nature08144
228. Hofmann, P. K., Cheerer, P., Hildebrand, P. W., Choe, H. W., Park, J. H., Heck, M., & Ernst, O. P. (2009). A G protein-coupled receptor at work: the rhodopsin model. *Trends in Biochemical Sciences, 34*(11), 540-552. https://doi.org/10.1016/j.tibs.2009.07.005
229. Abd-Elrahman, K. S., Hamilton, A., Vasefi, M., & Ferguson, S. S. G. (2018). Autophagy is increased following either pharmacological or genetic silencing of mGluR5 signaling in Alzheimer's disease mouse models. *Molecular Brain*, *11*(1), 4–11. https://doi.org/10.1186/s13041-018-0364-9
230. Ran, F. A., Hsu, P. D., Wright, J., Agarwala, V., Scott, D. A., & Zhang, F. (2013). Genome engineering using the CRISPR-Cas9 system. *Nature Protocols*, *8*(11), 2281–2308. https://doi.org/10.1038/nprot.2013.143
231. Jinek, M., Chylinski, K., Fonfara, I., Hauer, M., Doudna, J. A., Charpentier, E. (2012). A programmable Dual-RNA-Guided DNA Endonuclease in Adaptive Bacterial Immunity. *Science, 337*(6096), 816-821. https://doi.org/10.1126/science.1225829
232. Unniyampurath, U., Pilankatta, R., & Krishnan, M. N. (2016). RNA interference in the age of CRISPR: Will CRISPR interfere with RNAI? *International Journal of Molecular Sciences*, *17*(3). https://doi.org/10.3390/ijms17030291
233. Feng, Y., He, D., Yao, Z., & Klionsky, D. J. (2014). The machinery of macroautophagy. *Cell Research*, *24*(1), 24–41. https://doi.org/10.1038/cr.2013.168
234. Tanida, I., Ueno, T., & Kominami, E. (2008). LC3 and Autophagy. *Methods in Molecular Biology, 455*, 77-88. https://doi.org/10.1007/978-1-59745-157-4_4

235. Hill, S. M., Wrobel, L., & Rubinsztein, D. C. (2018). Post-translational modifications of Beclin 1 provide multiple strategies for autophagy regulation. *Cell Death & Differentiation, 26*, 617-629. https://doi.org/10.1038/s41418-018-0254-9
236. Cao, Y., & Klionsky, D. J. (2007). Physiological functions of Atg6/Beclin 1: a unique autophagy-related protein. *Cell Research, 17*, 839-849. https://doi.org/10.1038/cr.2007.78
237. Loeffler, D. A. (2019). Influence of Normal Aging on Brain Autophagy : A Complex Scenario. *Frontiers in Aging Neuroscience*, *11*(49). https://doi.org/10.3389/fnagi.2019.00049
238. Mizushima, N., & Yoshimori, T. (2007). How to Interpret LC3 Immunoblotting. *Autophagy*, *3*(6), 542–545. https://doi.org/10.4161/auto.4600
239. Fahnenstich, J., Nandy, A., Milde-Langosch, K., Schneider-Merk, T., Walther, N., & Gellersen, B. (2003). Promyelocytic leukaemia zinc finger protein (PLZF) is a glucocorticoid- and progesterone-induced transcription factor in human endometrial stromal cells and myometrial smooth muscle cells. *Molecular Human Reproduction, 9*(10), 611-623. https://doi.org/10.1093/molehr/gag080
240. Savage, A. K., Constantinides, M. G., Han, J., *et al.* (2008). The transcription factor PLZF directs the effector program of the NKT cell lineage. *Immunity, 29*(3), 391-403. https://doi.org/10.1016.j.immuni.2008.07.011